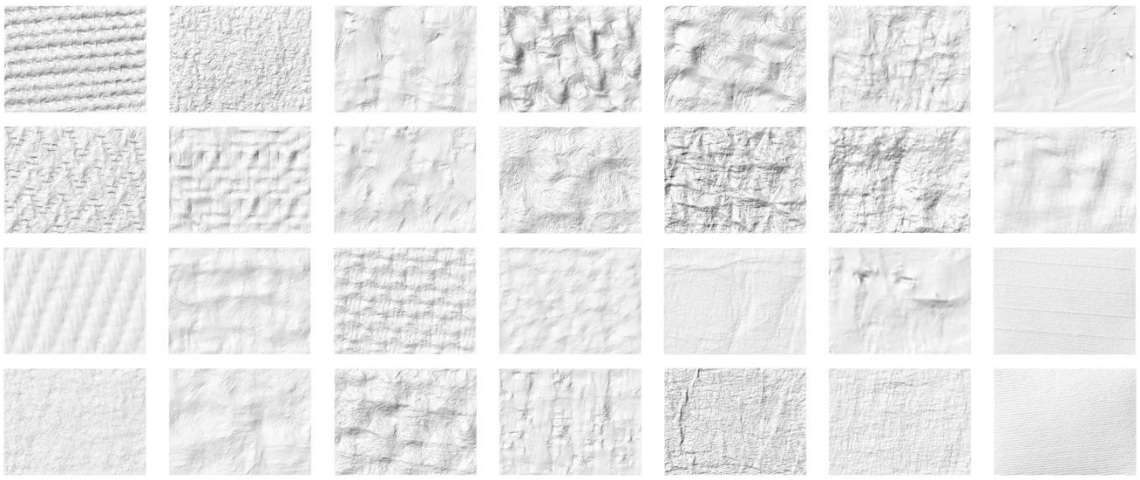

3D Microscopic Texture Interface in CAD: Cultivating Material Knowledge for the Practiced Digital Hand

Wei-Wei Chi

School of Architecture, College of Fine Arts,
Carnegie Mellon University,

Master of Computational Design
2019

Abstract

This thesis investigates the feasibility of incorporating 3D textures in design via the development of a prototype texture scanning device that allows real time sampling of physical material textures at a microscopic scale. Drawing from the state-of-the-art methods in computer vision, computer graphics, and electrical engineering, it describes the implementation of a low-cost, portable, open-source prototype texture scanning device. It presents the performance of the device through a technical examination of scanned outputs and a human-centered exploration of design opportunities with three expert cases. Finally, it shows the opportunities to augment design processes and to reintroduce material sensibility training, similar to that of the Bauhaus sensory training, through 3D sampling of real texture at a microscale.

Acknowledgements

This thesis would not have been possible without the support of the following individuals to whom I am sincerely grateful to.

Prof. Daragh Byrne for his patience, guidance, and insights throughout this thesis. His technical and theoretical knowledge in tangible computing was of great assistance for the development of this thesis. Opportunities Professor Byrne provided throughout my time at Carnegie Mellon University (CMU) were essential to my development as a researcher.

Prof. Daniel Cardoso Llach for his mentorship throughout my time at CMU. His valuable and constructive critiques have been crucial throughout the development of this thesis.

Prof. Roberta Klatzky for sharing her scientific perspectives on haptic perception of material, which were crucial in informing this thesis.

Prof. Matthew O'Toole for guiding me through the technical computer vision aspect of this thesis.

Jill Chisnell for lending the necessary reading materials and references for this thesis.

All of my CodeLab and CMU colleagues and friends, among them Jinmo Rhee, Özgüç Bertuğ Çapunaman, Runchang Kang, Zheng Luo, Ardavan Bidgoli, Emek Erdolu, Byeongjoo Ahn for late night discussion and for helping me mentally and physically throughout my two years at CMU.

My family for years of support in my education and for placing their confidence in me. Vanessa Baaklini, for her constant, generous, and unconditional support.

CMU Graduate Student Assembly and Provost Office for their generous financial support through GuSH Research grants.

Table of Contents

1. Introduction

Hands are essential in design; not only as a tool for drawing, sketching, and sculpting but as a sensory touch organ that is constantly cultivating knowledge. Donald A Schön proposed that design is a reflective conversation with materials in a design situation and one framework of knowing-in-action he explained was "Seeing/Drawing/Seeing".[1] Here, "Seeing" refers not only to the visual perception but "Seeing" as in designing with the body and senses. Schön shows that design is a reflective conversation and practices with material. In design, this form of learning is difficult to obtain only through formal knowledge, but it is essential to build up tacit knowledge through the practice of designing. One form of knowledge that a designer gets familiar with their hand is material knowledge, which includes their physical properties and perceptual properties. Though the physical properties of the material can be learned through formal methods which provide an objective numerical understanding of material, but using them in design requires both tacit knowledge and explicit knowledge of material. The traditional methods of material training involves cultivating the objective properties of material to understand the limits of material and cultivating subjective properties of material to understand expressive-sensorial aspect of material.

This thesis shows how a new understanding of material could be cultivated with the aid of a digital scanning prototype tool that provides a 3D texture reconstruction at a microscale. The encoding of the microscopic texture will be done through the prototype texture scanning system developed in this thesis. Furthermore, this thesis hopes to contribute to creating realistic haptic material texture rendering by encoding the haptic geometric model of the texture at a microscopic scale. The larger ambition of this thesis is to take a step towards a multimodal interface in Computer-Aided Design (CAD) by encoding various mode of sensory perception of material into the CAD workflow (sound, thermal effect of material, etc.). However, this thesis will focus on the micro-geometry of

[1] Schön, *The Reflective Practitioner : How Professionals Think in Action*, 133.

material texture difficult to distinguish with the normal human visual system, but the human hands could feel.

The thesis is organized as follows. The first chapter will define the dimensions of material knowledge which is discussed in this thesis, and it will introduce the background on the perceptual biases of computer-aided design softwares through historical and theoretical lenses, focusing on the perspective of Paul Dourish, Malcolm McCullough, Juhani Pallasmaa, and Daniel Cardoso Llach. The second chapter will guide the user through a brief literature survey of texture representation, encoding, and decoding techniques used in computer vision, computer graphics, and haptic rendering. In addition, the second chapter will show the historical evidence of understanding texture in design through the Bauhaus tradition of sensory training. The third chapter will describe the system implmentation of the texture scanning prototype. The fourth chapter will show results through a) qualitative description, b) quantitative statistically analysis of the 3D reconstruction, and c) Interview with experts in material-focused design fields (Computational Textile and Biomaterial). The fifth chapter provides a discussion of findings, the limitations of the system and its ability to aid the cultivation of material knowledge.

1.1 Objective and Subjective Dimension of Material Knowledge

Material knowledge, in this thesis, refers to the *know-what* of the material in both the explicit knowledge form which includes the objective scientific model of material and tacit knowledge form which includes subjective material experience. Figure 1 shows the categorization of material knowledge into four different types of knowledge: know-what, know-who, know-how, and know-why and each of these contain more or less tacit and explicit form.[2]

[2] Haug, "Acquiring Materials Knowledge in Design Education."

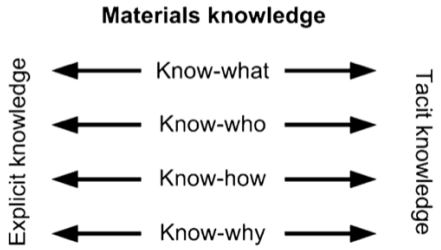

Figure 1: Forms of materials knowledge, reprinted from "*Acquiring materials knowledge in design education"*[3]

The know-what of the materials are shown in
Table 1. below. This thesis will refer to material knowledge as understanding the subjective evaluation and the objective evaluation of inherent material properties. The material properties can help designers to better understand the material and to design with the material.

	Inherent properties	Attributed properties
Subjective evaluation	Color (S), feel, sound (S), smell, etc.	Meaning, symbolism, aesthetics, etc.
Objective evaluation	Color (O), texture, sound (O), density, etc.	Price, delivery, time availability, etc.

Table 1: Material property types, reprinted from "*Acquiring materials knowledge in design education"*[4]

Many of these objective aspects of materials are becoming integrated into CAD through simulation and sensor-based data collection. However, thaspects of the "feel" and the touch of a material are still not part of the interfaces. Valentina Rognoli discussed the importance of the expressive-sensorial dimension of material in theoretical and practical

[3] Haug, 8.
[4] Haug, 8.

design.[5] Rognoli shows that the objective formalization of material in science is not enough for design but that design education and the design process require a more expressive-sensorial dimension of material that can be sensed.[6]

1.2 Multisensory Perception in Design for Material Knowledge

This form of expressive-sensorial dimension of material inspired by the Bauhaus tradition of the hands-on approach with the material. In *The New Vision*, by László Moholy-Nagy, he documented a form of sensory training with material through various tactile exercises which were a part of the Bauhaus curriculum.[7] These tactile exercises are used as a subjective evaluation of material rather than a more objective evaluation of material. Figure *2* shows one of the student texture tactile wheels, which is parameterized similar to the color wheel.

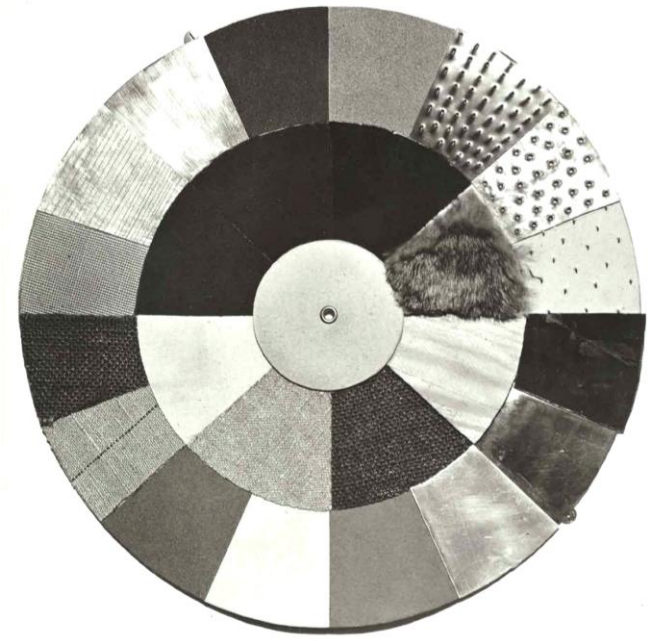

Figure 2: Walter Kaminski (Bauhaus, second semester, 1927) Revolving tactile table of two concentric circles with contrasting tactile values, from soft to hard, from smooth to rough, reprinted from "*The New Vision*"[8]

[5] Rognoli, *A Broad Survey on Expressive-Sensorial Characterization of Materials for Design Education*.
[6] Rognoli.
[7] Moholy-Nagy and Hoffmann, *The New Vision: Fundamentals of Design, Painting, Sculpture, Architecture*.
[8] Moholy-Nagy and Hoffmann, 26.

However, the Bauhaus tradition of using material and product samples to support the acquisition of material knowledge is undermined in the age of digital design technologies. Though practices of understanding material still exist in the design process, the abstracted visual representation in CAD and the final material form are hugely disconnected. The physical properties of the material in the process of design usually come after designing the visual representation.

To combat the occularcentric model of interaction in contemporary CAD, scholars, computer scientists, and designers propose a way to rebalance the hegemony of vision by incorporating the multimodal sensory model of interaction in computing. Ivan Sutherland, the father of computer graphics, envisioned one of the first multi-sensory experience systems. In his essay, The Ultimate Display, he ended the essay with, "The Ultimate display would, …, be a room within which computer can control the existence of matter… With appropriate programming such a display could literally be the Wonderland into which Alice walked."[9] Likewise, Malcolm McCullough's ideal model for the future of computing relies upon multimodal interfaces that support the touch. He stated, "Multimodal interaction seems at least as interesting multimedia documents as an immediate future for computing."[10] Though Juhani Pallasmaa was critical of new technology strengthening the hegemony of vision, he believes new technologies could also rebalance the senses.[11]

Drawing inspiration from the tactile table in *The New Vision*, new digital tools could be used to create a form of digital "sensory training" system which could incorporate new modality of sensory perception of material into CAD through new interfaces.

[9] Sutherland, "The Ultimate Display."
[10] McCullough, *Abstracting Craft: The Practiced Digital Hand*, 131.
[11] Pallasmaa, *The Eyes of the Skin : Architecture and the Senses*, 41.

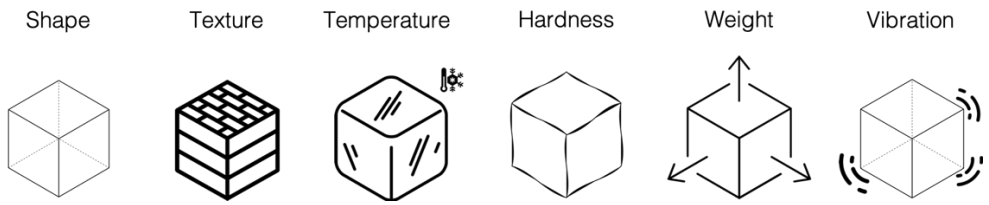

Figure 3: Haptic Perception of Material properties

Figure *3* shows various haptic perceptions of material properties that one can feel. Out of these haptic attributes of material, the texture attribute will be used in the prototype "sensory training" system, the texture of material is one attribute that is multisensory in nature combining the visual, haptic, and auditory perception among other sensorial attributes of material.[12] As evident in both Maria Montessori and László Moholy-Nagy's sensory training, the texture was used to train the sense of touch and understanding to material.[13] In addition, the texture is greatly related to the expressive-sensorial dimension of the material. This thesis will define texture as the microstructure and microgeometry of the material surface properties.

In this thesis, imaging and scanning of texture will be conducted at the microscopic scale, where each pixel is about 0.014mm in the real world. However, the texture of the sampled materials themselves can be considered as macrotextures; these sample materials have periods greater than 0.2mm. This follows the definition by Roberta Klatzky and Susan J. Lederman[14]. Even though scanned materials are macrotextures, I will consider the reconstructed scan as a microscopic texture because the system can capture at a higher resolution of 0.014mm per pixel. In the realm of haptic, it is known that the microstructure can be felt by the finger which result in different feel of material finishes.[15] Hence, geometric modeling of the microstructure is important for haptic applications. There is also evidence of using a microscope to understand material in

[12] Klatzky and J. Lederman, "Multisensory Texture Perception."
[13] Moholy-Nagy and Hoffmann, *The New Vision: Fundamentals of Design, Painting, Sculpture, Architecture*; Montessori 1870-1952, *The Montessori Method : The Origins of an Educational Innovation : Including an Abridged and Annotated Edition of Maria Montessori's The Montessori Method*.
[14] Klatzky and J. Lederman, "Multisensory Texture Perception," 215.
[15] Campion, *The Synthesis of Three Dimensional Haptic Textures: Geometry, Control, and Psychophysics*, 22.

design education. In *The New Vision,* Moholy-Nagy uses a microscope to capture microphotograph of various material to provide a new perspective of material on a different scale.[16] Moholy-Nagy stated, "Such a photograph (microphotograph) as this reveals the infinite richness of different aspects of materials. The exact, sharply defined photograph is the best approach to a new education in materials…" Achim Menges also shows the importance of understanding material at a microscopic scale and he uses microscopic scale to inform the computational design processes at the object scale.[17]

This thesis aims to test whether the digital equivalent of the "sensory training" is beneficial to design education and practices. To understand the benefit of such system in cultivating explicit and tacit knowledge of material surface texture, the thesis must address, "**How can novel representation and simulation of real material texture through digital method enrich material knowledge and design processes?**" To tackle this question, this thesis examines a digital "sensory training" prototype system that encodes real material texture in a 3D model at a microscopic scale. Hence, it is necessary to think about **"How to best encode and decode expressive-sensorial dimension of material properties into the computer representation?"**

1.3 Biases of Computer Interfaces

Current computer graphical interfaces have come a long way since the invention of the computer. They have moved through various stages of interaction model and representation throughout the decades. According to Paul Dourish, the timeline for the historical model of computer interaction can be presented as follows: electrical, symbolic, textual, and graphical.[18] The interactions model suggested by Dourish are also afforded by different form representations developed that the time for the computer interface. Each interaction model can be mapped to a specific representation within the computer interface: electrical to a physical circuit, symbolic to punch/control cards, textual to

[16] Moholy-Nagy and Hoffmann, *The New Vision: Fundamentals of Design, Painting, Sculpture, Architecture*, 35–39.
[17] Menges, "Material Resourcefulness: Activating Material Information in Computational Design."
[18] Dourish, "Where the Action Is: The Foundations of Embodied Interaction," 5.

words/characters, and graphical to visual representation. At each stages of the representation, the system become more abstracted from the material basis of a computer to the codified abstraction of these logic gates through invention of assembly languages, modern high level programming languages, and abstracted graphical icons. Though the graphical interaction and representation prevail in the current model of interaction, many of these representations still coexist in our current computer as they are built upon one another.

Daniel Cardoso Llach show that the motivation of creating these geometrical data structure were part of the bigger ideal of bridging the distance between design and manufacturing at MIT laboratories such as Servomechanisms Laboratory (later known as Electronic Systems Laboratory) in the 1940s. [19] These geometrical encoding allows the form of the design object to be represented in an interactive graphical format and allows automation of machine instruction for Computer-Aided Manufacturing (CAM). Such motivation for the data structure brings certain affordances to the Computer-Aided Design (CAD) and CAM tools that allows a designer to emphasize the visual form of a design artifact compared to the other sensory cue afforded by material of a design artifact. These biases can still be seen in the current CAD system as many of these modeling tools only support visual mode communication through a "viewport" concept, influenced by the Ivan Sutherland's SketchPad.

This dominance of vision is not only part of the computer interfaces, but it is rooted in the history of Western culture. From science to philosophy, vision traditionally has been used as the primary mode of sensory perception used to understand and experience the world. Juhani Pallasmaa noted that philosopher, such as Aristotle and Descartes, regarded "vision as the most noble of the senses."[20] Neuroscience studies have also shown visual perceptual dominance and its influence on other senses. McGurk effect and Rubber hand illusion are two pieces of evidence of human over-reliance on the visual perception.[21]

[19] Cardoso Llach, *Builders of the Vision: Software and the Imagination of Design*, 42–43.
[20] Pallasmaa, *The Eyes of the Skin : Architecture and the Senses*, 18, 22.
[21] MCGURK and MACDONALD, "Hearing Lips and Seeing Voices"; Botvinick and Cohen, "Rubber Hands 'Feel' Touch That Eyes See."

1.4 Immaterial Experience of Digital Design Media

The computer graphical interface had directly affected many professions and effectively changed the process of their workflows. In the field of design, the graphical interface allows for the creation of Computer-Aided Design (CAD) software that has changed the workflow of design. Such abstractions of design into the visual representation have biased the Computer-Aided Design process towards the visual form and undermined the full materiality of design artifacts. This is not to say that design professions have forgotten the physicality of the design artifacts, rather, the focus of design in the digital realm afford by Computer-Aided tools has placed the emphasis the visual form.

Furthermore, the romantic ideal of CAD and CAM working "seamlessly" together has not yet been fulfilled as the current model does not fully account for the complex behavior of the material in the real world and the design process still relies heavily on the designer's tacit understanding of the material. Though there are improvement in simulation system for modeling material behavior through numerical methods such as Finite Element Method (FEM) and Computational Fluid Dynamics (CFD) by solving large sets of partial differentiation equations, the current CAD system as many of these modeling tools have a generic model of material for physical simulation and requires physical prototyping and material experimentation.

In additions to reductive modeling of material properties, material experiences through non-visual perceptual senses are also undermined in the Computer-Aided Design software and the computer interface. Malcolm McCullough points out this bias of ocularcentric computer interface by questioning, "What good are computers, except perhaps for mundane documentation, if you cannot even touch your work?"[22] Juhani Pallasmaa also criticizes this visual bias and immaterial experience in the context of architecture design, especially in the digital era.[23] From the biases of the computer

[22] McCullough, *Abstracting Craft: The Practiced Digital Hand*, 25.
[23] Pallasmaa, *The Eyes of the Skin : Architecture and the Senses*, 22.

interface, many of today's CAD software does not account for the various modes of perception in the interaction model.

We can trace this detachment of the mental sphere of design and material sphere of materials and tools in design practices back to Renaissance architect and theorist Leon Battista Alberti.[24] In addition, the invention of Computer Aided Manufacturing (CAM) further industrialized the hands-on craftsmanship by automating manufacturing. Tim Ingold attributes of the problem of "regression of the hand" to this form of machine automation by stating "The fingertip interacts with the machine, through the 'interface' of button or key, but its gestures do not correspond with the material movements…"[25] Both CAD and CAM enhance the effect of separating representation of artifacts and physicality of material in the field of design. McCullough echo this view by stating, "… CAD/CAM is just another in a series of workplace mechanizations already including … deskilling of handwork,…"[26] Such a split is created by abstracting design artifacts and automating the manufacturing which forgoes the physicality of material in the digital world. In Builders of the Vision, Daniel Cardoso Lach states, "With the subsequent advent of design automation as a research goal, and the pervasiveness of the metaphor of the digital as weightless and immaterial, any trace of the material and embodied origins of software automation would soon be forgotten."[27]

1.5 Significance

The advent of Computer-Aided Design (CAD) has further enforced the Albertian ideal of the designer's role as mainly operating within the mental sphere of design. The Albertian split has an effect on the design education and process where material is secondary to the idea and concept. Though materiality is still part of many design educations and processes, the computational tools a designer uses does not facilitate material understanding during the process of design. Rather, designers are implicitly applying

[24] Cardoso Llach, *Builders of the Vision: Software and the Imagination of Design*, 3.
[25] Ingold, *Making: Anthropology, Archaeology, Art and Architecture*, 123.
[26] McCullough, *Abstracting Craft: The Practiced Digital Hand*, 189.
[27] Cardoso Llach, *Builders of the Vision: Software and the Imagination of Design*, 36.

their knowledge of material while designing with these computational tools. Though there are a multitude of CAD tools to simulate material for the purpose of understanding material, they are abstract and generalized physical models of material. Besides the physical dimension of material in design, the expressive-sensorial dimension of material is also important in design. However, the limits of the computer interfaces in stimulating senses beyond sight and sound forces the current computational tools to ignore the expressive-sensorial dimensions of material. To incorporate both the objective dimension and expressive-sensorial dimension of materials, the CAD tools must include physical simulation for objective dimension and sensory stimulation through multisensory interfaces for expressive-sensorial dimension.

1.6 Expected Contribution

Even though CAD tools incorporate some material modeling such as physical simulation or material visualization through texture mapping, many of the elements of material are still missing in the system. However, the current model of physical simulation abstracts the material toward generalized form. Such generalized abstracted models do not account for the uniqueness of each material and generalized the same type of material into one category. In addition, many of the CAD tools only present the material in a visual representation through texture mapping for rendering. Such representations do not fully reveal the expressive-sensorial dimension of materials, as it does not incorporate the complex multisensory perceptual aspect of material.

This thesis will address the immaterial and sensory biases enforced in the computational design tools by creating a provocative prototype tool inspired by the Bauhaus “sensory training” to bring a new perspective of material knowledge. In this thesis, the focus will be on the material texture at a microscale because at this scale we can model the microstructure which can be felt by the hand (for expressive-sensorial dimension of material) and form a new understanding of material through the microstructures. We can see this tradition of looking at texture at the microscale in the Bauhaus tradition of material education through both sensory training (tactile exercises) and visual understanding of microscopic surface structure. Though such a scale of understanding

material is not novel, there are a few works in reconstructing 3D texture at this scale in design for cultivating material knowledge.

2. Background and Related Work

2.1 Digital Texture Representation

Digital texture representation is concerned with the abstraction of material texture in the form of bits which can be used for simulation, visualization, and analysis. There are various texture representations in digital formats, but each of these representations is useful for the very particular task described above. The method of representation described below includes statistical, light-based, and geometrical representations.

2.1.1 Statistical

The statistical representation of texture is a form of representation that describes texture as distribution and encodes them into the distribution function, histogram, density, and Fourier space representation.[28] In material science, texture can be represented by the orientation distribution function. The orientation distribution function represents the material texture as a distribution of crystal orientation in 3D space.[29] Such representation is useful for mathematically analyzing material texture at the scale of crystalline structure, however, it reduces the texture into a probability function that describe the crystalline orientation useful in analyzing material performance and properties. If material is textureless, it is described as having a random crystalline orientation; Hence, there is no dominant orientation.

Histograms, density plots, and Fourier analysis are also used in Image Processing, Computer Graphics, and Computer Vision to quantify texture as spatial distribution and directionality in the image. Intensity histograms are used to understand the contrast of the texture by putting the image pixel into 255 bins of pixel intensity. The intensity histogram allows us to see the distribution of the pixel and identify the vividness of the

[28] Matsuyama, Miura, and Nagao, "Structural Analysis of Natural Textures by Fourier Transformation"; Niblack et al., "QBIC Project: Querying Images by Content, Using Color, Texture, and Shape"; Tamura, Mori, and Yamawaki, "Textural Features Corresponding to Visual Perception"; Dana and Nayar, "Histogram Model for 3D Textures."
[29] Bunge, "3 - Orientation Distributions."

pattern.[30] The directionality histogram is created by computing the derivative of the image in both the x and the y and the image is then bin according to the gradient angle. The directionality histogram allows the user to identify the general orientation of the visual pattern through the orientation histogram.[31]

In pure statistical form, some statistical measure of texture includes mean, variance, standard deviation, skewness, uniformity, and average entropy of the grey-scale pixel value.[32] The mean represents the average intensity of the image. The variance and standard represent the gray-level contrast, which can be a descriptor of relative smoothness. The skewness represents the bias of the image toward the darker or lighter side of an image. The uniformity represents the overall flatness of the image;It is the maximum when all levels are equal. The entropy measures the variability of the image; it measures 0 for constant image. All the formula below is derived from Rafael C. Gonzales and Paul Wintz.[33]

[30] Niblack et al., "QBIC Project: Querying Images by Content, Using Color, Texture, and Shape."
[31] Niblack et al.
[32] Gonzales and Wintz, *Digital Image Processing (2nd Ed.)*, 667.
[33] Gonzales and Wintz, *Digital Image Processing (2nd Ed.)*.

$$mean = m = \sum_{i=0}^{L-1} z_i p(z_i) \quad (1)$$

$$variance = \mu_2(z) = \sum_{i=0}^{L-1} (z_i - m)^2 p(z_i) \quad (2)$$

$$standard\ deviation = \mu_1(z) = \sum_{i=0}^{L-1} (z_i - m)^1 p(z_i) \quad (3)$$

$$skewness = \mu_3(z) = \sum_{i=0}^{L-1} (z_i - m)^3 p(z_i) \quad (4)$$

$$uniformity = U = \sum_{i=0}^{L-1} p^2(z_i) \quad (5)$$

$$entropy = e = -\sum_{i=0}^{L-1} p(z_i) \log_2 p(z_i) \quad (6)$$

$$where\ m\ is\ the\ mean,$$

$$L\ is\ the\ total\ number\ of\ bins,$$

$$z_i\ is\ the\ gray\ level\ of\ ith\ bins,$$

$$m\ is\ the\ mean$$

$$p(z_i)\ is\ the\ corresponding\ frequency\ of\ z_i\ gray\ level$$

Besides the 2D image histogram, there are 3D histogram models that use various viewing positions and light sources.[34] The angle of both the camera and light source affects the isotropic texture and requires multiple images to capture this effect. Using multiple images, the histogram model can be created for each of the images, and one material can be modeled using various viewing and light positions. Each of the viewing and light

[34] Dana and Nayar, "Histogram Model for 3D Textures."

position are parametrised as the polar coordinate system which includes azimuth and zenith angles. The combination of these histograms makes up the histogram model of 3D texture. However, histogram representation is limited because spatial information is abstracted. For example, if there are 50% white pixel (255) and 50% black pixel (0). Figure *4* shows multiple images that correspond to the same histogram.

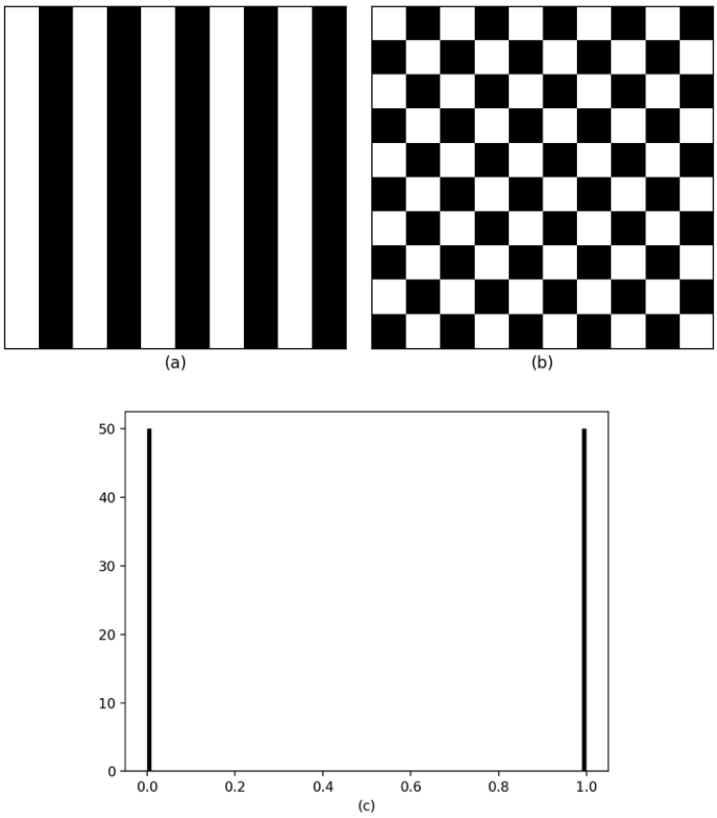

Figure 4: Different images with the same histogram distribution

Similarly, the Fourier spectrum is another form of analysis that could describe the periodicity and frequency of image intensity value.[35] The 2D Fourier transforms the x and y spatial domain of the image to u, v frequency domain. The center of the Fourier image corresponds to the low frequency component, and the higher frequency is the map away from the center.

[35] Matsuyama, Miura, and Nagao, "Structural Analysis of Natural Textures by Fourier Transformation."

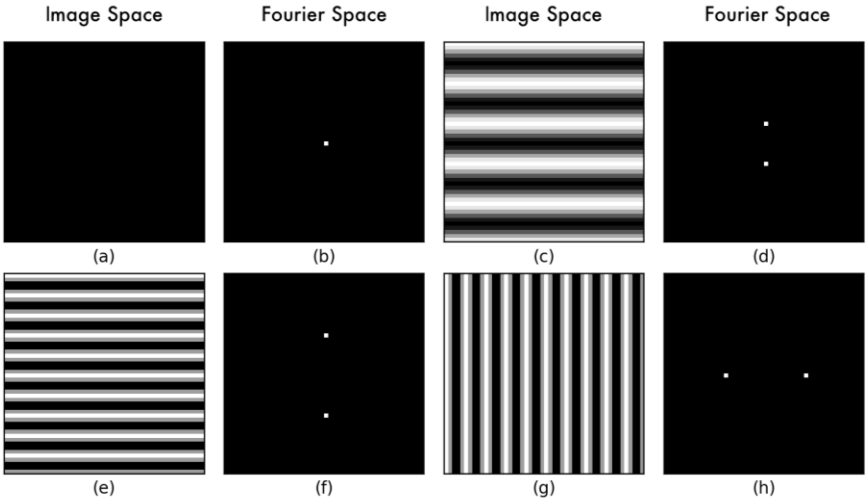

Figure 5: Simple 2D Fourier Transform

Figure *5*(b) shows a Fourier transform of the solid image Figure *5*(a). The center of the Figure *5*(b) is bright because solid image have no frequency (0 Hz). Figure *5*(d) and (f) are the Fourier transform of (c) and (e) respectively. Figure *5*(d) shows two dots that are closer to the center because the image, Figure *5*(c), has a lower frequency. Figure *5*(f) shows two dots which are further out from the center as the image, Figure *5*(e), has a higher frequency. Figure *5*(g) shows the 90° rotated image of Figure *5*(e), the Fourier spectrum also encodes such rotation, hence, the general spatial orientation can be still analyze through Fourier spectrum. The statistic-based representation is useful for quantitatively analyzing the properties of surface texture and it can statistically synthesize surface geometry close enough to the real texture but never the real geometry of material.

2.1.2 Light-Based

The light-based representation is an important form of representation used in the field of computer graphics for rendering. The light-based representation model abstract the material appearance of the surface into the function of irradiance and radiance with the polar coordinate system. One of the earliest such representations was the Bidirectional

reflectance distribution function (BRDF), introduced by Fred Nicodemus.[36] The BRDF function is defined as follows:

$$BRDF: f(\theta_i, \phi_i, \theta_r, \phi_r) = \frac{L(\theta_r, \phi_r)}{E(\theta_i, \phi_i)} \quad (7)$$

$$where\ \theta_i, \theta_r\ are\ the\ zenith\ angles,$$
$$\phi_i, \phi_r\ are\ the\ azimuth\ angles,$$
$$i\ and\ r\ are\ incident\ ray\ and\ reflect\ ray,$$
$$L\ is\ the\ radiance\ of\ the\ surface,$$
$$E\ is\ the\ irradiance\ of\ the\ surface.$$

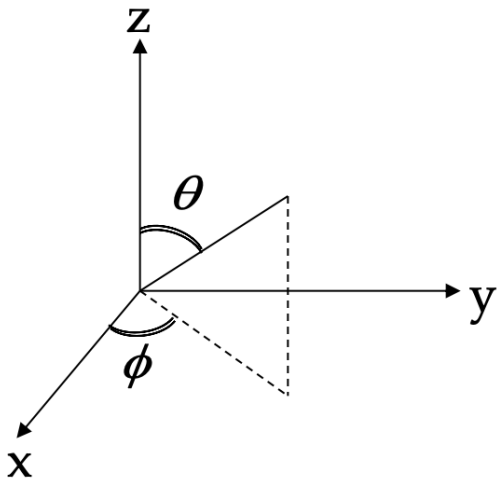

Figure 6: Polar Coordinate System

The BRDF returns the ratio of reflected radiance and incident irradiance on a given surface. The radiance is the amount of light being reflected by the surface and the irradiance is the amount of light received by the surface. These parameters relate to the surface normal as the zenith angles use normal as the origin or 0°. This representation shows how light is reflected at an opaque surface and abstract the surface with its interaction with light.

[36] Nicodemus, "Directional Reflectance and Emissivity of an Opaque Surface."

However, there have been extensions to BRDF, such as the Bi-directional texture function (BTF).[37] BRDF works well in the coarse scale where local intensity is uniform but at a fine scale, the texture surface geometry give rise to local intensity which changes the appearance of the material at a different view.[38] BTF was developed to render material texture at a finer scale but require less computational cost than the rendering geometry of the surface. BTF calculates the surface reflectance at every x, y position of the pixel and the average of all x and y positions is the BRDF function. This representation models the variation changes in each of the x, y positions with respect to the viewing and lighting direction.

$$BTF: f(x, y, \theta_i, \phi_i, \theta_r, \phi_r) = \frac{L(x, y, \theta_r, \phi_r)}{E(x, y, \theta_i, \phi_i)} \quad (8)$$

$$where\ x, y\ are\ the\ point\ on\ the\ surface\ where\ the\ light\ ray\ hit,$$
$$\theta_i, \theta_r\ are\ the\ zenith\ angles,$$
$$\phi_i, \phi_r\ are\ the\ azimuth\ angles,$$
$$i\ and\ r\ are\ incident\ ray\ and\ reflect\ ray,$$
$$L\ is\ the\ radiance\ of\ the\ surface,$$
$$E\ is\ the\ irradiance\ of\ the\ surface.$$

Both the BRDF and BTF abstract the material geometry and its normal into the function of light position, viewing position, radiance, and irradiance. Though this information can recover the geometry using methods such as Photometric Stereo (mentioned in Section 2.2.3.3), it is mainly useful for rendering and visualizing the surface texture and material appearance. One advantage of the light-based representation is that it does not require the large space for storing the geometry but it stores a smaller abstracted ratio which are useful for rendering. However, this form of representation is only useful for visual representation and not for haptic applications.

[37] Dana et al., "Reflectance and Texture of Real-World Surfaces."
[38] Koenderink and van Doorn, "Illuminance Texture Due to Surface Mesostructure."

2.1.3 Geometric

Texture in the geometric form can be seen as the normal map, depth map, 3D mesh, and 3D point cloud. The geometric representation will preserve the spatial information. For example, the normal map preserves the normal of the surface at each x, y location, but it abstracts the surface geometry of the texture into the field of normal vectors (See Figure 7). The depth map or height map preserves the elevation data of the geometry in a discrete form (See Figure 8). The height map encodes how far the pixel is from the viewpoint of the camera. The 3D mesh and 3D point cloud have a bigger degree of freedom as it full encode the location of the texture in the 3D space and does not project them into 2D height map or convert them into normal map (See Figure 9 and Figure 10).

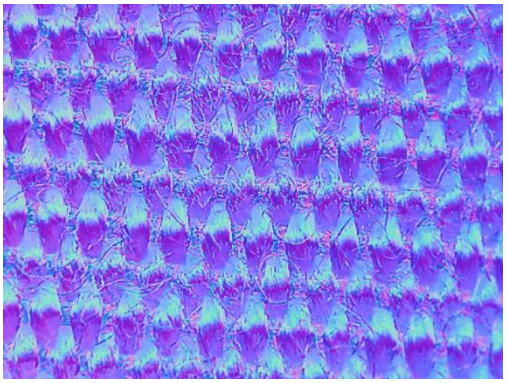

Figure 7: Normal Map

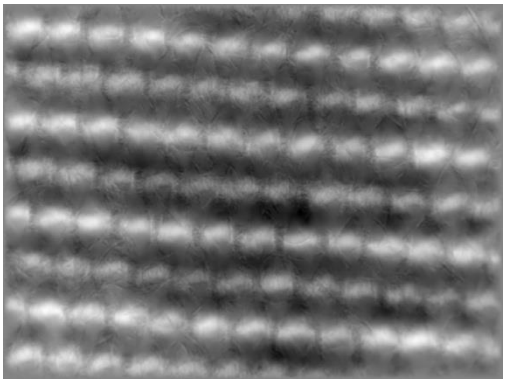

Figure 8: Depth Map

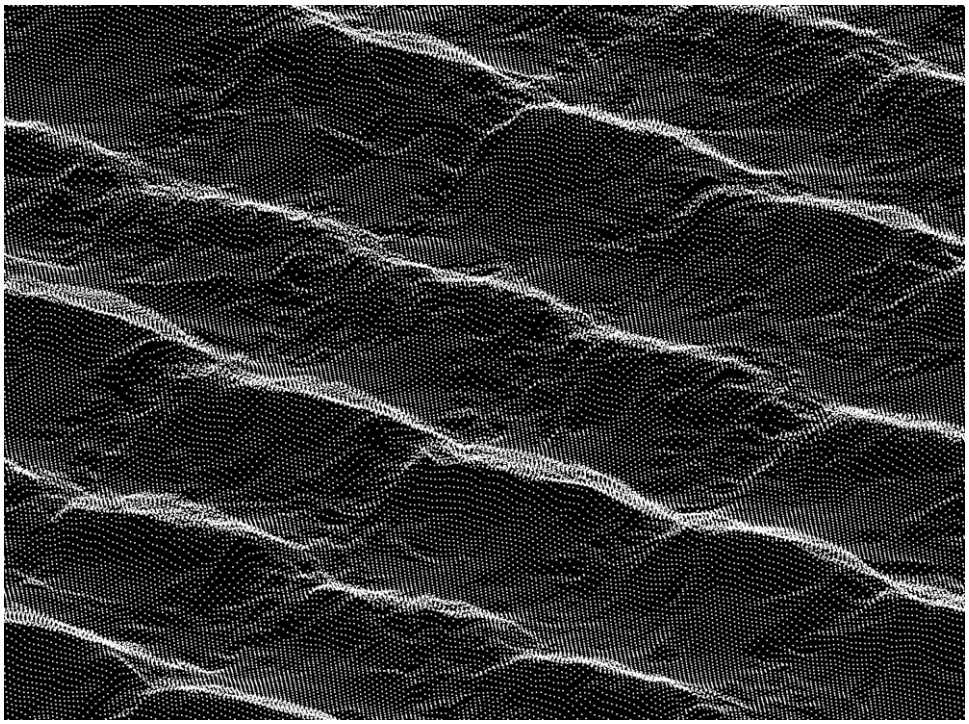

Figure 9: Point Cloud

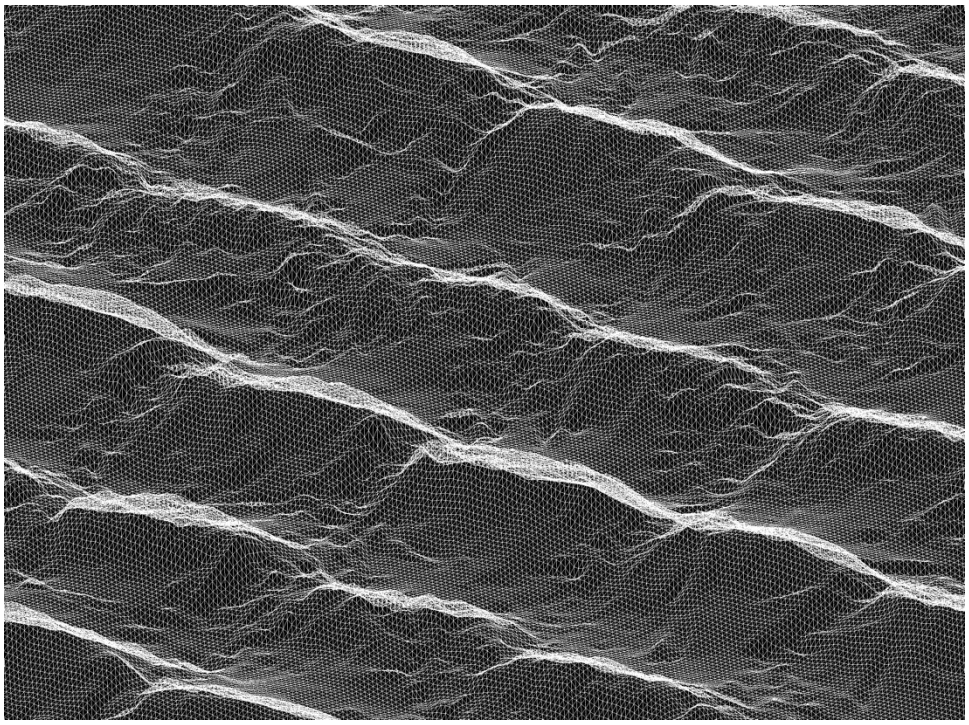

Figure 10: Mesh

Such geometrical modeling is used in many texture mapping contexts. Texture mapping was invented by Edwin E. Catmull in his 1974 Doctor of Philosophy dissertation.[39] Texture mapping involves simply mapping the appearance of the material onto the geometry without considering the geometrical deformation. Bump mapping is another texture rendering technique and was introduced in 1978 by James F. Blinn.[40] Bump mapping uses the height map or normal map to model the effect of light in the u, v texture space but it does not deform the original geometry of the 3D object. These texture mapping are great for rendering the visualization of the object, but it is harder to use for haptic rendering as it requires translation of representations. An alternative technique, such as displacement mapping, can be used to map the texture onto the 3D object. Displacement mapping deform the geometry of the original mesh; It does not only use abstracted light models but encodes the geometry of the texture. Hence, it is useful when trying to create haptic rendering because displacement mapping changes the surface of the 3D object. With the texture truly visible onto the 3D form, it would be easier to calculate the force and friction generated by the texture. The displacement map is ideal for both creating realistic rendering or 3D printing with such a change in texture. One of the disadvantages of displacement mapping is that it will destructively modify the original form of the mesh and require high computational cost.

2.2 Microscopic Texture Modeling

Modeling the texture of real materials can be done through various methods. Three of the methods that was considered for in this thesis includes: contact-based sensing, data-based modeling, and computer vision.

2.2.1 Contact-Based Sensing

Robert W. Patterson et al. develops one of the earlier contact-based sensing for touch sensing.[41] The system uses two Polyvinylidene fluoride (PVDF) transducers, with electrodes layer on either side of the PVDF transducer, which are then bonded by epoxy

[39] Catmull, "A Subdivision Algorithm for Computer Display of Curved Surfaces."
[40] Blinn, "Simulation of Wrinkled Surfaces."
[41] Patterson and Nevill, "The Induced Vibration Touch Sensor – a New Dynamic Touch Sensing Concept."

(See Figure *11*). The PVDF transducer picked up the ultrasonic vibration and two PVDF transducers were used to increase the sensitivity.

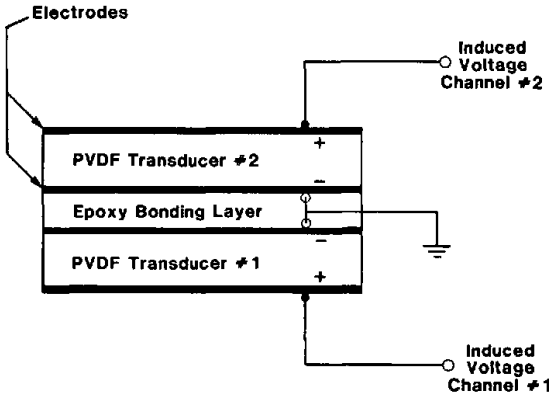

Figure 11: PVDF Transducer Sensor Design, reprinted from "*The induced vibration touch sensor - a new dynamic touch sensing concept*"[42]

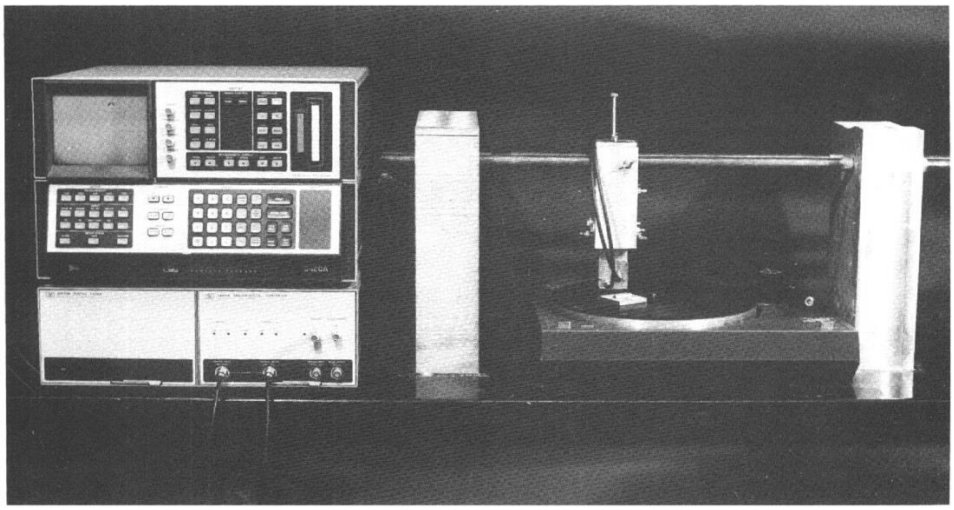

Figure 12: Prototype Probes and Experimental Setup, reprinted from "*The induced vibration touch sensor - a new dynamic touch sensing concept*"[43]

Contemporary contact-based force sensing follow similar setup for texture recognition but it added additional sensors for more information. It uses sensor fusion data of the force sensor, PVDF module, and strain gauge to gauge the 3D contact force applied (See

[42] Patterson and Nevill.
[43] Patterson and Nevill.

Figure 13).[44] In addition to the PVDF which senses vibration, this setup fuses the force applied by the user through a force sensor. Strain gauge are used to measure tangential forces. They also found that the laser displacement sensor, an optic based system, was able to capture more detail compared to their force-based pen.[45] They experimented on average grain sizes of 16, 23, 68, and 140 μm. At every size, the laser displacement sensor performs better than the contact force sensing. The resolution of the profile was about 0.2mm.

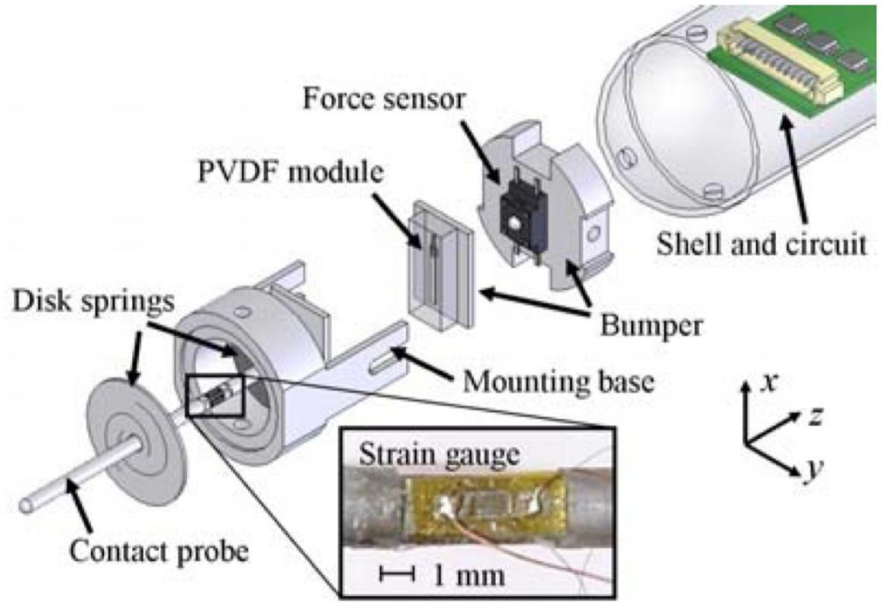

Figure 13: Prototype Pen Sensor Design, reprinted from "*The induced vibration touch sensor - a new dynamic touch sensing concept*"[46]

Another setup not using PVDF is from Heather Culbertson et al. which uses magnetic tracking sensor, accelerometer, and force sensor.[47] The magnetic tracking system was used to track the tool's position and orientation at 240Hz, the resolution of 0.5mm, and 0.1 degrees. Six-axis force sensor were used to measure the force and torque of the

[44] Ye et al., "Profile-Based Roughness Discrimination with Pen-Type Texture Sensor."
[45] Ye et al., 798–99.
[46] Ye et al., "Profile-Based Roughness Discrimination with Pen-Type Texture Sensor."
[47] Culbertson, Delgado, and Kuchenbecker, "One Hundred Data-Driven Haptic Texture Models and Open-Source Methods for Rendering on 3D Objects."

contact tip. The accelerometer were used to record the vibration or the frequency of the contact tip.

All contact force sensing is limited by the size of the contact tip and the sampling rate of the sensors. Though it can measure non-static physical motion of the texture, it can only measure one cross-section of the surface texture at one time. Contact-based sensor is useful for measuring material texture where fiber is constantly moving while interacting with them but it does not have good precision and resolution when comparing to vision based methods.

2.2.2 Statistical-Based Modeling

Statistical-Based modeling had been used in both texture synthesis and analysis. Most of the statistical-based modeling uses image based method to understand the distribution of the intensity for 2D image case and view and light dependent distribution of the image intensity for 3D texture cases. 3D Texture Surface Modeling by Kristin J. Dana and Shree K. Nayar, uses images from multiple views and illuminations to create the BTF dataset (See Figure 14).[48] These BTF dataset was used to model texture using the histogram and correlation modeling. The bidirectional histogram captures the image intensity distribution from multiple views and illuminations, and this creates a statistical model for a single material. Histogram modeling allows the data size to shrink from the image size $\times$ number of images to just the coefficient of the histogram distributions to describe the texture.

[48] Dana and K. Nayar, *3D Textured Surface Modeling*.

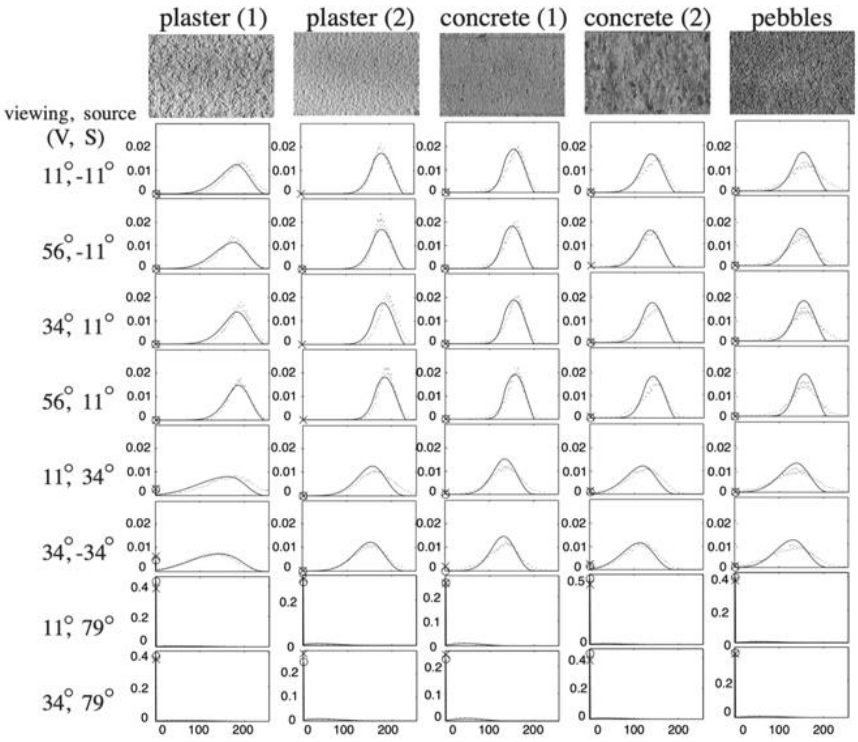

Figure 14: 3D Textured Histogram Modeling, reprinted from "*3D Textured Surface Modeling*"[49], All view are at 180° azimuth angle with varying zenith angle.

The histogram model in its raw form cannot synthesize the texture but with the combination of a linear filter bank and collection of a histogram from these filter bank result, it is possible to statistically synthesize texture based on a sample image. David J. Heeger and James R. Bergen show this method of using a linear filter bank at multi-resolution and matching the histogram of the response to these linear filters provides notably good results (See Figure 15).[50]

[49] Dana and K. Nayar.
[50] Heeger and Bergen, "Pyramid-Based Texture Analysis/Synthesis."

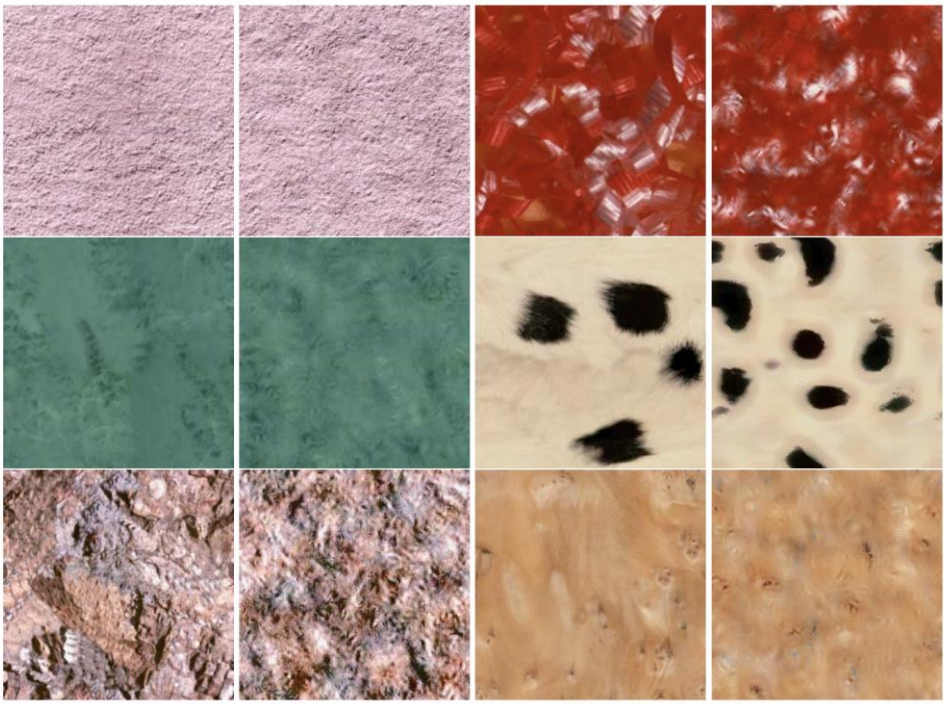

Figure 15: Results, reprinted from "*Pyramid-Based Texture Analysis/Synthesis*"[51]; Left image: Original, Right Image: Synthetic

Another method of synthesis uses a Markov Random Field (MRF) to synthesize and model texture given a sample image (See Figure *16*).[52] MRF is a graphical model of a joint probability distribution. They assume that "the probability distribution of brightness values for a pixel given the brightness values of its spatial neighborhood is independent of the rest of the image."[53] With this method, they were able to recreate the texture through a probabilistic model by sampling the image and enlarging them. The MRF could encode the periodicity of the texture and solve it through multiple iterations.

[51] Heeger and Bergen.
[52] Efros and Leung, "Texture Synthesis by Non-Parametric Sampling."
[53] Efros and Leung.

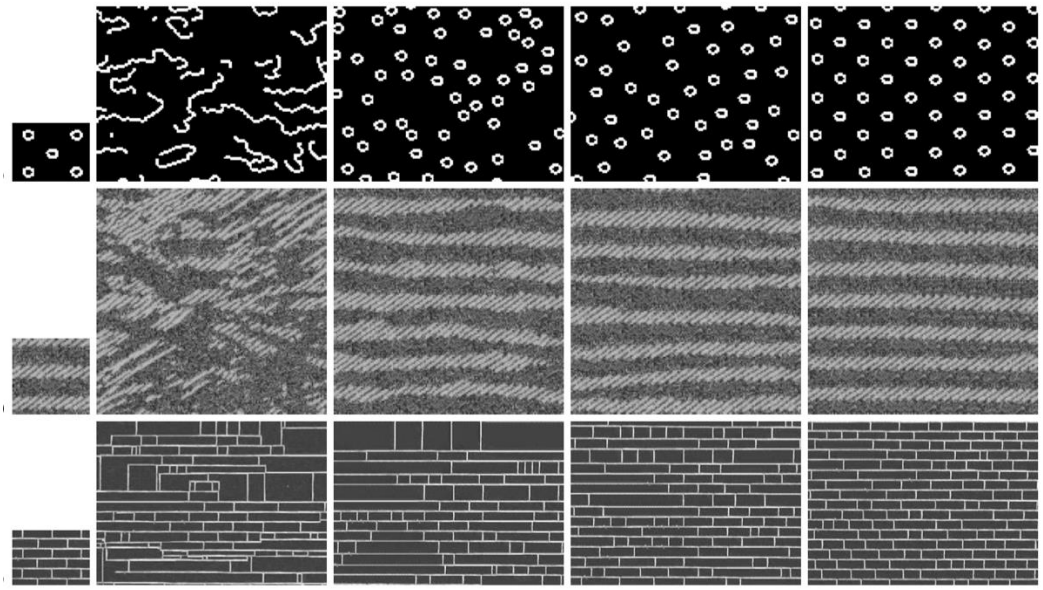

Figure 16: Result, reprinted from "*Texture Synthesis by Non-parametric Sampling*" with various sampling window sizes[54]; Left to Right: sample texture, synthesized image using windows of width 5, 11, 15, and 23 pixels, respectively.

Besides 2D image texture synthesis and analysis, there are also methods to synthesize 3D texture using stochastic methods. Jason P. Fritz and Kenneth E. Barner show methods to use the probability distribution function, Fourier spectral synthesis, and filtering to produce synthetic 3D haptic texture.[55] Though Fritz and Barner did not use external sample, their method can be used on sampled 3D texture to synthesize similar but larger 3D texture.

The advantage of statistical modeling the texture is that it reduces the texture to just a distribution and probability from an image. As mentioned above in statistical representation (Section 2.1.1), histogram distribution and statistics, it can be used to understand high-level concept such as smoothness. It can synthesize a new texture based on the sample texture. However, it does not represent the real material texture of the particular object as it is stochastically produced.

[54] Efros and Leung.
[55] Fritz and Barner, "Stochastic Models for Haptic Texture."

2.2.3 Computer Vision-Based Geometric Modeling

Computer Vision-Based modeling includes using computer vision methods to reconstruct the 3D shape of the surface texture. There are various methods to extract 3D shapes, such as multi-view stereo[56], structured light (laser and coded structured light)[57], photometric stereo[58], and other Shape-from-X methods.

2.2.3.1 Multi-View Stereo

Multi-view stereo uses two or more camera views to triangulate features in the image space (See Figure 17). On the microscopic scale, it is hard to get two cameras focused on the same area, and it is costly to create a system that does so.

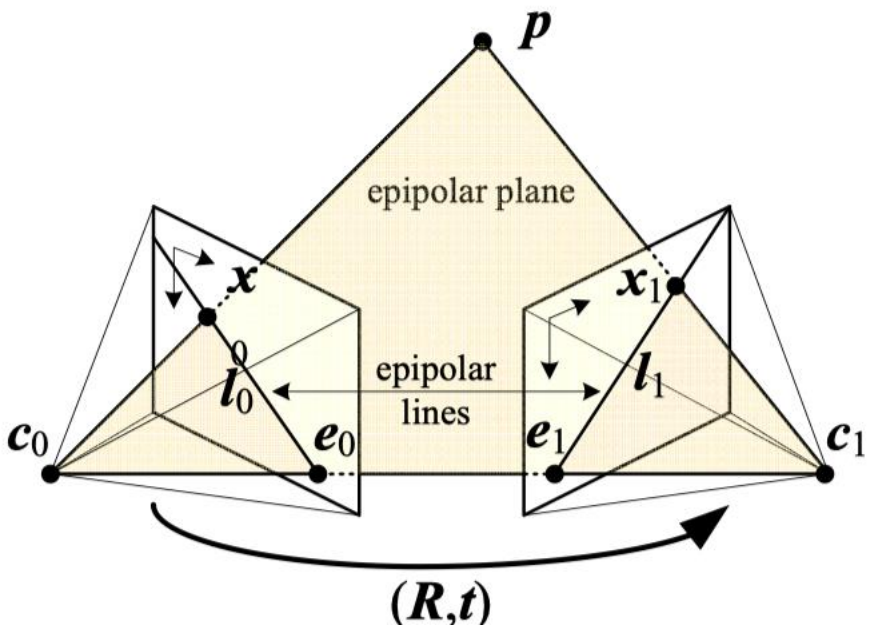

Figure 17: Multi-view Stereo Representation, reprinted from "*Computer Vision: Algorithm and Applications*"[59]

[56] Fua, "A Parallel Stereo Algorithm That Produces Dense Depth Maps and Preserves Image Features."
[57] Levoy et al., "The Digital Michelangelo Project: 3D Scanning of Large Statues."
[58] Woodham, "Photometric Stereo: A Reflectance Map Technique For Determining Surface Orientation From Image Intensity."
[59] Szeliski, *Computer Vision: Algorithms and Applications*, 471.

The multi-view stereo system involves finding a corresponding point and matching it to the point in the second camera. The correspondence problem is especially hard without unique features, so it does not work well for the object with a regular pattern or textureless object. For the two reasons above, a multi-view stereo does not work well for microscopic texture reconstruction.

2.2.3.2 Structured light

Structured light reconstruction involves using a laser light stripe or projecting coded structure onto the surface.

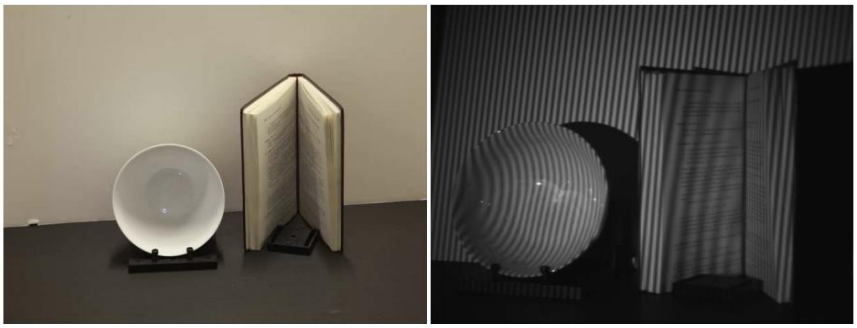

Figure 18: Coded Structured Light, reprinted from "*A parallel stereo algorithm that produces dense depth maps and preserves image features*."[60]

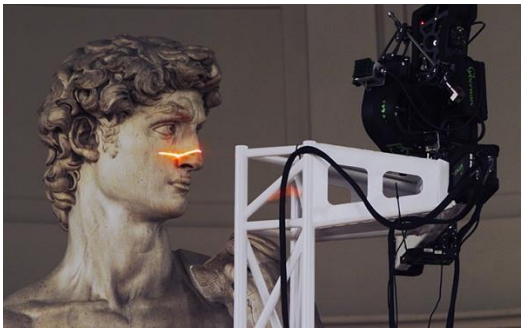

Figure 19: Laser Light Stripe Structured Light, reprinted from "*The digital Michelangelo project: 3D scanning of large statue*."[61]

[60] O'Toole, Mather, and Kutulakos, "3D Shape and Indirect Appearance by Structured Light Transport."
[61] Levoy et al., "The Digital Michelangelo Project: 3D Scanning of Large Statues."

The structured light method uses light projection onto the matte surface and sees the way the light distorts to recover the shape (See Figure 18 and Figure 19). This works well at object scale but the structured light setup at the microscopic scale will requires complex setup and expensive small equipment to let the laser or light strip through the surface. It is not feasible to create a low-cost system with such setup in mind.

2.2.3.3 Photometric Stereo

Photometric Stereo uses various lighting conditions and reflectance models to recover the geometry of the object. Classical photometric stereo assumes that the reflectance model follows a Lambertian model, which assumes that the surface is matte.[62] It assumes a model where the light, normal, and pixel intensity are linear. Equation (9) shows the linear modeling of the Lambertian surface. Photometric stereo uses this linear equation and inverse it to recover the normals.

$$I = \rho N \cdot L \qquad (9)$$

$$where\ I\ is\ Image,$$
$$\rho\ is\ the\ diffuse\ albedo,$$
$$N\ is\ Normal,$$
$$and\ L\ is\ the\ Light\ Vector$$

[62] Woodham, "Photometric Stereo: A Reflectance Map Technique For Determining Surface Orientation From Image Intensity."

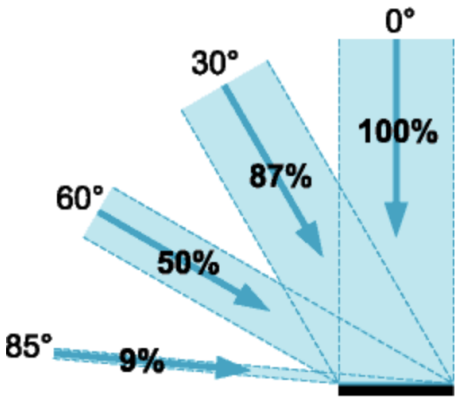

Figure 20: Lambert's cosine law Relief texture, reprinted from "*Light Measurement Handbook*"[63]

In the Lambertian model, the photometric stereo follows Lambert's cosine law.[64] The Lambert's cosine law states that the radiant intensity observed from a diffuse surface is directly proportional to the cosine angle between surface normal and incident light (See Figure 20). In layman's term, the light is highest when the angle is 0° and lowest when the angle is 90°.

The classical photometric stereo at an object scale assumed that: 1) light sources are far enough that the intensity is even on the captured image, 2) projection is orthographic, 3) surface is a uniform Lambertian reflectance, and 4) there are no shadows, highlights, occlusion or interreflection.[65] In the object scale, the first two assumptions can be usually tackled using the simple method as space is usually not a big limitation and camera calibration could be done with a checkerboard pattern to transform perspective to orthographic projection. In the micro-scale photometric stereo, the assumption light sources are far could be harder to fulfilled as there is a physical form factor limitation of a microscope. This causes the problem of spatially varying illumination in the captured image, which could create an error in 3D shape reconstruction.

[63] Ryer, Light, and Light, "Light Measurement Handbook."
[64] Ryer, Light, and Light.
[65] Woodham, "Photometric Stereo: A Reflectance Map Technique For Determining Surface Orientation From Image Intensity."

Some early work in microgeometry recovery work uses the specular effect of material to find the texture relief using specialize setup with a concave parabolic mirror and a point light source achieving 0.1mm spatial resolution (See Figure 21).[66] The system does not encounter spatially varying illumination because they could place the light source far enough away as the setup was big and it does not produce a high spatial resolution. Similarly, Sunghwan Shin and Seungmoon Choi were able to place the point light source far enough, so it does not have a spatially varying illumination effect.[67]

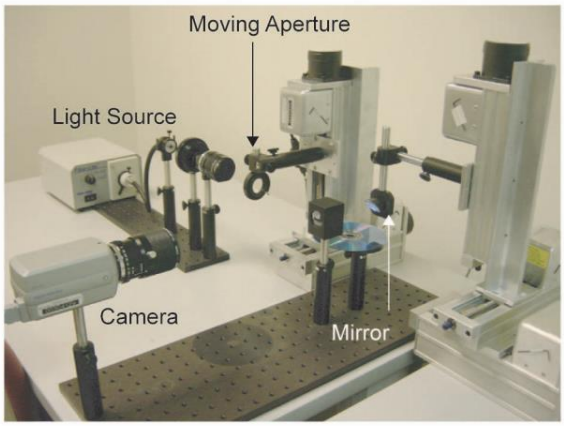

Figure 21: Texture Capture Setup, reprinted from *"Relief texture from specularities"*[68]

Another recent method in capturing microgeometry uses an elastomeric sensor that has a fixed known BRDF to reconstruct surface texture (See Figure 22).[69] Micah K. Johnson et al. could model the spatially varying illumination and inter-reflections of glass by using a quadratic model derived from a truncated spherical-harmonic shading model. This nonlinear model helps correct the error from the linear photometric stereo methods. However, the elastomeric sensor capture the microgeometry of the object with the pressure which works on many surfaces, however, the pressure could cause a shift in the anisotropic texture of fabric and furs.

[66] Wang and Dana, "Relief Texture from Specularities."
[67] Shin and Choi, "Geometry-Based Haptic Texture Modeling and Rendering Using Photometric Stereo."
[68] Wang and Dana, "Relief Texture from Specularities."
[69] Johnson et al., "Microgeometry Capture Using an Elastomeric Sensor."

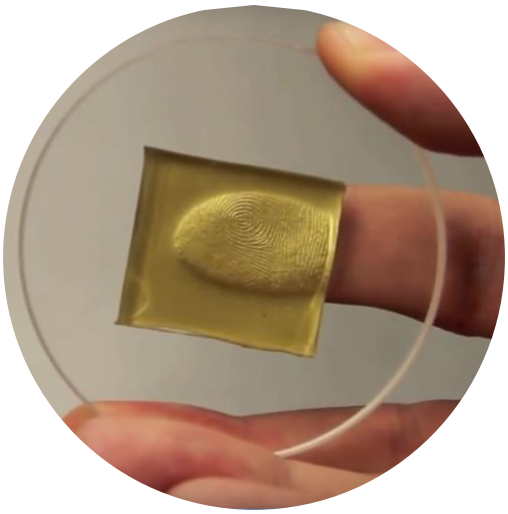

Figure 22: Elastomeric sensor to create a fixed albedo, reprinted from "*Microgeometry capture using an elastomeric sensor*"[70]

Both of the methods above require complex and costly setup and special materials to perform the reconstruction. To apply the technology to the material classification and reconstruction of the textile surface, researchers have created a low-cost DIY variant of the close range photometric stereo[71]. In these low-cost approaches, spatially varying illumination is a big issue in producing accurate 3D reconstruction. Christos Kamporuis et al. handle this by using a 2x2 grid chrome ball to calibrate the light and interpolate the light vectors at each pixel.[72] Dimitris Gorpas et al. approach the problem in a simpler method by flat-fielding using white card images in various illumination.[73]

2.3 Texture Haptic Rendering

Haptic simulation can be done through an active and passive feedback system. An active system uses actuators while the passive system relies on real material objects. Under an

[70] Johnson et al.
[71] Gorpas, Kampouris, and Malassiotis, "Miniature Photometric Stereo System for Textile Surface Structure Reconstruction"; Kampouris et al., "Fine-Grained Material Classification Using Micro-Geometry and Reflectance BT - Computer Vision – ECCV 2016."
[72] Kampouris et al., "Fine-Grained Material Classification Using Micro-Geometry and Reflectance BT - Computer Vision – ECCV 2016."
[73] Gorpas, Kampouris, and Malassiotis, "Miniature Photometric Stereo System for Textile Surface Structure Reconstruction."

active system, it can be further divided into physical systems and electrical systems. In the physical system, the haptic display will use physical forces such as sound, air, magnetic, and mechanical force. In an electrical system, it uses the property of electricity and receptors on the skin to simulate the haptic feedback. Creating a texture-based haptic display is especially hard when using physical forces because of the limited spatial resolution of the mechanical actuators. The finer spatial resolution required by texture must use electrovibration, electrostatic, and electrotactile (electrocutaneous).

2.3.1 Physical Actuation

Physical actuation haptic rendering hardware uses motors to drive an array of tactile pins and reorient the surface of the tactile pin. Hrvoje Benko et al. developed two systems: NormalTouch and TextureTouch which uses servo motor to actual the tactile pins.[74] Figure 23 and Figure 24 show the prototype system of NormalTouch and TextureTouch, respectively.

Figure 23: NormalTouch, reprinted from "*NormalTouch and TextureTouch: High-Fidelity 3D Haptic Shape Rendering on Handheld Virtual Reality Controllers*"[75]

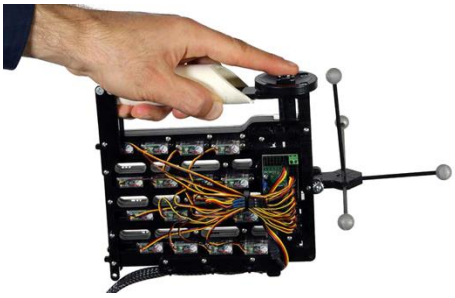

Figure 24: TextureTouch, reprinted from "*NormalTouch and TextureTouch: High-Fidelity 3D Haptic Shape Rendering on Handheld Virtual Reality Controllers*"[76]

The NormalTouch will angle the plate according to the shape in the virtual world and it use Interlink Electronics FSR-402, off-the-shelf force transducer, to detect touch. The

[74] Benko et al., "NormalTouch and TextureTouch: High-Fidelity 3D Haptic Shape Rendering on Handheld Virtual Reality Controllers."
[75] Benko et al.
[76] Benko et al.

TextureTouch uses small servo motors (HiTec HS-5035HD) to drive each of the tactile pins.

Limitations of the physical actuation system include bulkiness and low resolution. As you can see from Figure 24, it requires 16 servos to drive a 4x4 grid of tactile pins. The 4x4 grid is a low resolution, and it is not feasible to create a high resolution tactile physical actuation system without using tiny motors.

2.3.2 Electrostatic / "Electrovibration"

One implementation of electrostatic uses a thin layer of indium tin oxide (ITO) on top the screen and it is cover wiith a silica on top of the ITO.[77] Figure *25* shows the schematic of the implementation.

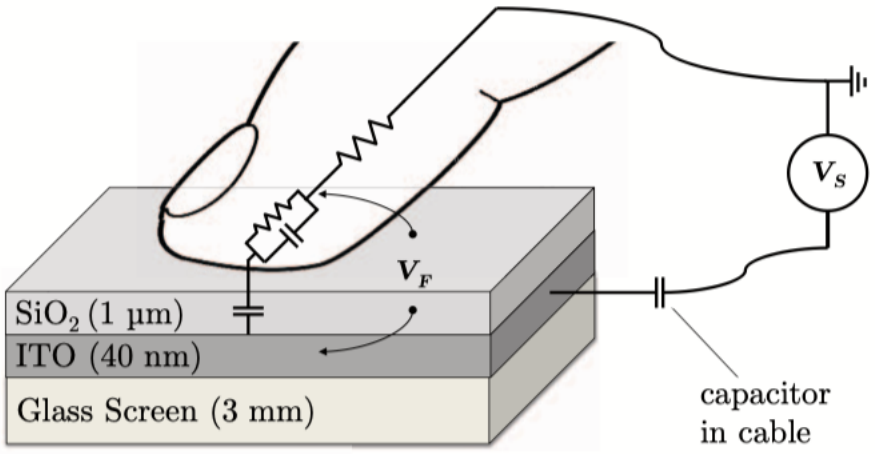

Figure 25: Electrostatic System Schematic, reprinted from "*Fingertip Friction Modulation due to Electrostatic Attraction*"[78]

This system generates an electrostatic force on the finger when "potential drop from the ITO to the conducting tissue beneath the stratum corneum (outer layer of skin)."[79] The

[77] Meyer, Peshkin, and Colgate, "Fingertip Friction Modulation Due to Electrostatic Attraction."
[78] Meyer, Peshkin, and Colgate.
[79] Meyer, Peshkin, and Colgate.

silica and stratum corneum acts as an insulator in series; it does not directly interact with the user's mechanoreceptive afferent nerve. The electrodes and finger as conductive skin create an electrical force field that can simulate friction. The electrostatic display, as opposed to electrovibration, runs the current through the user's body when touching the polymer surface.

Olivier Bau et al. differentiated the electrovibration from electrostatic by stating that the electrostatic have an intermediate element (indirect) while electrovibration does not (direct).[80] This literature review consider both electrostatic implementation above and electrovibration proposed by Olivier et al. to be the same as there are no intermediate elements in the electrostatic implementation suggested by David J. Meyer et al. (See Similarity between Figure 25 and Figure 26).

The discovery of electrovibration dates back to 1953 when Edward Mallinckrodt, A. L. Hughes, and William Sleator, Jr. accidentally discovered the effect of friction induced by electricity.[81] Mallinckrodt et al. found that when the finger dragged over a conductive surface with an insulating layer on a 110V signal, there is a lack of smoothness. Mallinckrodt et al. successfully implement a friction-based textural display. Recent attempt to research the effect was by Disney Research, where they implement the idea to bring textural haptic feedback to the touchscreen (See Figure 26).[82] The frequency and amplitude modulation of the AC voltage signal will change the friction on the touch surface. The frequency directly affects the smoothness of the texture, where the low frequency is perceived as rougher than a higher frequency. The amplitude modulation effect is dependent on the frequency, at the higher frequency and higher amplitude feel smoother while at the lower frequency and higher amplitude feel sticky.[83] The advantage of the electrovibration is that it does not pass the current through the body of the user.

[80] Bau et al., "TeslaTouch: Electrovibration for Touch Surfaces."
[81] Mallinckrodt, Hughes, and Sleator, "Perception by the Skin of Electrically Induced Vibrations."
[82] Bau et al., "TeslaTouch: Electrovibration for Touch Surfaces."
[83] Bau et al., 4.

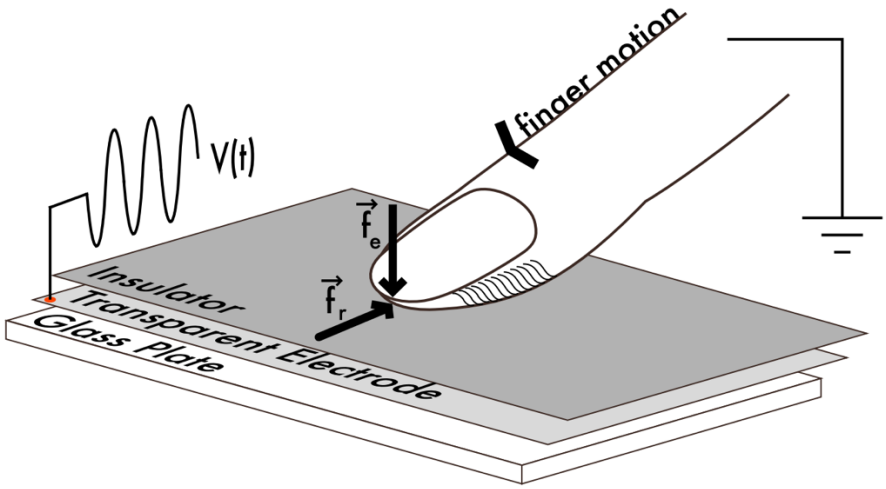

Figure 26: Electrovibration Schematic, reprinted from "*TeslaTouch: Electrovibration for Touch Surfaces*"[84]

The disadvantage of electrostatic/electrovibration implementation is that when the humidity on the skin is different, the conductivity of the skin fluctuates, producing various haptic feedbacks. It also requires that the finger must be dragged on a conductive surface, and it cannot simulate the texture if no physical force is applied.

2.3.3 Electrotactile

The electrotactile or also known as electrocutaneous uses electricity to directly stimulate the afferent nerve, which sends the signal directly to the central nervous system bypassing the physical stimulation. The electrotactile display could be traced back to the Robert M. Strong and Donald E. Troxel in 1970.[85] One of the contemporary implementations uses only three electrodes to stimulate the afferent nerve on the finger and augment the texture of real materials.[86]

[84] Bau et al., "TeslaTouch: Electrovibration for Touch Surfaces."
[85] Strong and Troxel, "An Electrotactile Display."
[86] Yoshimoto et al., "Roughness Modulation of Real Materials Using Electrotactile Augmentation BT - Haptics: Neuroscience, Devices, Modeling, and Applications."

Shunsuke Yoshimoto et al. were able to fuse and augment the texture of real objects by directly modulating nerve activity onto afferent nerves bypassing the mechanical stimulation of the mechanoreceptors at the finger (See Figure 27).[87] They did not modulate the frequency of the voltage signal but modulate the pulse density of the electrical stimulus. The signal has a pulse width of 200 μs and the electrical pulse ranges from 1 to 100 pulses per second (pps). They also control the pulse amplitude to account for the finger pressure on the object. The pulse density increases according to the finger velocity and texture and they found the pulses send were similar in neurophysiological level to sinusoidal mechanical stimulus.

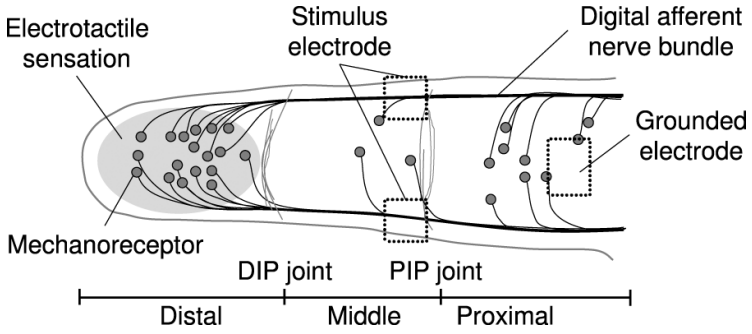

Figure 27: Position of electrode placement on the afferent nerves, reprinted from "*Material Roughness Modulation via Electrotactile Augmentation*"[88]

For the experiment, they could fuse and augment texture sensation on 6 different materials: sandpaper, wood, velcro tape, urethane, taurillon leather and tracing paper. Yoshimoto et al. found that with more pulses, there is an increase in perceived roughness at a microscale and macroscale. However, it was more apparent in the microscale changes and less significant in a macroscale. Similar to electrostatics, the disadvantage of the electrotactile implementation depends on the humidity on the skin. There are also personal differences in the bioimpedance so the signal range has to be adjusted to meet the sensitivity of the individual. The advantage of this technique is that the user needs not

[87] Yoshimoto et al.
[88] Yoshimoto et al.

drag their finger onto a predefined surface and allows easier implementation of texture simulation for 3D shapes.

2.4 Digital Texture in Design

2.4.1 Sensory Training

In *The New Vision,* Chapter II: The material, Moholy-Nagy extensively discussed the understanding material through sensory training.[89] Such sensory training, he claims is important as it is "indispensable in human development to pass through all the stages of rudimentary experience in every field of sensory activity; thus man little by little attains his own expression and finds the forms to use."[90] He believes that the fundamental sensory experience helps designers build material knowledge through the tacit method for design. As such, the curriculum involves training the "five senses" and one of the first exercises were tactile exercises. Various tactile exercises were conducted with students to improve their sensory perception of material and students were required to identify material based solely by touch alone in order to form acute sense of haptic material knowledge (See Figure *28,* Figure *29,* and Figure *30*). Most of these tactile exercises revolved around understanding the material through feeling various material properties such as texture, softness and other haptic sensations.

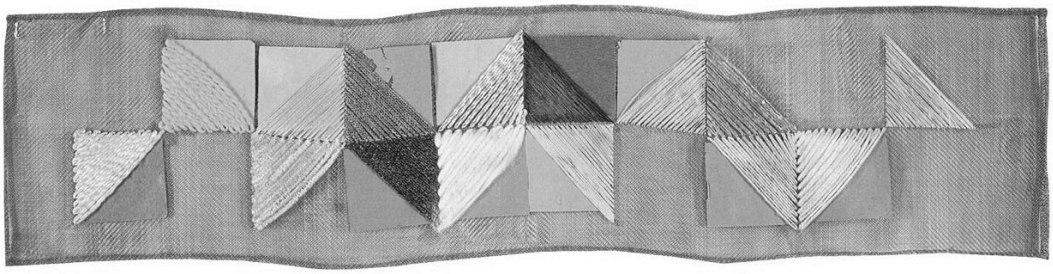

Figure 28: Otti Berger (Bauhaus, second semester, 1928) Tactile table of threads, reprinted from "*The New Vision*"[91]

[89] Moholy-Nagy and Hoffmann, *The New Vision: Fundamentals of Design, Painting, Sculpture, Architecture*.
[90] Moholy-Nagy and Hoffmann, 23.
[91] Moholy-Nagy and Hoffmann, 24.

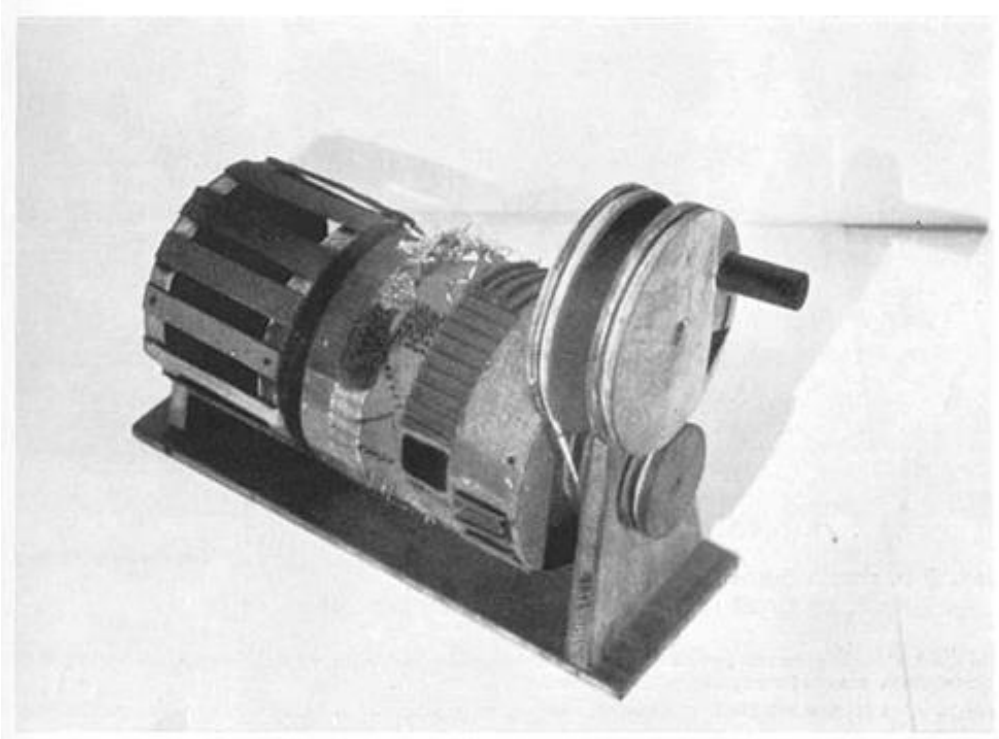

Figure 29: Rudolf Marwitz (Bauhaus, second semester, 1928) Revolving tactile drum with contrasting tactile values; materials arranged in rows, reprinted from "*The New Vision*"[92]

[92] Moholy-Nagy and Hoffmann, 25.

Figure 30: The blind test tactile charts of the New Bauhaus students, reprinted from "*The New Vision*"[93]

2.4.2 Microscopic Texture

Section 1.2 briefly discussed a new way to see texture at a microscopic scale in the era of the Bauhaus training. Moholy-Nagy saw the relevance of microscope texture or which he called “structure” in both science and design (See Figure 31). He stated, “The exact, sharply defined photograph (microphotograph) is the best approach to a new education in materials, since its concentration of emphasis offers a quick, though an indirect approach to actual experience with the material.”[94] This scale of looking at material in design offers new ways to see material, but such a scale is typically where the finger operates in. The resolution of the finger offers superior understanding material texture properties that the eyes do not.

[93] Moholy-Nagy and Hoffmann, 32.
[94] Moholy-Nagy and Hoffmann, 39.

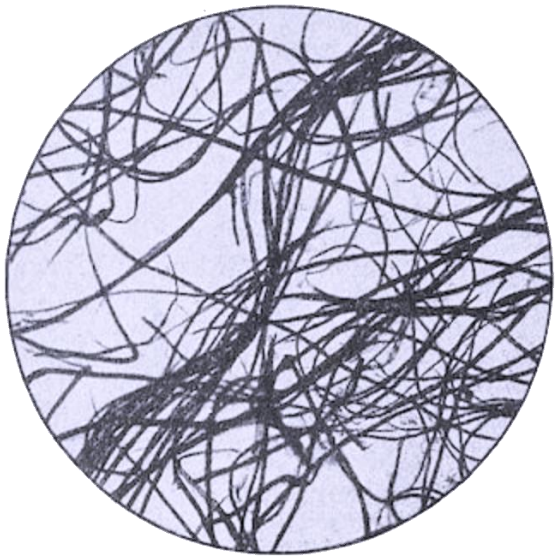

Figure 31: Structure of wrapping paper (microphotograph), reprinted from "*The New Vision*"[95]

More recently, Menges's investigation of material structure on the microscopic scale allows him to exploit the anisotropic microstructure of wood to understand the elastic bending behavior wood for the computational design process.[96] This form of material investigation to exploit specific material properties could generate a new design process that put material at the forefront of design and fabrication. This process enhances the form of finding methods by basing the form on the material affordances and properties. Such an understanding of material could push design toward more materially informed design.

Besides understanding the texture and material through vision and touch, Moholy-Nagy also have exercises in surface treatment where the goal is to create surface texture through various tools on various materials (paper, fabric, etc.) (See Figure 32). He believes such results can build up a better understanding between man and material and stated, "Many people will perhaps not be convinced of the justification of such exercises until some practical application is pointed out….But we are, in the first period of

[95] Moholy-Nagy and Hoffmann, 35.
[96] Menges, "Material Resourcefulness: Activating Material Information in Computational Design"; Menges, "Material Information: Integrating Material Characteristics and Behavior in Computational Design for Performative Wood Construction."

Bauhaus teaching, much less concerned with such applications than with the fundamental relationship of man to material, which may be built up by such exercises as this."

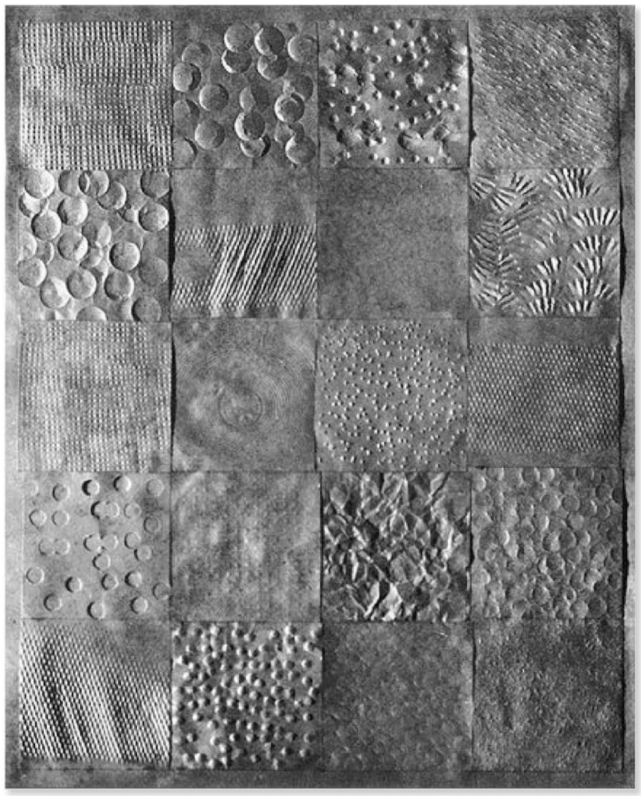

Figure 32: Gerda Marx (Bauhaus, second semester, 1927) Surface treatments of paper (a single material, different tools), reprinted from "*The New Vision*"[97]

[97] Moholy-Nagy and Hoffmann, *The New Vision: Fundamentals of Design, Painting, Sculpture, Architecture*, 48.

3. System Implementation

From the literature review above, we can see that there are multiple ways to encode and decode texture data. Though there are various methods to extract 3D shapes, such as multi-view stereo[98], structured light (laser and coded structured light)[99], photometric stereo[100], and other Shape-from-X methods, it was necessary to test the feasibility of each of the methods to use at a micro-scale with mostly off-the-shelf components. Out of all these methods, photometric stereo requires the least need for special components as USB microscope could be bought relatively at a cheap price and light-ring could be fabricated using off-the-shelf LEDs. Furthermore, Shin and Choi showed that photometric stereo using the ordinary camera with a photometric stereo provides them with a 10-micrometer spatial resolution.[101]

This chapter will introduce the software and hardware aspects of the system implementation (See Appendix D for Open-sourced Github Page). The hardware section will walk through reasoning behind the selection of the low-cost off-the-shelf hardware. The software section will introduce a theoretical Lambertian model for photometric stereo and describe various calibration steps to implement photometric stereo at a microscopic scale.

3.1 Hardware (Microscopic Photometric Stereo)

3.1.1 Camera

The first step in creating the computer vision-based reconstruction is to choose an appropriate camera and lens that would allow the capture of microscopic surfaces. At the beginning, the plan was to build a custom microscopic camera using off-the-shelf Raspberry Pi Cam with a custom macro lens. However, after testing the Raspberry Pi

[98] Fua, "A Parallel Stereo Algorithm That Produces Dense Depth Maps and Preserves Image Features."
[99] Levoy et al., "The Digital Michelangelo Project: 3D Scanning of Large Statues."
[100] Woodham, "Photometric Stereo: A Reflectance Map Technique For Determining Surface Orientation From Image Intensity."
[101] Shin and Choi, "Geometry-Based Haptic Texture Modeling and Rendering Using Photometric Stereo."

Cam and exploring the literature on microscope optics, the plan of building a relatively good microscope using Raspberry Pi Cam was not ideal. For this reason, it was necessary to hack a microscope to eliminate the difficulties of dealing with complex optical systems. To hack the microscope to perform the photometric stereo technique, the microscope should be cheap, able to interface with the computer through USB and have enough space to mount a set of controllable LEDs. The Adafruit USB Microscope could fulfill all of these requirements and it also has an 8 LEDs ring on it for lighting the area of capture (See Figure 33).[102] In addition to all the requirements, it also included an adjustable focal length, so it is easier to adjust to another size of the image.

Figure 33: Z-Star Microelectronics Corp. Venus USB Microscope - 5MP interpolated 220x magnification/8 LEDs

3.1.2 LEDs

Since the microscope already included the LEDs Ring, it was used as a reference to create the custom LEDs Ring circuit using AutoDesk EAGLE software. The LEDs Ring was sized at 26mm for outer diameter and 15 mm for the inner diameter. The front of LEDs ring is used to place 8 NeoPixel Nano at 45° interval. Each NeoPixel Nano is about 2.4mm by 2.7mm and includes an integrated driver to control and chain all the NeoPixels

[102] Adafruit, "USB Microscope - 5MP Interpolated 220x Magnification / 8 LEDs ID: 636 - $79.95 : Adafruit Industries, Unique & Fun DIY Electronics and Kits."

through data in and out.[103] The back of the circuit was connected each of the Neopixel to the voltage and ground. Six 0.1μF capacitors were used to prevent damage to the NeoPixels. The circuit diagram (Figure *36*) shows that connection was straightforward with a ground connectedto all the ground, voltage connected to all the voltage, and data out is connected to data in. From the schematic, AutoDesk Eagle was used to autoroute the path of the circuit, it effectively came up with 100% connection of the schematic shown below.

For the circuit fabrication, an online vendor, OSHPark, was used for their fast delivery time.[104] The fabricated custom LEDs ring was used to replace the LEDs Ring that came with the microscope. Since the original LEDs ring does not have the same pinouts, it was necessary to drill two holes on the side of the USB microscope without damaging the focus gear mechanism. Figure *34* shows the custom LEDs ring inserted into the LED slot in the microscope with the wire coming out from two sides.

[103] Adafruit, "NeoPixel Nano 2427 RGB LEDs w/ Integrated Driver Chip - 10 Pack ID: 3484 - $4.95 : Adafruit Industries, Unique & Fun DIY Electronics and Kits."
[104] Osh, "OSH Park ~."

Figure 34: LEDs Light Ring in the Microscope

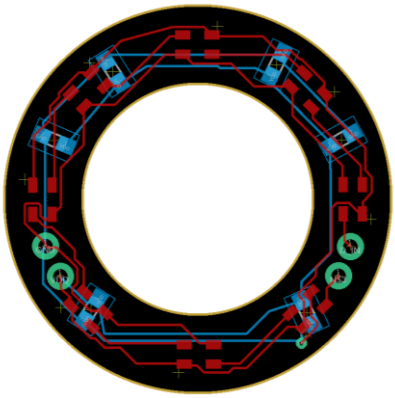

Figure 35: Custom NeoPixel Nano Ring Circuit

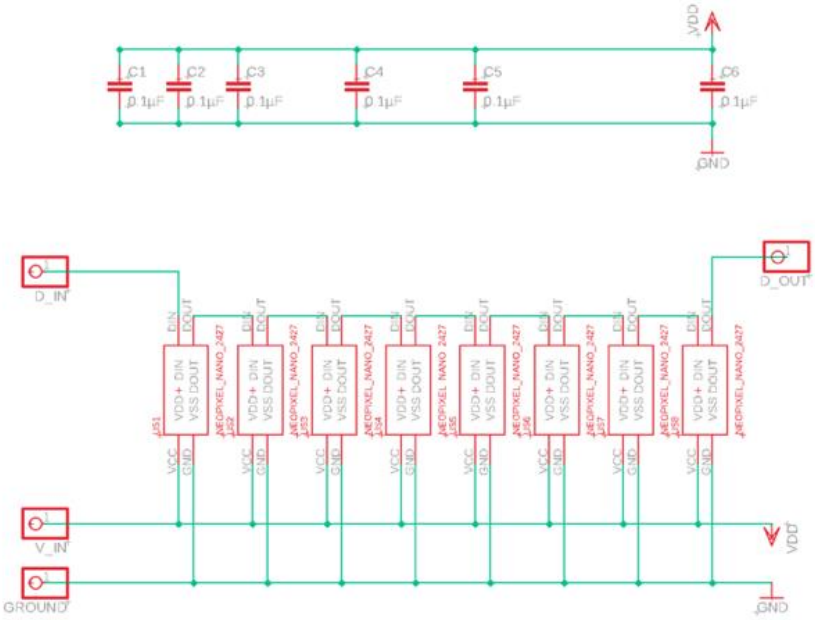

Figure 36: Custom NeoPixel Nano Ring Schematics

3.1.3 Integrated vs. Laptop Configuration

The next consideration for the haptic texture modeling tool is whether the system would be integrated embedded system (Raspberry Pi, Figure 37) or would use a micro-controller and a computer to control the microscope. Since, the initial vision of the project was to combine the Haptic Texture Modeling Tool and Haptic Texture Rendering Tool into an integrated tool with a scanner, screen, and haptic rendering device, Raspberry Pi would be

better in creating such integrated system. Though micro-controller with the computer could perform better, the Raspberry Pi is also more portable and would allow easier use in an outdoor context. On the other hand, Raspberry Pi is underpowered when compared to a laptop. The integrated configuration will include Raspberry Pi 3B+, 7inch Raspberry Pi Multi-touch screen, and an USB microscope with a custom LEDs ring.

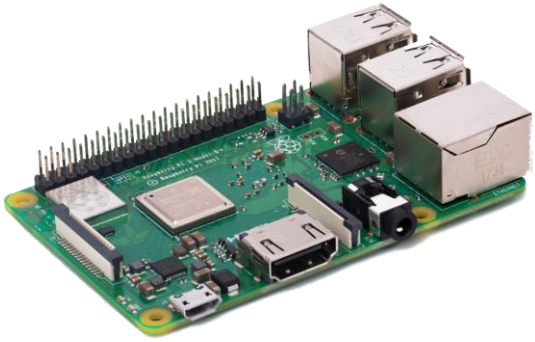

Figure 37: Raspberry Pi 3B+[105]

Figure 38: Raspberry Pi 7 inch Touch Display[106]

[105] Raspberry Pi, “Raspberry Pi Store.”
[106] Raspberry Pi.

3.2 Software

For the software aspect of the haptic texture modeling tool, we use the traditional photometric stereo proposed by Robert J. Woodham.[107] This traditional method requires: 1) calibration of the light source, 2) light source are evenly distributed among the surface, 3) orthographic camera, 4) shadow, inter-reflectance, and 5) specularity are not considered in the model. As mentioned above in Section 1.1, the photometric stereo was chosen because it was feasible in the microscale. In addition to these, the photometric stereo method proves to be mathematically linearly when using the Lambertian model so it could be efficiently solved in the Raspberry Pi.

3.2.1 Light Vector Calibration Process

The calibration process includes scanning a specular sphere with a known radius in multiple illumination settings. The specular sphere is used to exploit the effect of light reflecting on the specular surface to find the normalized light directional vector. Figure *39* shows how the light direction is calculated using the normal vector on the brightest spot of the sphere.

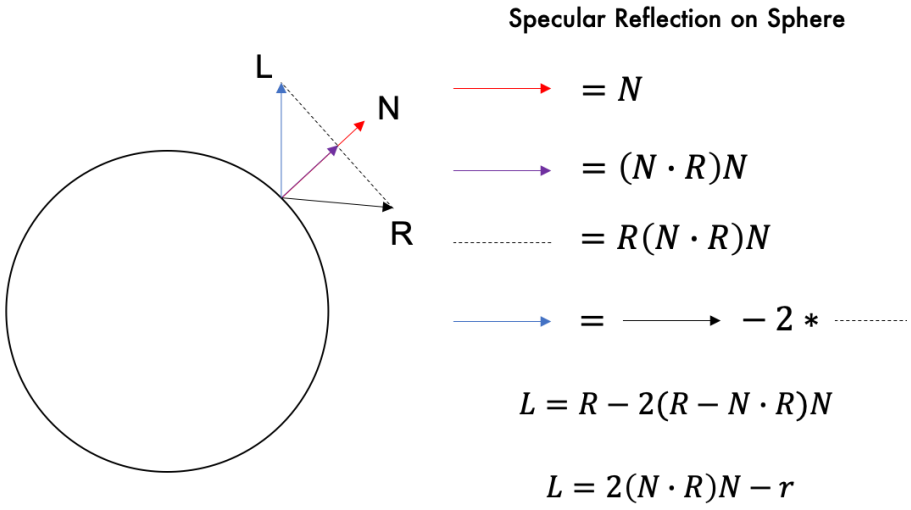

Figure 39: Law of Reflection[108]

[107] Woodham, "Photometric Stereo: A Reflectance Map Technique For Determining Surface Orientation From Image Intensity."
[108] "Photometric Stereo."

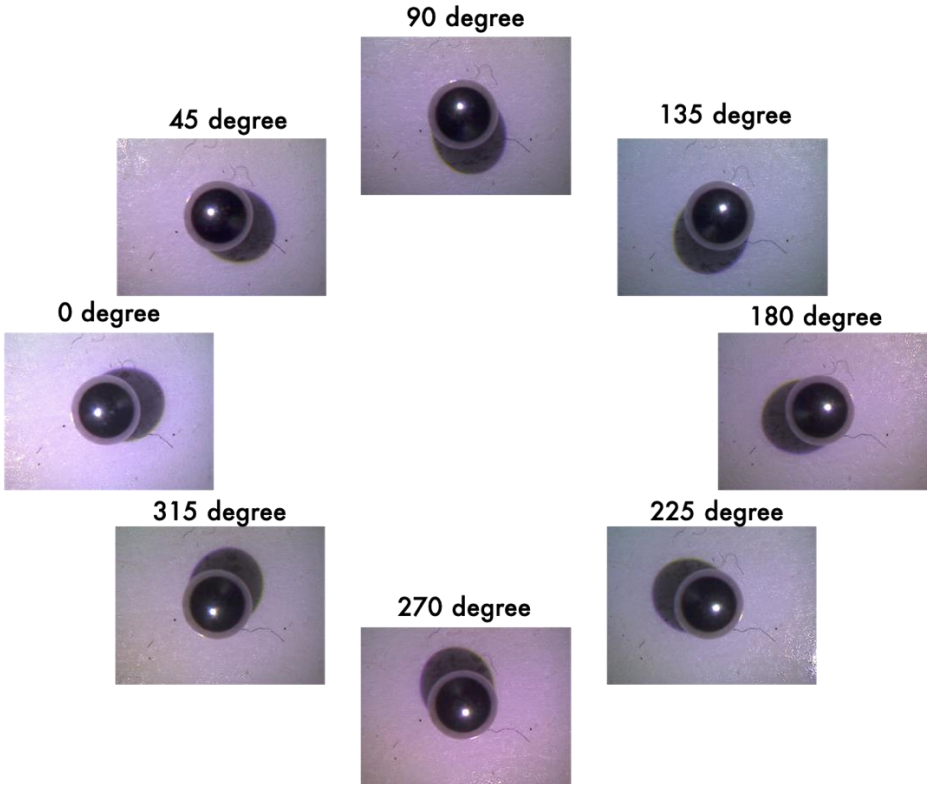

Figure 40: Calibration Photos

Figure 40 shows the images of 3mm diameter metal ball bearing from various illumination settings. The step for calibration involves: 1) localizing the sphere, 2) finding the center of the circle, 3) finding the center of the brightest pixel, 4) calculating the normal at the brightest spot given the sphere known diameter using the Law of Reflection, 5) calculating normalized light vector. In order to localize the sphere, the Hough circle function from OpenCV was used.[109] The brightest spot was found by finding the highest pixel value (255) and finding the center of this set of pixels. Subsequently, the brightest pixel spot was used to find the normal from a relative position between the center of the circle and the center of pixel. Finally, the equation will return the normalized light vector, as shown in Figure *41*.

[109] "OpenCV: Hough Circle Transform."

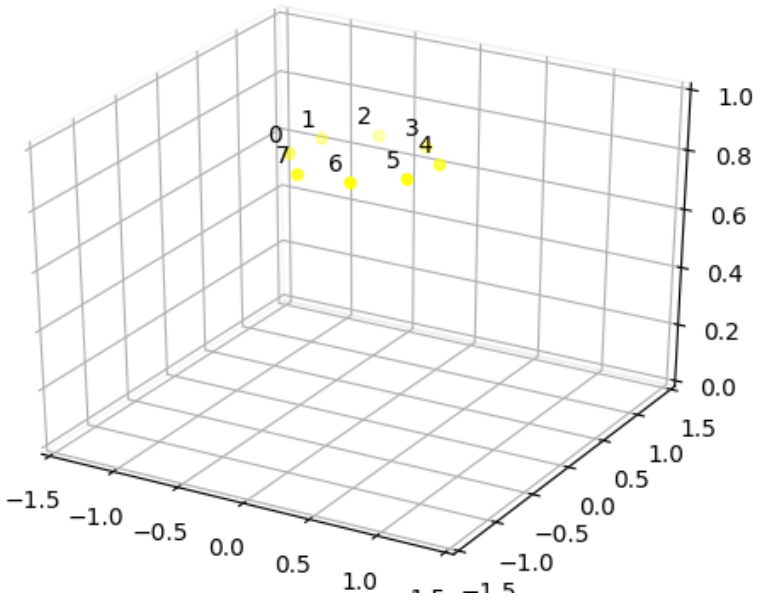

Figure 41: Calibrated Normalized Light Vectors

3.2.2 Image Flat-fielding Calibration Process

The Woodham's photometric stereo assumes that it evenly distributes the light on the scene.[110] However, since the LED point light source is only about 20 mm away from the surface, it causes the capture images to have spatially varying illumination. The spatially varying illumination causes errors in the normal map because of the uneven distribution of lighting from the LEDs. The uneven distribution of the lighting is caused by the inverse square law of light propagation. This can be counteracted through nonlinear modeling of illumination using spherical harmonics.[111] Though there are more complex iterative methods to correct the spatially varying illumination, the flat-field correction is a fast and effective correction method. Flat-fielding process is used to remove the effect of the inverse-square law of light propagation and it used in image processing to compensate gains and offset the dark frame noise.[112] Fan et al. and Angelopoulou and

[110] Woodham, "Photometric Stereo: A Reflectance Map Technique For Determining Surface Orientation From Image Intensity."
[111] Johnson et al., "Microgeometry Capture Using an Elastomeric Sensor."
[112] Angelopoulou and Petrou, "Evaluating the Effect of Diffuse Light on Photometric Stereo Reconstruction."

Petrou show flat-fielding correct the error by drastically lower the error when compared to the non-flat-field method.[113]

The standard flat-fielding operation requires both the dark field image and the flat-field image. For this case, I assumed the dark field image close to 0 as the hardware does not allow external light to propagate in. For the flat-fielding method, images of a white paper was captured with multiple illuminations. These photos are noisy, as the paper has a small texture at a microscale, therefore, the images have to be fitted to a low degree polynomial curve. For this flat-fielding purpose, the image was fitted to the 5th polynomial curve. The fitted parameter was tested from 2nd to 10th degree, 2nd to 4th-degree polynomial curve fitted the image but comparing the result, the 5th-degree polynomial curve fitted the corners better than the other curve. From the 6th to 10th degree, the curve was too complex, and no longer resembled the illumination field. Figure *42,* Figure *43,* and Figure *44* show the images of the curve fitting process to remove noise from the white paper image.

[113] Angelopoulou and Petrou; Fan et al., "Deviation Correction Method for Close-Range Photometric Stereo with Nonuniform Illumination."

Figure 42: White Paper Image (0° Azimuth)

Figure 43: Fitted Grayscale Gradient of Illumination Field (5th Degree Polynomial)

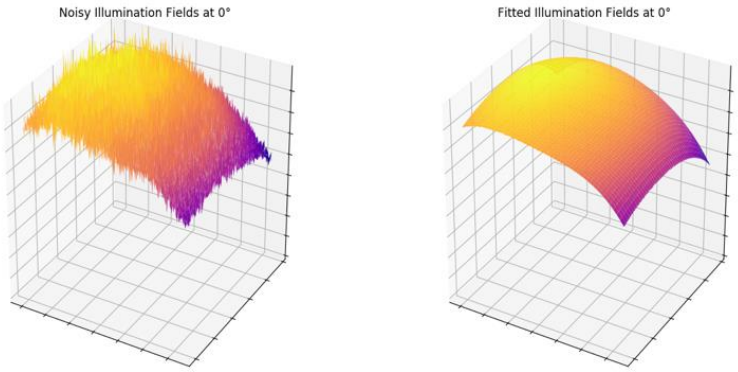

Figure 44: 3D Curve of White Paper Image and Fitted Grayscale Gradient of Illumination Field (0° Azimuth, 5th Degree Polynomial)

Assuming the dark field image is extremely close to 0, let I_k be the kth input image, $gray(I_k)$ be the gray-scale version of the input image, D be dark field image, and f_k be the 2D 5th degree polynomial function of the kth illumination field.

$$I'_k = \frac{I_k - D}{f_k - D}\overline{gray(I_k - D)}, for\ k \in [1, K] \quad (10)$$

$$where\ I_k\ is\ the\ k^{th}\ Original\ Image,$$
$$f_k\ is\ the\ k^{th}\ 2D\ fitted\ function\ (Flat - Field\ Image),$$
$$I'_k\ is\ the\ k^{th}\ Flatfield\ Corrected\ Image,$$
$$D\ is\ the\ Dark\ Field\ Image.$$

Assuming the dark field image is extremely close to 0, we can ignore the D, dark field image, and rewrite the formula as:

$$I'_k = \frac{I_k}{f_k}\overline{gray(I_k)}, for\ k \in [1, K] \quad (11)$$

$$where\ I_k\ is\ the\ k^{th}\ Original\ Image,$$
$$f_k\ is\ the\ k^{th}\ 2D\ fitted\ function\ (Flat - Field\ Image),$$
$$I'_k\ is\ the\ k^{th}\ Flatfield\ Corrected\ Image.$$

I_k is divide pixel-wise by the function f_k, and to preserve the initial dynamic range, this is multiplied by the mean value of $gray(I_k)$.

3.2.3 Shadow

Assuming that the texture materials are planar surfaces, the effect of shadows is limited by the height of the fiber of the textile material. If the height of the fibers is sufficiently large, the effect of the shadow can become significant, which would cause depth error. The system assumes that the fibers of the fabric are sufficiently small enough to not cast shadows.

3.2.4 Classical Photometric Stereo

According to classical photometric stereo theory, the image formation model is as follows:

$$I^k(p) = \rho N(p) \cdot L^k \qquad (12)$$

$$where\ I^k(p)\ is\ the\ kth\ Image\ at\ pixel\ p,$$
$$\rho\ is\ the\ diffuse\ albedo,$$
$$N(p) is\ Normal\ at\ pixel\ p,$$
$$and\ L\ is\ the\ kth\ Light\ Vector.$$

This image formation model assumes the Lambertian reflectance model with uniform illumination and an orthographic camera. To simply the linear model, the scalar albedo (ρ) and normal (N) into G. Each of the images are flattened and vertical stacked them into an image matrix (I). This form can be represented as follows:

$$I = G \cdot L \qquad (13)$$

$$where\ I\ is\ the\ Image\ Matrix,$$
$$G\ is\ Normal\ and\ diffuse\ Albedo,$$
$$and\ L\ is\ Normalized\ Light\ Vector.$$

The matrix form of this equation (13) can be written as follows:

$$\begin{bmatrix} I_{1,1} & \cdots & I_{1,p} \\ \vdots & \ddots & \vdots \\ I_{m,1} & \cdots & I_{m,p} \end{bmatrix} = \begin{bmatrix} G_{1,1} & G_{1,2} & G_{1,3} \\ \vdots & \vdots & \vdots \\ G_{p,1} & G_{p,2} & G_{p,3} \end{bmatrix} \cdot \begin{bmatrix} L_{1,1} & \ldots & L_{1,m} \\ L_{2,1} & \ldots & L_{2,m} \\ L_{3,1} & \ldots & L_{3,m} \end{bmatrix} \qquad (14)$$

$$where\ m\ is\ the\ number\ of\ images,$$
$$p\ is\ the\ number\ of\ pixels.$$

We can solve this form of a linear equation using the linear least square form:

$$G^* = \min_G \|I - G \cdot L\|^2 \qquad (15)$$

$$where\ N = \frac{G^*}{\|G^*\|}$$

The normal N is normalized to get rid of the scalar value ρ as it was combined in equation (13). From N, we can derive surface gradients as follows:

$$p = -N_x/-N_z \ and \ q = -N_y/-N_z \qquad (16)$$

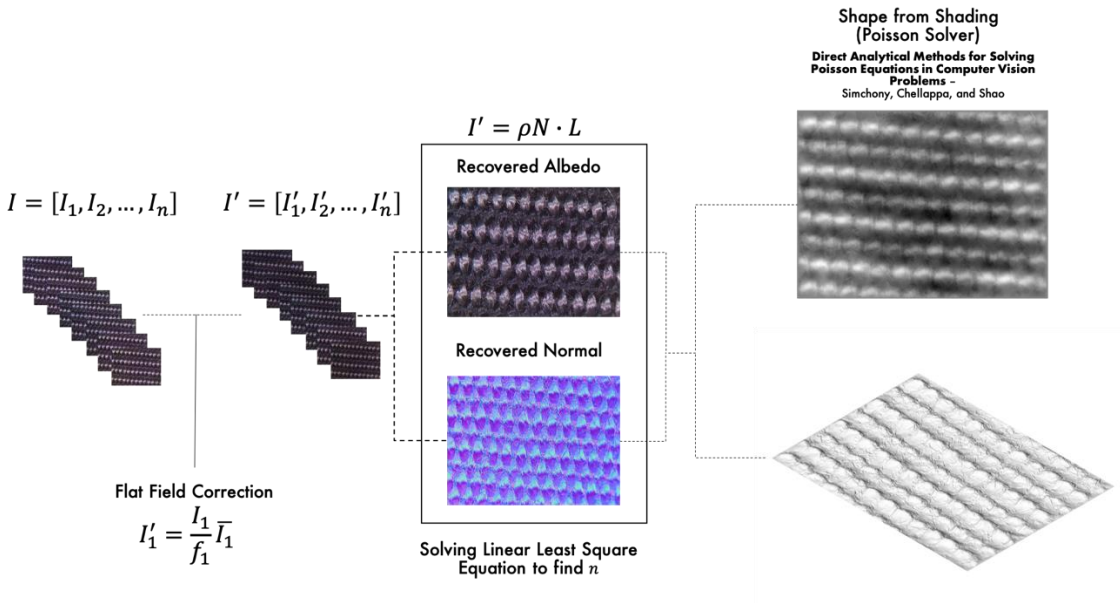

Figure 45: Photometric Stereo and Shape from Shading Process

Figure *45* shows the process of photometric stereo used in the 3D texture scanning prototype. The process first take multiple photos from various lighting azimuth angle and

the raw image is pre-process through the flat-fielding process. The pre-processed image is put into a matrix form and using least square method from Numpy, it reconstructs the normal. Subsequently, a shape-from-shading algorithm is used to reconstruct the depth map from the normal. Since the depth map provides a grid of height, it can be saved as a 3D format such as .ply and .obj.

3.2.5 3D Reconstruction

For the surface reconstruction, shape-from-shading algorithms must be considered as we acquired the surface normal can provide the gradient of x and y with respect to z. There are various shape-from-shading algorithms and Amit Agrawal et al. compare various shape from shading methods.[114] These methods include Poisson Solver, Frankot-Chellappa, Alpha-Surface, M-estimator, Regularization, and Diffusion. Out of these, this thesis tested Poisson Solver, Frankot-Chellappa, M-estimator, and Simchony Integration. Most of the methods tested are solved using Fourier Transform, Cosine Transform, and Sine Transform. These methods transform the image into the 2D frequency domain and integrate the gradient in this domain. This is done because it is computationally more efficient to integrate into the frequency domain. Out of all the methods tested, the most stable, accurate, computationally efficient for Raspberry Pi was the Poisson Solver using Sine Transform. T. Simchony et al.'s sine transform Poisson equations solver was used to recover the surface.[115] The code for this Poisson reconstruction was derived from Dr. Ramesh Raskar.[116]

3.2.6 Visualization

One challenge using Python to implement the current system is the visualization dependencies and libraries available for the python language. The visualization libraries require other back-end dependencies which are structured in a very complicated manner. I tested various libraries such as Vispy, Pygame, PyQtGraph, and Kivy. Each of these libraries is useful for creating a different type of visualization, Vispy for 3D scientific visualization, Pygame for general 2D visualization and interaction, PyQtGraph was useful

[114] Agrawal, Raskar, and Chellappa, "What Is the Range of Surface Reconstructions from a Gradient Field? BT - Computer Vision – ECCV 2006."
[115] Simchony, Chellappa, and Shao, "Direct Analytical Methods for Solving Poisson Equations in Computer Vision Problems."
[116] Raskar, "Code A: Matlab Code for Poisson Image Reconstruction from Image Gradients."

for graphing and plotting in 2D and 3D, and lastly Vispy for GUI visualization. After testing various libraries, the Vispy library was the most efficient and least complicated library. Since Vispy does not have good support for the GUI implementation and uses Qt widget, which is harder to control, I used a grid-based system to create squares and use them as a button. This causes some delay in the GUI system, as it is not threaded from the visualization. Another problem I encountered was that visualization system could not be run in sequence with the computation done by the photometric stereo, hence the Threading and Queue libraries from python were used to multi-thread the processes.

Figure 46: Interface and Visualization of 3D Texture Scanner System Prototype

4. Evaluation

In this chapter, the prototype system will be evaluated by analyzing: 1) the general performance of the algorithm, 2) the reconstruction evaluation of material samples, 3) interview with three participants to find the use case scenario in the field of the participant's expertise including computational textile and bio-plastic fabrication.

4.1 System Evaluation

The current 3D texture scanning prototype captures a patch about 9.5x7.0mm of the material sample. Since the scanner is capturing 640x480 images, each pixel of the image represents about 0.014mm of the object. The resolution could be increased to create denser results, but the computation time will drastically increase. The current scanning and reconstruction require about 20 to 30 seconds to compute.

For the quantitative evaluation, the scanning performance will be evaluated through various material samples. These samples include twenty textile, five bio-plastics, and three 3D prints [include powder print, PLA (Polylactic Acid) print using Fused Deposition Modeling (FDM), resin print using Stereolithography (SLA)]. Furthermore, a sandpaper test will be conducted on a wood block with a different grit of sandpaper (80, 100, 120, 180, 220). The textile samples were from the Room&Board free fabric swatches.[117] I selected the samples with variety in mind (color, material, and texture size). The bio-plastics samples were from the course "IDeATe: Orgoformation: Designing with Biological Matter", 48233. The 3D prints were designed by Özgüç Bertuğ Çapunaman.

The normalized depth map and gray-scale albedo image of the material was used to analyze the statistical difference between visual texture and geometric texture. Though visual texture is affected by geometry[118], visual texture is a combination of color, edges, and geometry. The system should see differences between geometric texture and visual

[117] Room&Board, "Free Fabric & Leather Swatches - Fabrics & Materials."
[118] Koenderink and van Doorn, "Illuminance Texture Due to Surface Mesostructure."

texture as it decomposes the images into color texture (albedo), and geometric texture (3D geometry). The differences will be higher in the surface with multiple color, as the color pattern is a form of visual texture that is not part of the geometric texture. To evaluate this difference, statistical analysis derived in section 2.1.1 will be used. The statistical analysis includes calculating the mean, variance, standard deviation, skewness, uniformity, and entropy. 2D Fourier analysis of both gray-scale albedo image and depth map were used to verify whether there is structure similarity in the gray-scale albedo and depth map.

In addition to the statistical histogram analysis, the results will be qualitatively analyzed through visual inspection of the normal map, depth map, and 3D reconstruction. The qualitative evaluation will include 6 case studies (three successful cases and three distorted cases). In each of the case studies, reason would be given for the cause of distortion and success with respect to the Lambertian model of reflection.

4.2 Qualitative Evaluation of Reconstructed Texture

This section will evaluate the reconstruction of 28 sample materials through six case studies (three successful, three unsuccessful). These case studies will include samples distinct in material composition and color.

4.2.1 Material Samples Used

The 3D texture scanning prototype was tested on the material samples shown in Figure *47* (see Appendix B for the material composition of the samples).

Figure 47: Material Samples Tested

4.2.2 Reconstructed Albedo

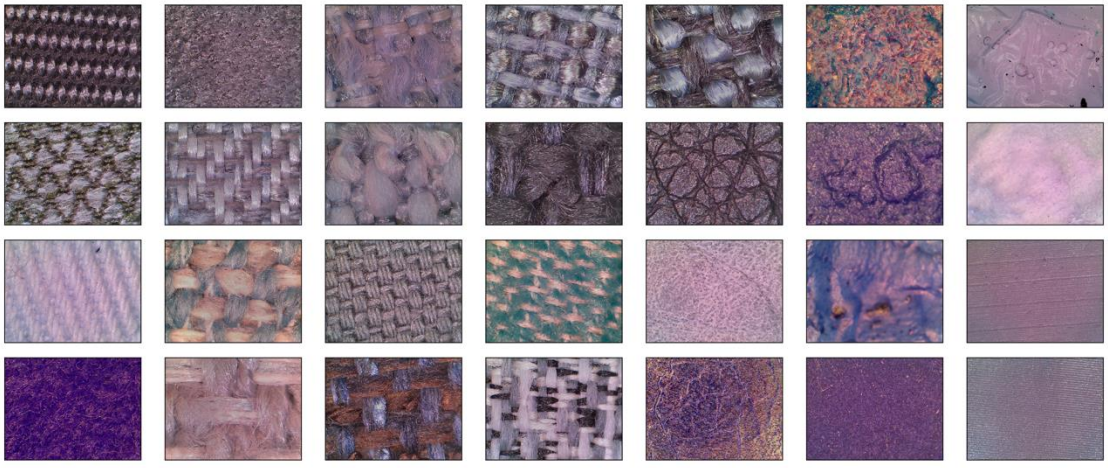

Figure 48: Recovered Albedo from Photometric Stereo

Figure *48* shows the recovered albedo from the material samples using the photometric stereo method. The result shows that most of the recovered albedo stay true to the original color of the material sample except for the material at Row 4, Column 1 which turned from red to purple. This is the result cause by discrete RGB component of the LED which does not have true white but uses the combination of red, green, and blue to produce white. The discrete components of red, green, and blue sometimes leak the color or get occluded so the white color is not even.

4.2.3 Reconstructed Normal

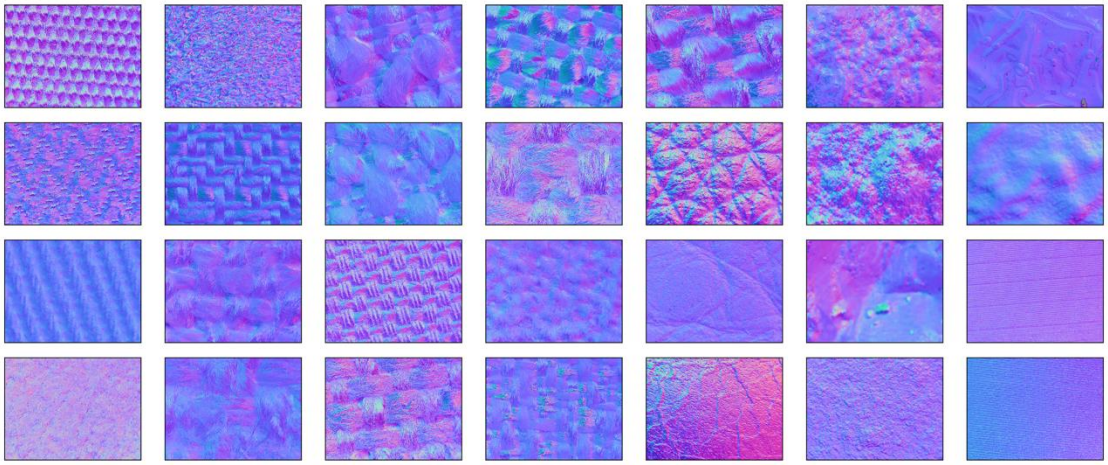

Figure 49: Normal Map Reconstructed using Photometric Stereo

Figure 50: Sphere Normal Map Guide

Figure *49* shows the reconstructed normal map using the photometric stereo technique. Normal map shows the normalized direction of vector in each pixel. Using the sphere normal map guide, we can map the corresponding color to the direction of the normal. For example, if the normal is pointing up (towards the viewer), the color is purple.

4.2.4 Reconstructed Normalized Depth Map

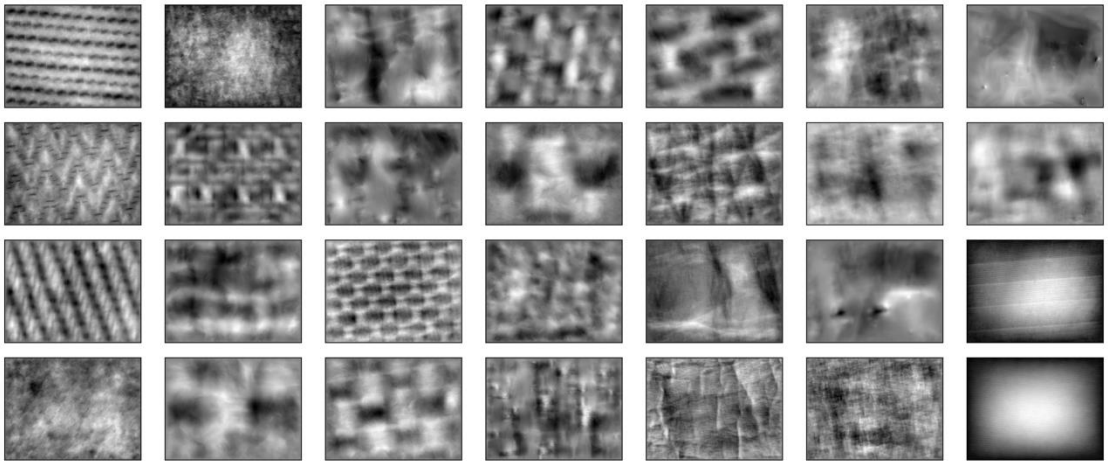

Figure 51: Reconstructed Normalized Depth Map using Shape-from-Shading

Figure *51* shows the reconstructed normalized depth map. The normalization linearly remaps the minimum depth to zero and maximum depth to one. This means that the normalized depth map only shows the relative difference between the highest and lowest points. Therefore, it cannot be used to compare against other depth maps, as they are essentially in a different range. The depth gives us a relative sense of depth for each of the materials. However, it can also accentuate the small error if the surface is relatively flat (Row 3, Column 7) and (Row 4, Column 8). From the depth map, most of the texture of the material seems to be visible and shows some similarity with the Albedo. The depth map keeps most of the low frequency changes in the texture and does not preserve high frequency edges from Albedo. This results from the shape-from-shading algorithm, which assumes that the surface can be integrated smoothly.

4.2.5 Reconstructed 3D Surface Rendering

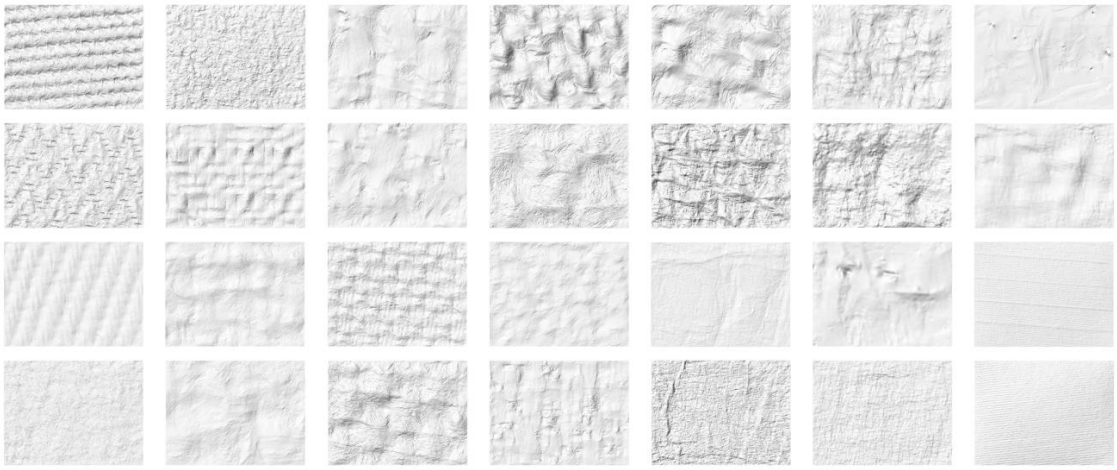

Figure 52: Rendering of Reconstructed Surface

Figure *52* shows the rendering of the 3D surface from the top view. 3D model rendering provide a more realistic view compare to the normalized depth. Such 3D models can be used to compare between various material as it is not normalized. One observation from the top view, is that bigger texture grain tends to have lower variance in height. For example, (Row 3, Column 2), (Row 4, Column 2), (Row 1, Column 3), (Row 2, Column 3), and (Row 2, Column 4) tends to be have lower height. This is because larger grain size the smoother the change in height (low frequency) while smaller grain size the drastic the changes in height over the area (high frequency). Using these 3D reconstruction, some of the selected materials were 3D printed at a 5:1 scale to see how enlarged texture could be used to provide new sensibility of the material (See Appendix C).

4.2.6 Successful Cases of Reconstruction

4.2.6.1 Successful Case 1 (100% polyester micro-weave, Single Color) (Row 2, Column 1)

(a) Material

(b) Albedo

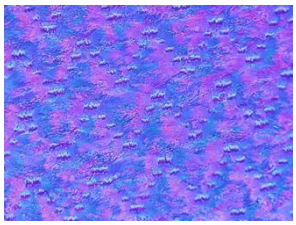

(c) Normal Map

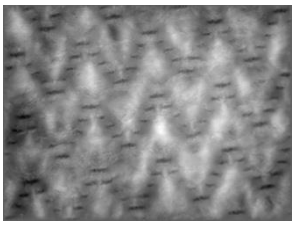

(d) Normalized Depth Map

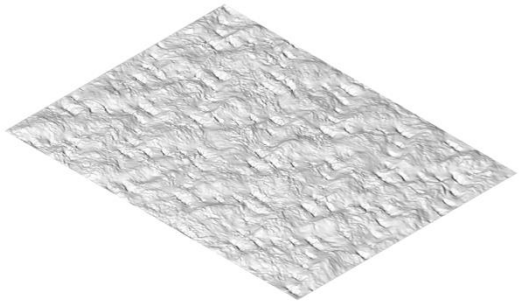

(e) 3D Rendering

Figure 53: Case Studies, Material Sample (Row 2, Column 1)

This successful case 1 material is the 100% polyester micro-weave. From the 3D rendering, the result shows the texture created by micro-weaves and weaving patterns. The algorithm was successful in capturing the details of geometry in both the normal map and 3D reconstruction. From a normal map, it can be seen that all the weave facing in the same direction. The algorithm was able to perform well as it does not have complex color.

4.2.6.2 Successful Case 2 (Matte Resin Print, Single Color) (Row 3, Column 7)

(a) Material

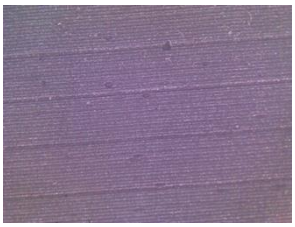

(b) Albedo

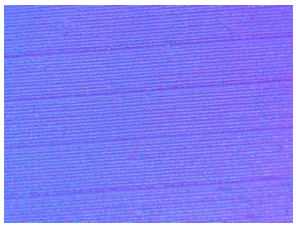

(c) Normal Map

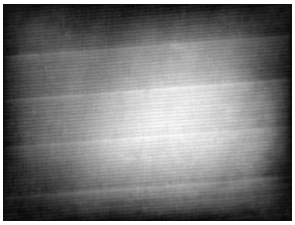

(d) Normalized Depth Map

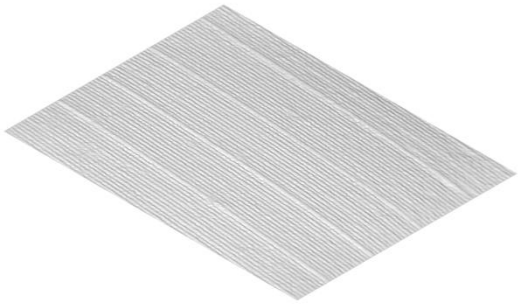

(e) 3D Rendering

Figure 54: Case Studies, Material Sample (Row 3, Column 7)

The successful case 2 material is a gray matte resin print using SLA method. The 3D rendering reconstruction shows an accurate capture of the print layer and even the small sub-millimeter imperfection from print can be seen on the 3D rendering. Comparing the albedo to the 3D reconstruction, it captures the major and minor lines from the 3D printed layers.

4.2.6.3 Successful Case 3 (100% polypropylene bouclé, Multi-Color) (Row 1, Column 5)

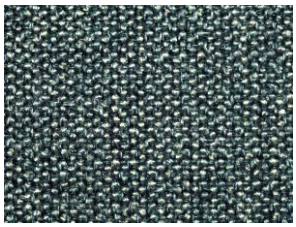

(a) Material

(b) Albedo

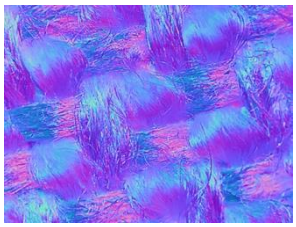

(c) Normal Map

(d) Normalized Depth Map

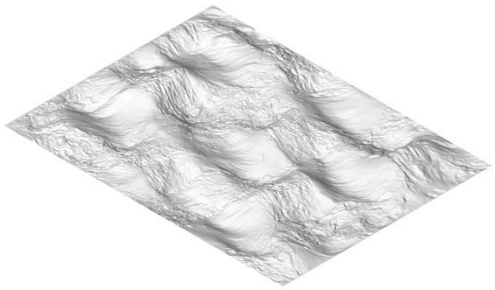

(e) 3D Rendering

Figure 55: Case Studies, Material Sample (Row 1, Column 5)

The successful case 3 material is 100% polypropylene bouclé. The 3D rendering reconstruction shows an accurate capture of material even though they are two different colors. There are no artifacts on the normal map when compared to the fail cases in section 4.2.7. Looking at the structure of the albedo image, the depth map and 3D rendering capture the 3D texture fairly accurately.

4.2.7 Fail Cases of Reconstruction

4.2.7.1 Fail Case 1 (50% polyester and 50% olefin jacquard, Multi-Color) (Row 4, Column 4)

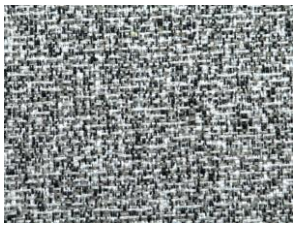

(a) Material

(b) Albedo

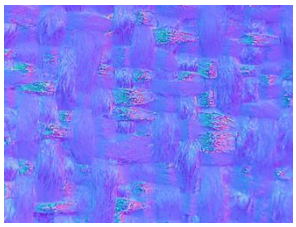

(c) Normal Map

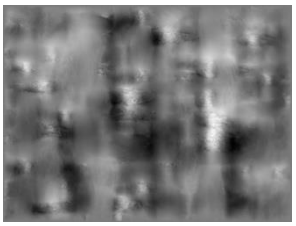

(d) Normalized Depth Map

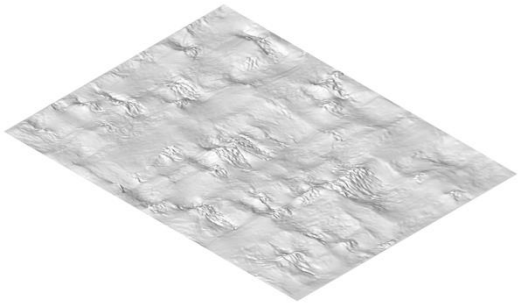

(e) 3D Rendering

Figure 56: Case Studies, Material Sample (Row 4, Column 4)

The fail case 1 material is a mixture of 50% polyester and 50% olefin jacquard. One of the main reason this system fail was because it is made up of two materials which have very different reflectances. The 3D model shows an inaccurate structure as compared to the albedo. The normal map also shows artifacts where not all the left-to-right stitches have the same normal direction. The black fibers have different normal direction when compared to the white fibers. This error causes the reconstruction to be flattened.

4.2.7.2 Fail Case 2 (51% olefin and 49% polyester jacquard, Multi-Color) (Row 1, Column 3)

(a) Material

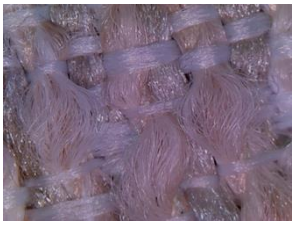

(b) Albedo

(c) Normal Map

(d) Normalized Depth Map

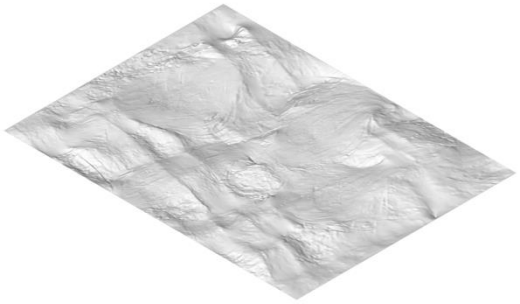

(e) 3D Rendering

Figure 57: Case Studies, Material Sample (Row 1, Column 3)

The fail case 2 material is a mixture of 51% olefin and 49% polyester jacquard. Similar to section 4.2.7, one of the main reason this system fail to reconstruct this sample was because it comprises two materials which have very different reflectances. Another reason for the failed reconstruction is the big fibers creating shadows which the model does not account for. The shadow causes some areas to be darker and distort the normal direction. The reconstruction near the shadow tend to become exaggerated as the normal changes became drastic.

4.2.7.3 Fail Case 3 (Tapioca Bioplastic, Single Color) (Row 1, Column 7)

(a) Material

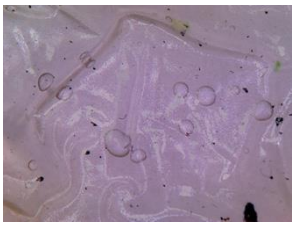

(b) Albedo

(c) Normal Map

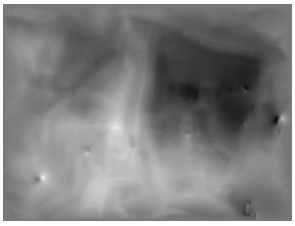

(d) Normalized Depth Map

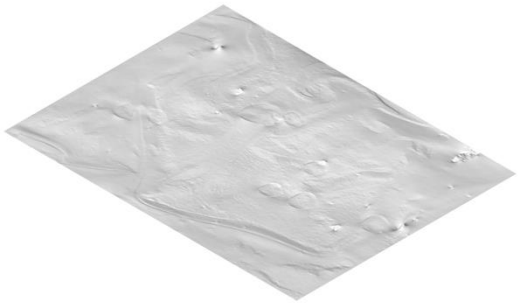

(e) 3D Rendering

Figure 58: Case Studies, Material Sample (Row 1, Column 7)

The fail case 3 material is a clear bio-plastics without any additional materials. Though the system can detect some elevation of the material, the reconstructed is flattened. This is caused by the transparency property of the material, which tends to create interreflection and complicate light modeling. Inter-reflection is known to underestimate the depth in photometric stereo, therefore it result in a flatten reconstruction.[119] The small dimple structures and bubble could be seen on the 3D rendering even though bubbles are inside the material. This shows that reconstruction fail in the case of transparent material.

[119] Nayar, Ikeuchi, and Kanade, "Shape from Interreflections."

4.3 Quantitative Statistical Analysis of Reconstructed Texture

4.3.1 Histogram Analysis (Seperating Albedo Texture and Geometric Texture)

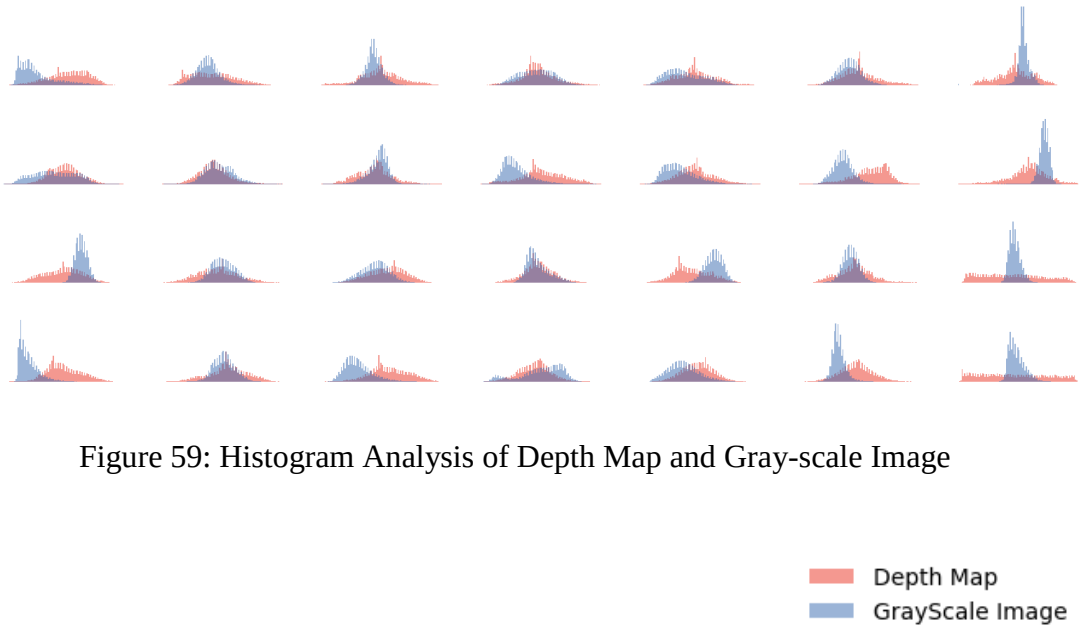

Figure 59: Histogram Analysis of Depth Map and Gray-scale Image

The histogram analysis shows the differences between normalized depth map and gray-scale images. The histogram shows the difference between texture from gray-scale image, which is a combination of color texture and geometric texture and texture from depth map which is only the geometric texture without influence of color. From the broad overview of all the histogram shown in Figure *59*, there are some histograms which are drastically different.

4.3.2 Histogram Case 1: (80% polyester and 20% rayon bouclé, Multi Color) (Row 4, Column 3)

(a) Gray-scale Image

(b) Normalized Depth Map

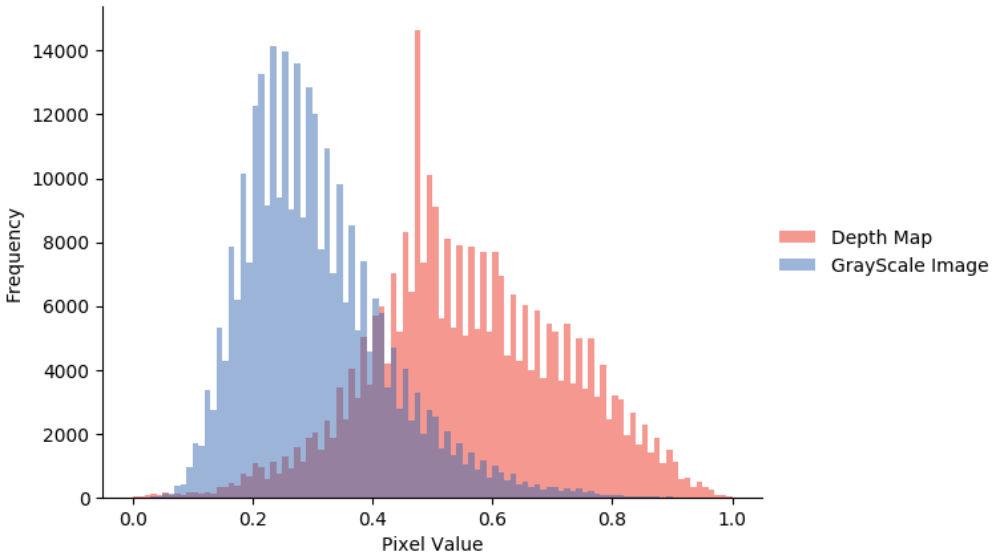

(c) Histogram

Figure 60: Histogram Analysis, Material Sample (Row 1, Column 1)

The material for Histogram Case 1 is the dark color polyester (80%) and rayon (20%) bouclé. From the histogram, it can be seen that the gray-scale histogram is skewed toward the lower pixel value, while the normalized depth map tends to be more evenly distributed. This shows that the albedo biases the visual texture towards the lower end of the pixel value. The skew shows the bias of the color in the distribution even though, the texture is the regular in the pattern which can be seen by the normal distribution of the depth map.

4.3.3 Histogram Case 2: (100% cotton twill, Single Color) (Row 3, Column 1)

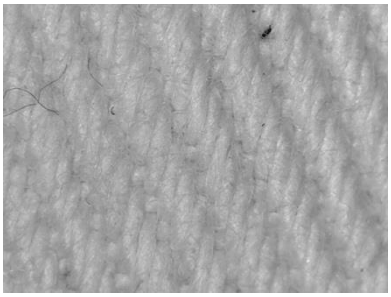

(a) Gray-scale Image

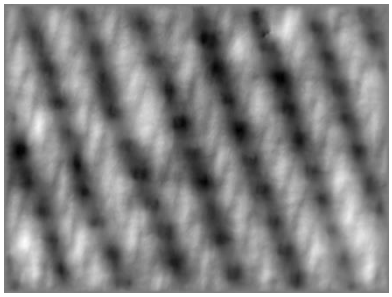

(b) Depth Map

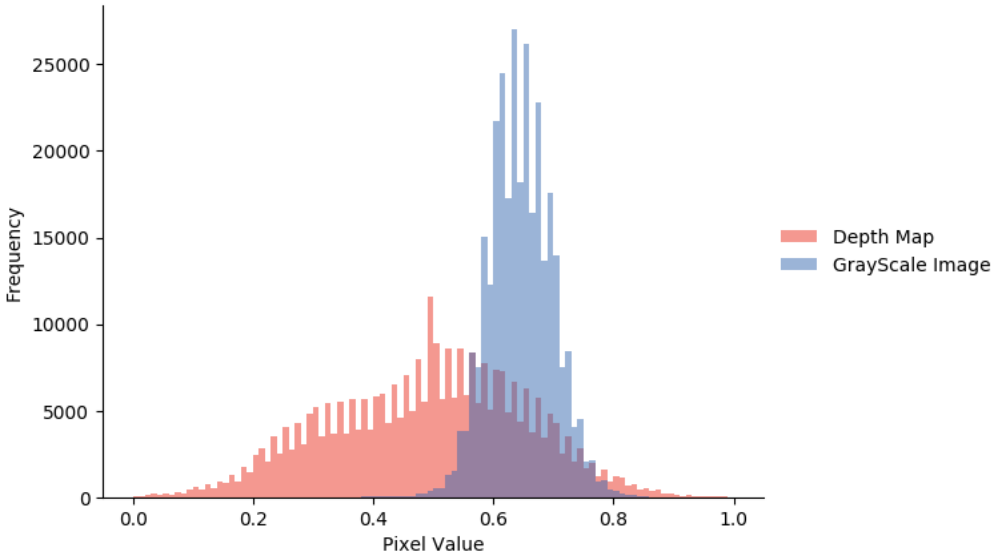

(c) Histogram

Figure 61: Histogram Analysis, Material Sample (Row 3, Column 1)

The material for Histogram Case 2 is the white cotton (100%) twill. From the histogram, it can be seen that the gray-scale histogram is skew toward the higher pixel value which is cause by overall color of the material while the normalized depth map is more evenly distributed. Similar to Histogram Case 1: (80% polyester and 20% rayon bouclé, Multi Color) (Row 4, Column 3), this shows that the albedo causes biases in the visual texture but in this case towards the higher end of the pixel value. Similar to section 4.3.2 above, the skew shows the biases of the visual texture in the distribution even though the texture of the material is actually periodical.

4.3.4 Histogram Case 3: (50% polyester and 50% olefin jacquard, Multicolor Color) (Row 4, Column 4)

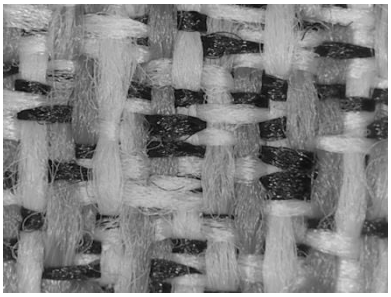

(a) Gray-scale Image

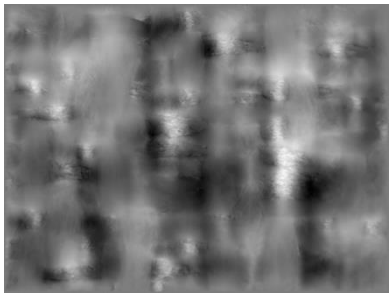

(b) Depth Map

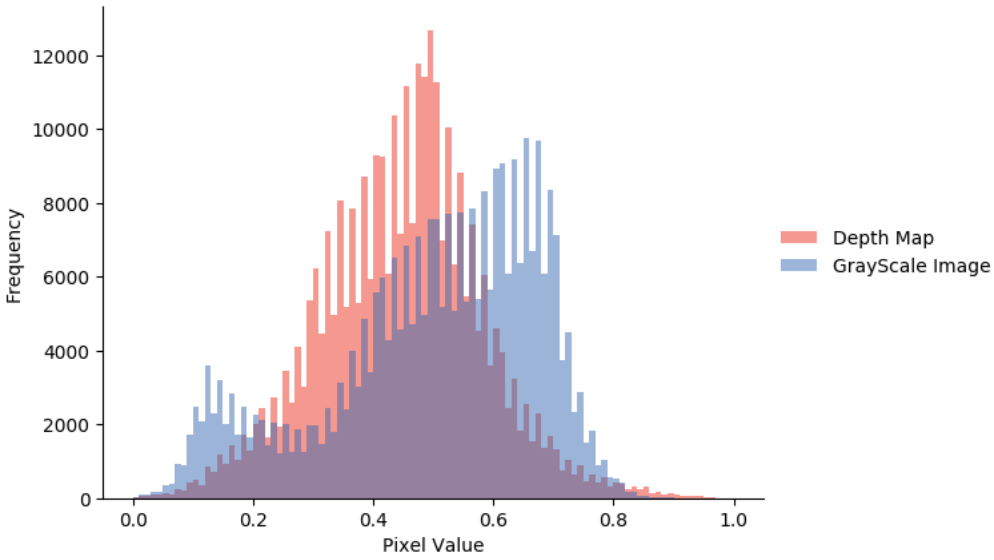

(c) Histogram

Figure 62: Histogram Analysis, Material Sample (Row 4, Column 4)

The material for Histogram Case 3 is the black and white color mixture of 50% polyester and 50% olefin jacquard. From the histogram, it can be seen that the gray-scale histogram has two peaks instead of one. This is caused by the high contrasting black and white color patterns in the gray-scale image. The contrasting color pattern is a form of albedo texture that can be seen visually, but it does correspond to the geometric texture that can be felt. The two peaks shown above shows the visual texture tends to bias toward color and depth map provide a more accurate means to show geometric texture.

4.4 Sandpaper Test

For the sandpaper test, the reconstruction of a block of wood sanded by different various grit of sandpaper (80, 100, 120, 180, 220) will be visually analyzed. Figure 63 shows the wood block that was used in the experiment. Each of the section with sanded with only a single grit of sandpaper without slowly progressing from 80 to 220.

Figure 63: Wooden Block sanded using different grit of sandpaper

Figure *65* shows the results of the wood treated with a different grit of sandpaper. From the reconstruction, we can see that Figure *65*(a), 80 grit sandpaper, tends to have a larger coarse texture compared to the other grit. Figure *65*(b)(c)(d) shows the general trends of becoming smoother as the grit becomes higher. However, Figure *65*(e) shows a very grainy structure that looks rougher. This effect is caused by skipping grits when sanding wood where finer sandpaper could not remove bigger structure on the wood which coarser sand paper could remove. Figure *64* shows this effect of skipping grits causing irregular structure in the wood surface.

Figure 64: Effect of Skipping Grits on Wood, reprinted from Woodworker's Journal[120]

[120] Dresdner, "Spending Less Time and Effort on Sanding - Woodworking | Blog | Videos | Plans | How To."

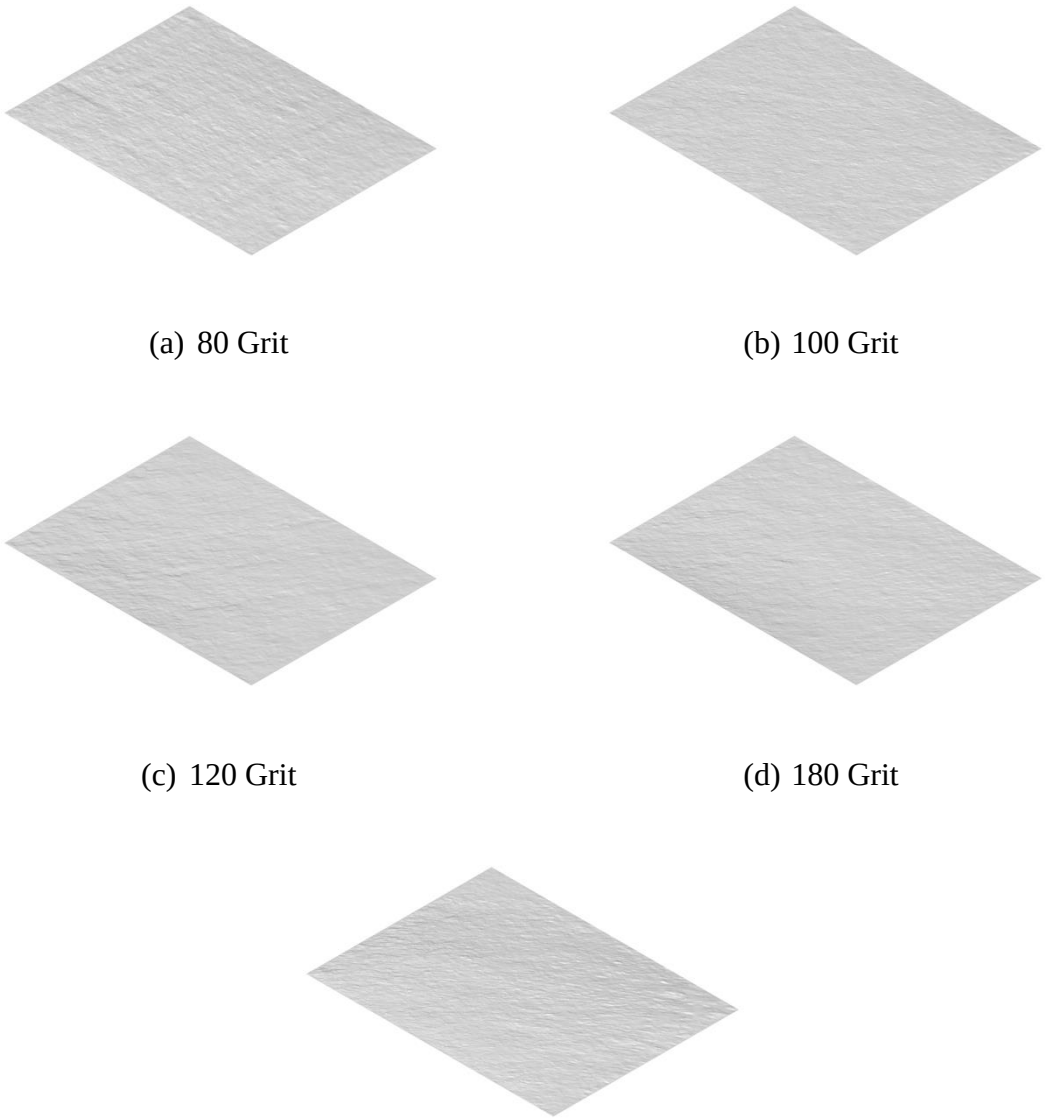

(a) 80 Grit (b) 100 Grit

(c) 120 Grit (d) 180 Grit

(e) 220 Grit

Figure 65: 3D Reconstruction of Sanded Wood using varying sandpaper grit

4.5 Technical Limitation

One limitation of the current system is that it works well with flat surfaces as microscope focus does not work well when it is too close to the sensor. Improvement could be made to have a wider depth of field in order to accommodate for the non-flat material. Since the proposed 3D texture scanner work in the case of Lambertian model, it does not deal

particularly well with specular reflection. In addition, some specular properties of material are more apparent in micro scale than they are at object scale. Hence, this causes a model to exaggerate the error from these specular highlights. For cases where the textile samples are ideally matte, the prototype was able to reproduce relatively good 3D reconstruction. In addition to the specular reflection of material, shadow causes many problems in the current model.

(a) Image Capture with 180° Light

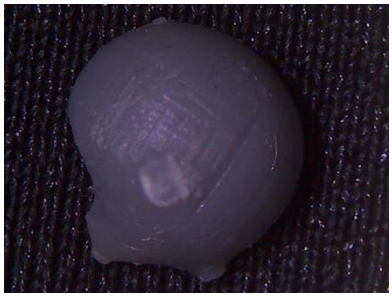

(b) Image Capture with 45° Light

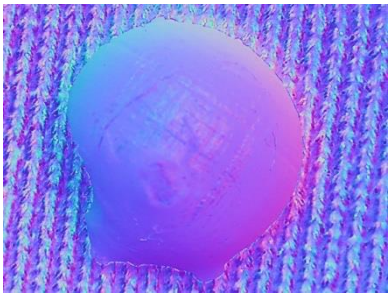

(c) Normal Map

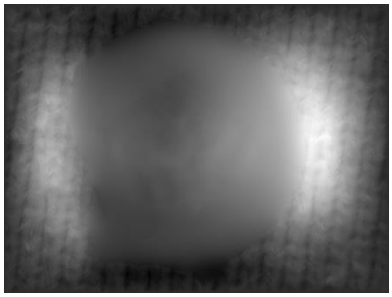

(d) Normalized Depth Map

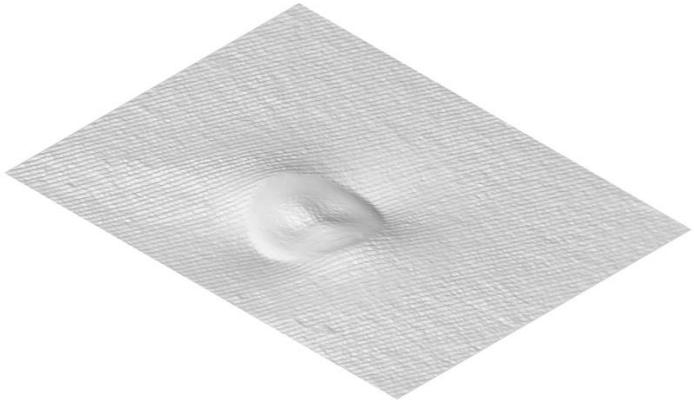

(e) 3D Reconstructed Rendering

Figure 66: Specular and Shadow Effect on Lambertian Photometric Stereo

Figure *66* shows the effect of shadow and specularities on the reconstruction algorithm. The result shows that the height at specular spots is overestimated and height near shadow area are underestimated.

Besides the reductive reflection model, the current system does not calibrate the effect of LEDs position so the images at various azimuth have different overall temperatures. This is because some color tends to reach the location better at a particular angle since position the RGB diode is in a different location at each azimuth angle. Further image pre-processing would be helpful in eliminating some noise caused by the varying color in the different azimuth angle of the light.

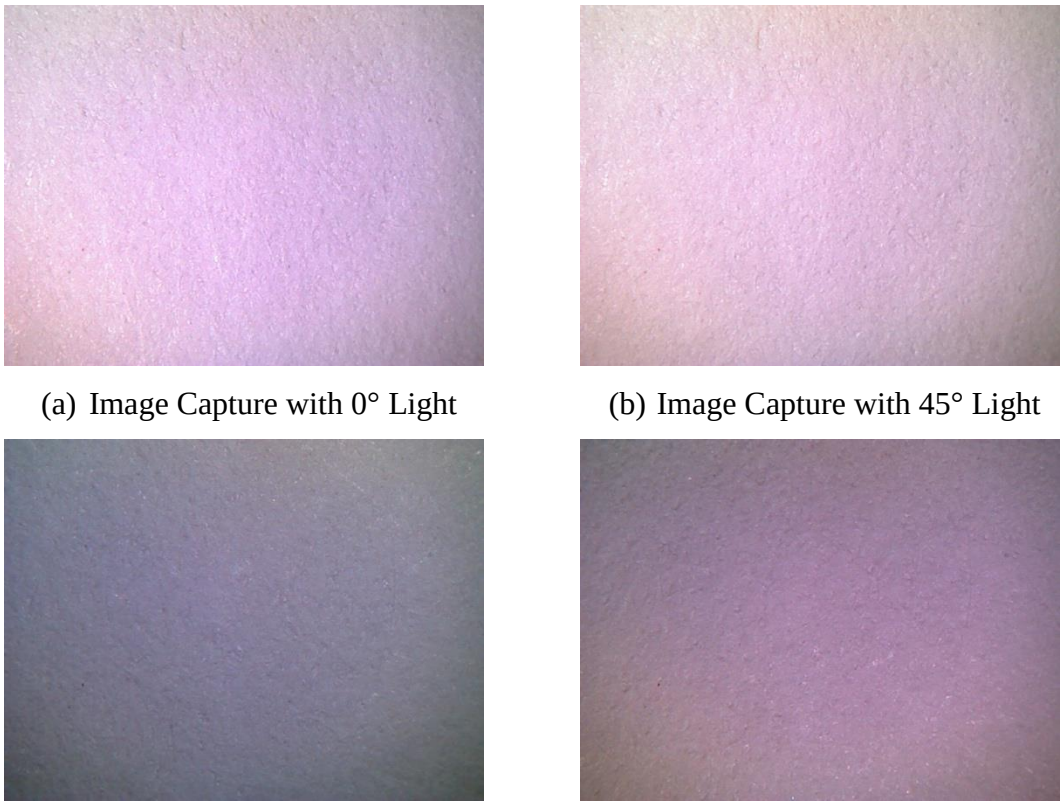

(a) Image Capture with 0° Light (b) Image Capture with 45° Light

(c) Image Capture with 135° Light (d) Image Capture with 270° Light

Figure 67: Uncalibrated RGB LEDs

4.6 Experts Interviews

To inform the use case scenario of the texture scanning system, an interview and discussion with the 3D texture scanning prototype system was conducted. The interview will investigate the possible applicability in the field of the participants. The participants were one graduate student and two professors from Carnegie Mellon University. The participants' fields of expertise include computer science, architecture and electrical engineering. More specific, two of the participants were conducting research in the field of computational textile (textile modeling, simulation, CAD and fabrication), and one of the participant was conducting research in a new form of material synthesis in the context of build environment (bio-plastic material modeling, simulation and fabrication).

The question of the interview will be set in the context of the participant's academic research field. The interview ranged from 25 to 55 minutes. The interview and discussion were based around the 3D texture scanning prototype tools and its applicability in the research field of the participants. The interview and discussion start with showing the prototype in action by scanning some samples and seeing the visualization of recovered 3D texture along with normal map, depth map, and histogram of a depth map. In addition to the low resolution visualization on the prototype screen, the 3D model file of previously captured textures were shown on the Rhinoceros 5. Participants were allowed to suggest different materials to scan and see the both successful and fail results on the prototype screen. The questions in the interview and discussion includes: "What are the possible use case of such tools in the {field of the participants}?", "What the important aspect of understanding geometry at this scale?", "In terms of understanding material in {field of the participants}, how important is geometry when compared to physics of the material?", "Would haptic rendering useful, in addition to the visualization and 3D model, for understanding material through haptic perception?" From these questions, participants speculate on answers and formulate more questions which then become part of the interview and discussion.

For the interview, the results are grouped based on the central theme discussed by the participants. The themes involve a speculative use case scenario and a general impression of the system. The following are the themes that emerged from the discussion:

4.6.1 Measurement tool for understanding material behavior.

All the participant suggested that there is a need for quantitative measurement tool that analyze material structure which affect their behavior in the real world.

- P1 commented, "[In the 3D textile context], that kind of simulation feedback [3D fabric simulation] is going to be useful in the future. To get there, we need a **measurement system.** "
- P2 remarked, "Especially when you are investigating new materials, that the **understanding of material behavior over time**."
- P3 stated, "System like this would **provide some quantification** [of texture]…"

4.6.2 Fine tuning physics simulation through real world material structure

The participant finds the challenge of modeling unknown material accurately in physics simulation and they believe that modeling the microstructure would help predict material behavior.

- P1 remarked, "The challenge is to measure real world sample and **tune the constant of the physics** so that they actually match"
- P2 remarked, "**Enabling a higher resolution of tuning** between the kind of material and fabrication."
- P3 remarked, "**Understanding the structure** is critical to that step how do we do draping on [Textile CAD] software."

4.6.3 Cataloging new unknown material

Developing a catalogue of unknown material using the prototype texture scanner was seen as one possible use case scenario.

- P1 remarked, "There might be advantages in system that allows you to give people **point of reference for new material** … without having the thing [physical materials]."

- P2 remarked, “This tool can help catalogue **material affects and material expression** of these things we know nothing about [Bioplastic], which will help **bridge the gap between material, fabrication, and environment**.”
- P3 suggested, “…**Identifying different fabric** that you don’t know intrinsically how they were made... This system could potentially detect that.”

4.6.4 Finding a similar substitute material

Identifying similar material through microscopic structure analysis to substitute for more expensive material.

- P1 remarked, “When you are doing design with expensive fabric, … you may want to provide them with **physical comparison for this stand in material**.”

4.6.5 Accessibility of the Prototype (Low Cost)

The 3D texture scanner prototype was seen as a low-cost alternative to the higher end industrial laser profilometer.

- P3 mentioned, “This concept is **accessible** [when compared to high tech texture scanner] … you can hold camera to something and it gives you a rudimentary scan.”

4.7 Discussion

The experiment described in the previous chapter shows a preliminary success in reconstructing material 3D structure at the microscopic scale using a low-cost method. Such effort in understanding material microstructure is useful in understanding material performance in relation to its microstructure. In addition, the 3D microgeometry at this scale also could be used as a part of a haptic model in addition to the force-based model for simulating material roughness in the digital realm. From the various interview themes, it shows that such microscopic texture capturing tools are useful in design fabrication where modeling the behavior of the unknown material is essential. Menges shows that understanding the anisotropic properties of wood can be used as part of the generative

driver in design computation rather than an afterthought.[121] Such material understanding of material microstructure can refine the knowledge of material behavior. By combining, the material behavior at the object scale and also understanding the microstructure can open up new design processes and opportunities.

4.7.1 Cultivating Objective Material Knowledge

From the six material case studies (three successes, three failures), the prototype shows various successes and challenges of the system. The 3D texture scanner prototype was able to reconstruct normal map (.png), depth map (.png), and 3D mesh (.obj & .ply) file for use in the Computer-Aided Design software. Such files are not only useful for graphical texture mapping for visualization, it can be used to analyze the material structure through the 3D meshes. As the theme from the interview shows, the potential use case should be to analyze and model material structure quantitively for the purpose of understanding material behavior. This form of cultivating the objective material knowledge which are useful in designing and fabrication with unknown material. This is not to say that such tools could not be use with known material. Looking at the material structure at a different scale provide a different material knowledge which may be useful in the object scale design and fabrication. Menges shows that though wood have been use in many designs and fabrication, there are microscale elements which can open up to a new form of design process and fabrication method.[122] For example, an understanding of anisotropic properties of wood at the microscopic level allows a designer to know which direction the wood can bend more. Such understanding material can be derived from modeling the 3D microstructure of the wood on the surface and thesis proposed prototype provide the ability to cultivate objective material knowledge through 3D reconstruction of surface microstructure.

4.7.2 Cultivating Subjective Material Knowledge

The bigger goal of this thesis is to help cultivate both the objective knowledge (quantitative measurement) and subjective knowledge (feel of the material). The feel of

[121] Menges, “Material Resourcefulness: Activating Material Information in Computational Design.”
[122] Menges.

material could be modeled by combining both geometrical modeling and physics-based modeling of the material texture. This prototype contributes a step towards realistic haptic modeling of material that could be rendered using various haptic rendering methods. The ability to mimic and reproduce the material roughness in the computational method may be helpful when material of a large quantity is not available. The haptic rendering that could provide the feel of material for the subjective understanding of material will be addressed in the future work. Following the Bauhaus traditional of sensory training, if the technology of haptic rendering hardware and software are improved, the digital version of sensory training could provide access to hundreds of thousands of materials feeling at your fingertips. Such a system would allow students and designers to understand the material feels of many samples which they may not able to get. However, this abstract form of sensory stimulation would still miss some complex properties of material that are harder/impossible to model.

5. Conclusions

5.1 Conclusions

This thesis provides a new perspective of material through the lense of a 3D microscopic texture scanner prototype which could enrich our understanding of material for design and inform both the objective and subjective material knowledge in the age of digitalization. By zooming into the microscopic view of the material and reconstructing them in 3D, the thesis provide a new method to understand material surface structure in the context of design and it is also a step towards better material-informed haptic simulation by modeling the one (microgeometry modeling of material) of the various material properties. Furthermore, the thesis provide a brief literature survey on methods of representation, encoding, and decoding in order to pick the most relevant methods for capturing and rendering 3D microscopic texture. Through this literature survey, the thesis identify various advantages and disadvantages of representation, encoding and decoding haptic texture which inform the method which was used in this thesis.

The result from the prototype shows promising results in its ability to scan 3D texture at the microscopic scale. The prototype provides various model files (.ply, .obj, depth map, normal map) which can be used in various CAD and image processing software. Such results are useful in various aspect of design which includes: material modeling (data collection for various unknown materials), a new perspective of seeing and feeling material through micro scale, and sampling texture for generative and parametric design system. In addition to careful documentation and analysis of the result, the interview verified that such a system could be use for tuning the physics of simulation for each unique material (material tuning), providing a way to catalogue unknown material (material modeling), and finding similar materials (classification). The interview was able spark and verify that the prototype can enrich material knowledge through the process of modeling unknown material using their microscopic structure.

The purpose of scanning texture at the microscopic scale allows us to not only model the 3D structure of the material surface but also to take a step toward better modeling for

haptic texture simulation. The bigger goal of the proposed system is to create one aspect of the interface for the “Practiced Digital Hand” which includes haptic simulation and rendering of material properties. This thesis takes a step towards this goal by modeling the 3D microgeometry of material texture, which will be useful in haptic rendering. Such tools can bring the sensorial aspects of material into the realm of design digital media and provide some material response in the CAD software.

5.2 Contribution

This thesis proposes an open sourced 3D microscopic reconstruction system using low cost off-the-shelf components for microtexture analysis. Such photometric stereo system are usually done at the object scale and microscopic photometric stereo includes expensive component such as laboratory microscope, expensive macro lens system, and complicated gel-based sensors. The current method only uses an off-the-self camera with custom open-sourced design LEDs ring. This thesis was able to show a proof of concept for capturing and reconstructing 3D texture at the microscopic scale using a few low-cost components.

Following the Bauhaus tradition of sensory training, this thesis tries to create a digitally informed version of sensory training by using modern technology. The thesis was able to extend one of the sensory training components (looking at microscopic texture image to looking at 3D microscopic reconstruction of texture). It also provides a step towards modeling haptic texture that could be used for virtual tactile training.

In addition, the thesis provides a brief survey of technical literature in terms of representation, encoding, and decoding of visual and haptic texture. Each of the relevant literature includes at least three subcategories which could be useful in understanding the computational method of codifying texture.

5.3 Next Steps

One immediate next step toward improving the system is to be model the more type of material which does not follow Lambertian model and follows a more complex lighting

model such as Phong model of reflection.[123] Phong model of reflection would allow the Photometric Stereo image formation model incorporate both Lambertian and specular surface. There are also efforts to create a more generalized and "robust" form of photometric stereo which account for shadows and specular surfaces.[124] However, they are still failed when there are a certain percentage of specularities.

With recent advances in haptic rendering hardware and software, it would be possible to use the model created in thesis with texture synthesis algorithm to create larger texture grid and render one aspect of material properties (geometric roughness). However, it has to be noted that the realistic rendering of material properties is still far from reality.

Another potential use case of this scanner is to use the scan produce to sample and remix for the purpose of design. Sayjel Vijay Patel et al. proposed various use a case of sample texture in design (generative system, remixing system, parametric system).[125] This potential to generate and remix new texture is interesting as a creative application and also as a method to fabricate new texture assuming commercial 3D printers can print at sub-micrometer scale.

[123] Phong, "Illumination for Computer Generated Pictures."
[124] Wu et al., "Robust Photometric Stereo via Low-Rank Matrix Completion and Recovery"; Ikehata et al., "Robust Photometric Stereo Using Sparse Regression."
[125] Patel and Tam, "3D Sampling Textures for Creative Design and Manufacturing"; Patel and Mueller, "3dj: 3d Sampling Haptic and Optically Performative Textures Remixed from 3d Scans BT - Modelling Behaviour: Design Modelling Symposium 2015"; Patel, Tam, and Mueller, "3DJ: An Analytical and Generative Design System for Synthesizing High-Performance Textures from 3D Scans BT - Design Computing and Cognition '16."

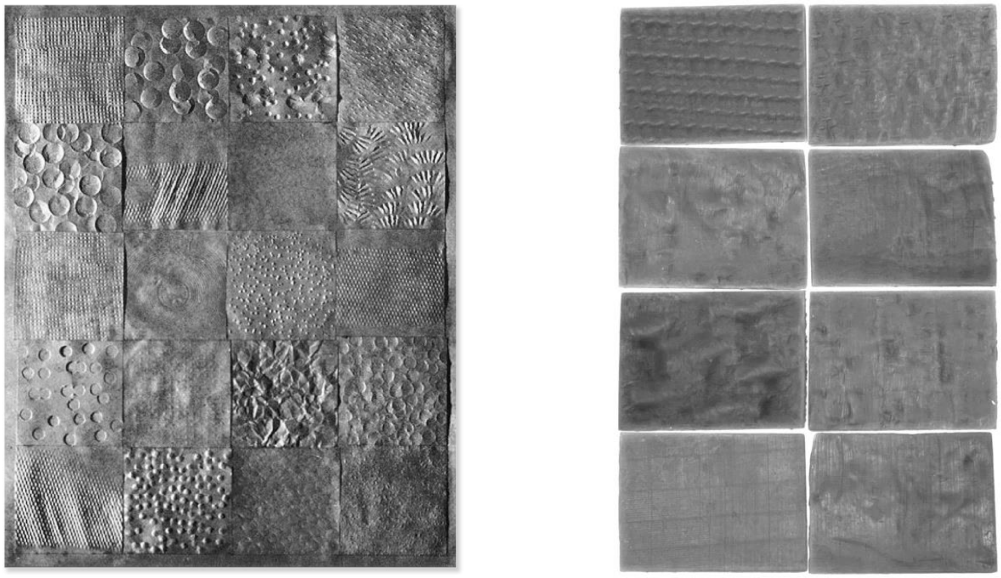

(a) Gerda Marx (Bauhaus, second semester, 1927), reprinted from "*The New Vision*"[126]

(b) 3D Print of Reconstructed Texture (See Appendix C for more detail)

Figure 68: Comparison of Bauhaus Surface Treatment and 3D Print of Reconstructed Texture

Using the approach outlined to generate 3D prints of the enlarge texture (See Appendix C), we can extend the Bauhaus tradition of seeing the image texture a microscopic scale to feeling the texture at the microscopic scale. This yields the to create new forms of sensitization training that fuses the haptic sensory training and microscopic texture experiment from the Bauhaus (See Figure 68). It also affords opportunities to extend the Bauhaus tradition into mixed digital and physical workflows. The scanning and capture of microscopic textures can be used to develop a digital library of resources for training that could be 3d printed and felt in the hand or could be introduced in digital contexts to create other formats for sensitization. Such exercises could be used to understand the material structure which are beyond our perception. Though there are no direct practical application of such exercise in design (similar to the Bauhaus Sensory Training and Surface Treatment exercise), this form of exercise could build new relationship between material and designers in the microscopic scale.

[126] Moholy-Nagy and Hoffmann, *The New Vision: Fundamentals of Design, Painting, Sculpture, Architecture*, 48.

6. Bibliography

Adafruit. “NeoPixel Nano 2427 RGB LEDs w/ Integrated Driver Chip - 10 Pack ID: 3484 - $4.95 : Adafruit Industries, Unique & Fun DIY Electronics and Kits.” Accessed April 29, 2019. https://www.adafruit.com/product/3484.

———. “USB Microscope - 5MP Interpolated 220x Magnification / 8 LEDs ID: 636 - $79.95 : Adafruit Industries, Unique & Fun DIY Electronics and Kits.” Accessed April 29, 2019. https://www.adafruit.com/product/636?gclid=Cj0KCQjw7YblBRDFARIsAKkK-dKSUk1Gbe9_k_1rE4I5sQKVTTZ1l0X2s2HcsvUIrSEOT8lXgzRG5SEaAkbhEALw_wcB.

Agrawal, Amit, Ramesh Raskar, and Rama Chellappa. “What Is the Range of Surface Reconstructions from a Gradient Field? BT - Computer Vision – ECCV 2006.” edited by Aleš Leonardis, Horst Bischof, and Axel Pinz, 578–91. Berlin, Heidelberg: Springer Berlin Heidelberg, 2006.

Angelopoulou, Maria E, and Maria Petrou. “Evaluating the Effect of Diffuse Light on Photometric Stereo Reconstruction.” *Mach. Vision Appl.* 25, no. 1 (January 2014): 199–210. https://doi.org/10.1007/s00138-013-0507-z.

Bau, Olivier, Ivan Poupyrev, Ali Israr, and Chris Harrison. “TeslaTouch: Electrovibration for Touch Surfaces.” In *Proceedings of the 23Nd Annual ACM Symposium on User Interface Software and Technology*, 283–92. UIST ’10. New York, NY, USA: ACM, 2010. https://doi.org/10.1145/1866029.1866074.

Benko, Hrvoje, Christian Holz, Mike Sinclair, and Eyal Ofek. “NormalTouch and TextureTouch: High-Fidelity 3D Haptic Shape Rendering on Handheld Virtual Reality Controllers.” In *Proceedings of the 29th Annual Symposium on User Interface Software and Technology*, 717–28. UIST ’16. New York, NY, USA: ACM, 2016. https://doi.org/10.1145/2984511.2984526.

Blinn, James F. “Simulation of Wrinkled Surfaces.” In *Proceedings of the 5th Annual Conference on Computer Graphics and Interactive Techniques*, 286–92. SIGGRAPH ’78. New York, NY, USA: ACM, 1978. https://doi.org/10.1145/800248.507101.

Botvinick, Matthew, and Jonathan Cohen. “Rubber Hands ‘Feel’ Touch That Eyes See.” *Nature*

391, no. 6669 (1998): 756. https://doi.org/10.1038/35784.

Bunge, H.-J. “3 - Orientation Distributions.” In *Texture Analysis in Materials Science*, edited by H.-J. Bunge, 42–46. Butterworth-Heinemann, 1982. https://doi.org/https://doi.org/10.1016/B978-0-408-10642-9.50008-8.

Campion, Gianni. *The Synthesis of Three Dimensional Haptic Textures: Geometry, Control, and Psychophysics*, 2011. https://doi.org/10.1007/978-0-85729-576-7.

Cardoso Llach, D. *Builders of the Vision: Software and the Imagination of Design*. *Builders of the Vision: Software and the Imagination of Design*, 2015. https://doi.org/10.4324/9781315798240.

Catmull, Edwin Earl. “A Subdivision Algorithm for Computer Display of Curved Surfaces.” The University of Utah, 1974.

Culbertson, H, J J López Delgado, and K J Kuchenbecker. “One Hundred Data-Driven Haptic Texture Models and Open-Source Methods for Rendering on 3D Objects.” In *2014 IEEE Haptics Symposium (HAPTICS)*, 319–25, 2014. https://doi.org/10.1109/HAPTICS.2014.6775475.

Dana, K J, and S K Nayar. “Histogram Model for 3D Textures.” In *Proceedings. 1998 IEEE Computer Society Conference on Computer Vision and Pattern Recognition (Cat. No.98CB36231)*, 618–24, 1998. https://doi.org/10.1109/CVPR.1998.698669.

Dana, Kristin J, Bram van Ginneken, Shree K Nayar, and Jan J Koenderink. “Reflectance and Texture of Real-World Surfaces.” *ACM Trans. Graph.* 18, no. 1 (January 1999): 1–34. https://doi.org/10.1145/300776.300778.

Dana, Kristin, and Shree K. Nayar. *3D Textured Surface Modeling*, 1999.

Dourish, Paul. “Where the Action Is: The Foundations of Embodied Interaction,” 256, 2001.

Dresdner, Michael. “Spending Less Time and Effort on Sanding - Woodworking | Blog | Videos | Plans | How To.” Accessed May 13, 2019. https://www.woodworkersjournal.com/spending-less-time-and-effort-on-sanding/.

Efros, A A, and T K Leung. “Texture Synthesis by Non-Parametric Sampling.” In *Proceedings of the Seventh IEEE International Conference on Computer Vision*, 2:1033–38 vol.2, 1999.

https://doi.org/10.1109/ICCV.1999.790383.

Fan, Hao, Lin Qi, Nan Wang, Junyu Dong, Yijun Chen, and Hui Yu. “Deviation Correction Method for Close-Range Photometric Stereo with Nonuniform Illumination.” *Optical Engineering* 56, no. 10 (October 2017): 1–13. https://doi.org/10.1117/1.OE.56.10.103102.

Fritz, Jason P, and Kenneth E Barner. “Stochastic Models for Haptic Texture.” In *Proc.SPIE*, Vol. 2901, 1996. https://doi.org/10.1117/12.263011.

Fua, Pascal. “A Parallel Stereo Algorithm That Produces Dense Depth Maps and Preserves Image Features.” *Machine Vision and Applications* 6, no. 1 (1993): 35–49. https://doi.org/10.1007/BF01212430.

Gonzales, Rafael C, and Paul Wintz. *Digital Image Processing (2nd Ed.)*. Boston, MA, USA: Addison-Wesley Longman Publishing Co., Inc., 1987.

Gorpas, Dimitris, Christos Kampouris, and Sotiris Malassiotis. “Miniature Photometric Stereo System for Textile Surface Structure Reconstruction.” In *Proc.SPIE*, Vol. 8791, 2013. https://doi.org/10.1117/12.2018913.

Haug, Anders. “Acquiring Materials Knowledge in Design Education.” *International Journal of Technology and Design Education* 29, no. 2 (March 2019): 405–20. https://doi.org/10.1007/s10798-018-9445-4.

Heeger, David J, and James R Bergen. “Pyramid-Based Texture Analysis/Synthesis.” In *Proceedings of the 22Nd Annual Conference on Computer Graphics and Interactive Techniques*, 229–38. SIGGRAPH ’95. New York, NY, USA: ACM, 1995. https://doi.org/10.1145/218380.218446.

Ikehata, S, D Wipf, Y Matsushita, and K Aizawa. “Robust Photometric Stereo Using Sparse Regression.” In *2012 IEEE Conference on Computer Vision and Pattern Recognition*, 318–25, 2012. https://doi.org/10.1109/CVPR.2012.6247691.

Ingold, Tim. *Making: Anthropology, Archaeology, Art and Architecture*. Routledge, 2013.

Johnson, Micah K, Forrester Cole, Alvin Raj, and Edward H Adelson. “Microgeometry Capture Using an Elastomeric Sensor.” In *ACM SIGGRAPH 2011 Papers*, 46:1--46:8. SIGGRAPH ’11. New York, NY, USA: ACM, 2011.

https://doi.org/10.1145/1964921.1964941.

Kampouris, Christos, Stefanos Zafeiriou, Abhijeet Ghosh, and Sotiris Malassiotis. “Fine-Grained Material Classification Using Micro-Geometry and Reflectance BT - Computer Vision – ECCV 2016.” edited by Bastian Leibe, Jiri Matas, Nicu Sebe, and Max Welling, 778–92. Cham: Springer International Publishing, 2016.

Klatzky, Roberta, and Susan J. Lederman. “Multisensory Texture Perception.” In *Multisensory Object Perception in the Primate Brain*, 211–30, 2010. https://doi.org/10.1007/978-1-4419-5615-6_12.

Koenderink, Jan J, and Andrea J van Doorn. “Illuminance Texture Due to Surface Mesostructure.” *J. Opt. Soc. Am. A* 13, no. 3 (March 1996): 452–63. https://doi.org/10.1364/JOSAA.13.000452.

Levoy, Marc, Kari Pulli, Brian Curless, Szymon Rusinkiewicz, David Koller, Lucas Pereira, Matt Ginzton, et al. “The Digital Michelangelo Project: 3D Scanning of Large Statues.” In *Proceedings of the 27th Annual Conference on Computer Graphics and Interactive Techniques*, 131–44. SIGGRAPH ’00. New York, NY, USA: ACM Press/Addison-Wesley Publishing Co., 2000. https://doi.org/10.1145/344779.344849.

Mallinckrodt, Edward, A L Hughes, and William Sleator. “Perception by the Skin of Electrically Induced Vibrations.” *Science* 118, no. 3062 (1953): 277–78. https://doi.org/10.1126/science.118.3062.277.

Matsuyama, Takashi, Shu-Ichi Miura, and Makoto Nagao. “Structural Analysis of Natural Textures by Fourier Transformation.” *Computer Vision, Graphics, and Image Processing* 24, no. 3 (1983): 347–62. https://doi.org/https://doi.org/10.1016/0734-189X(83)90060-9.

McCullough, Malcolm. *Abstracting Craft: The Practiced Digital Hand*. Cambridge, MA, USA: MIT Press, 1996.

MCGURK, HARRY, and JOHN MACDONALD. “Hearing Lips and Seeing Voices.” *Nature* 264, no. 5588 (1976): 746–48. https://doi.org/10.1038/264746a0.

Menges, Achim. “Material Information: Integrating Material Characteristics and Behavior in Computational Design for Performative Wood Construction.” In *LIFE in:Formation, On Responsive Information and Variations in Architecture: Proceedings of the 30th Annual*

Conference of the Association for Computer Aided Design in Architecture (ACADIA). ACADIA. New York, New York: Cooper Union, Pratt Institute, 2010.

———. “Material Resourcefulness: Activating Material Information in Computational Design.” *Architectural Design* 82, no. 2 (2012): 34–43. https://doi.org/10.1002/ad.1377.

Meyer, D J, M A Peshkin, and J E Colgate. “Fingertip Friction Modulation Due to Electrostatic Attraction.” In *2013 World Haptics Conference (WHC)*, 43–48, 2013. https://doi.org/10.1109/WHC.2013.6548382.

Moholy-Nagy, L, and D M Hoffmann. *The New Vision: Fundamentals of Design, Painting, Sculpture, Architecture*. New Bauhaus Books. W.W. Norton & Company, inc., 1938. https://books.google.com/books?id=haRPAAAAMAAJ.

Montessori 1870-1952, Maria. *The Montessori Method : The Origins of an Educational Innovation : Including an Abridged and Annotated Edition of Maria Montessori's The Montessori Method*. Lanham, MD : Rowman & Littlefield Publishers, [2004] ©2004, n.d. https://search.library.wisc.edu/catalog/999962597602121.

Nayar, Shree K, Katsushi Ikeuchi, and Takeo Kanade. “Shape from Interreflections.” *International Journal of Computer Vision* 6, no. 3 (1991): 173–95. https://doi.org/10.1007/BF00115695.

Niblack, Carlton Wayne, Ron Barber, Will Equitz, Myron D Flickner, Eduardo H Glasman, Dragutin Petkovic, Peter Yanker, Christos Faloutsos, and Gabriel Taubin. “QBIC Project: Querying Images by Content, Using Color, Texture, and Shape.” In *Proc.SPIE*, Vol. 1908, 1993. https://doi.org/10.1117/12.143648.

Nicodemus, Fred E. “Directional Reflectance and Emissivity of an Opaque Surface.” *Appl. Opt.* 4, no. 7 (July 1965): 767–75. https://doi.org/10.1364/AO.4.000767.

O’Toole, M, J Mather, and K N Kutulakos. “3D Shape and Indirect Appearance by Structured Light Transport.” *IEEE Transactions on Pattern Analysis and Machine Intelligence* 38, no. 7 (2016): 1298–1312. https://doi.org/10.1109/TPAMI.2016.2545662.

“OpenCV: Hough Circle Transform.” Accessed April 29, 2019. https://docs.opencv.org/3.1.0/da/d53/tutorial_py_houghcircles.html.

Osh. “OSH Park ~.” Accessed April 29, 2019. https://oshpark.com/.

Pallasmaa, Juhani. *The Eyes of the Skin : Architecture and the Senses*. Chichester: Wiley, 2012.

Patel, Sayjel V, and Caitlin T Mueller. “3dj: 3d Sampling Haptic and Optically Performative Textures Remixed from 3d Scans BT - Modelling Behaviour: Design Modelling Symposium 2015.” edited by Mette Ramsgaard Thomsen, Martin Tamke, Christoph Gengnagel, Billie Faircloth, and Fabian Scheurer, 527–41. Cham: Springer International Publishing, 2015. https://doi.org/10.1007/978-3-319-24208-8_44.

Patel, Sayjel V, Mark K M Tam, and Caitlin T Mueller. “3DJ: An Analytical and Generative Design System for Synthesizing High-Performance Textures from 3D Scans BT - Design Computing and Cognition ’16.” edited by John. S Gero, 477–94. Cham: Springer International Publishing, 2017.

Patel, Shivang, and Kingston Tam. “3D Sampling Textures for Creative Design and Manufacturing,” 2017.

Patterson, Robert W, and Gale E Nevill. “The Induced Vibration Touch Sensor – a New Dynamic Touch Sensing Concept.” *Robotica* 4, no. 1 (1986): 27–31. https://doi.org/10.1017/S0263574700002447.

Phong, Bui Tuong. “Illumination for Computer Generated Pictures.” *Commun. ACM* 18, no. 6 (June 1975): 311–17. https://doi.org/10.1145/360825.360839.

“Photometric Stereo.” Accessed April 29, 2019. http://www.cs.cornell.edu/courses/cs4670/2018sp/lec25-photometric-stereo.pdf.

Raskar, Ramesh. “Code A: Matlab Code for Poisson Image Reconstruction from Image Gradients.” Accessed April 29, 2019. http://web.media.mit.edu/~raskar/photo/code.pdf.

Raspberry Pi. “Raspberry Pi Store.” Accessed May 14, 2019. https://www.raspberrypi.org/products.

Rognoli, Valentina. *A Broad Survey on Expressive-Sensorial Characterization of Materials for Design Education*. *Middle East Technical University Journal of the Faculty of Architecture*. Vol. 27, 2010. https://doi.org/10.4305/METU.JFA.2010.2.16.

Room&Board. “Free Fabric & Leather Swatches - Fabrics & Materials.” Accessed

April 29, 2019. https://www.roomandboard.com/ideas-advice/explore-materials/fabrics.

Ryer, Alex, Ultraviolet Light, and Visible Light. “Light Measurement Handbook,” 1997.

Schön, Donald A. *The Reflective Practitioner : How Professionals Think in Action*, 1983.

Shin, S, and S Choi. “Geometry-Based Haptic Texture Modeling and Rendering Using Photometric Stereo.” In *2018 IEEE Haptics Symposium (HAPTICS)*, 262–69, 2018. https://doi.org/10.1109/HAPTICS.2018.8357186.

Simchony, T, R Chellappa, and M Shao. “Direct Analytical Methods for Solving Poisson Equations in Computer Vision Problems.” *IEEE Transactions on Pattern Analysis and Machine Intelligence* 12, no. 5 (1990): 435–46. https://doi.org/10.1109/34.55103.

Strong, R M, and D E Troxel. “An Electrotactile Display.” *IEEE Transactions on Man-Machine Systems* 11, no. 1 (1970): 72–79. https://doi.org/10.1109/TMMS.1970.299965.

Sutherland, Ivan E. “The Ultimate Display.” In *Proceedings of the IFIP Congress*, 506–8, 1965.

Szeliski, Richard. *Computer Vision: Algorithms and Applications*. 1st ed. Berlin, Heidelberg: Springer-Verlag, 2010.

Tamura, H, S Mori, and T Yamawaki. “Textural Features Corresponding to Visual Perception.” *IEEE Transactions on Systems, Man, and Cybernetics* 8, no. 6 (1978): 460–73. https://doi.org/10.1109/TSMC.1978.4309999.

Wang, Jing, and Kristin J Dana. “Relief Texture from Specularities.” *IEEE Trans. Pattern Anal. Mach. Intell.* 28, no. 3 (March 2006): 446–57. https://doi.org/10.1109/TPAMI.2006.63.

Woodham, Robert J. “Photometric Stereo: A Reflectance Map Technique For Determining Surface Orientation From Image Intensity.” In *Proc.SPIE*, Vol. 0155, 1979. https://doi.org/10.1117/12.956740.

Wu, Lun, Arvind Ganesh, Boxin Shi, Yasuyuki Matsushita, Yongtian Wang, and Yi Ma. “Robust Photometric Stereo via Low-Rank Matrix Completion and Recovery.” In *Proceedings of the 10th Asian Conference on Computer Vision - Volume Part III*, 703–17. ACCV’10. Berlin, Heidelberg: Springer-Verlag, 2011. http://dl.acm.org/citation.cfm?id=1966049.1966105.

Ye, Xianming, Byungjune Choi, Sungchul Kang, and Hyouk Ryeol Choi. “Profile-Based

Roughness Discrimination with Pen-Type Texture Sensor." *International Journal of Control, Automation and Systems* 8, no. 4 (August 2010): 793–800. https://doi.org/10.1007/s12555-010-0411-5.

Yoshimoto, Shunsuke, Yoshihiro Kuroda, Yuki Uranishi, Masataka Imura, and Osamu Oshiro. "Roughness Modulation of Real Materials Using Electrotactile Augmentation BT - Haptics: Neuroscience, Devices, Modeling, and Applications." edited by Malika Auvray and Christian Duriez, 10–17. Berlin, Heidelberg: Springer Berlin Heidelberg, 2014.

7. Figures

8. Appendix

Appendix A: 28 Sample Material Reconstructions

Acrylic (100%) Weave

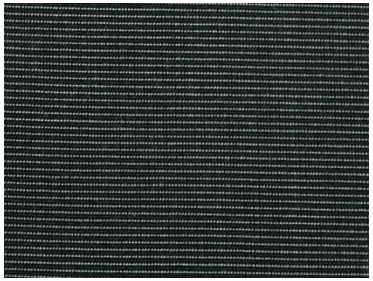

Material Scanned

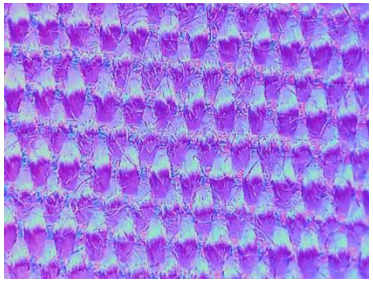

Normal Map

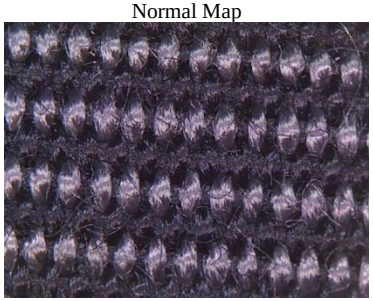

Albedo

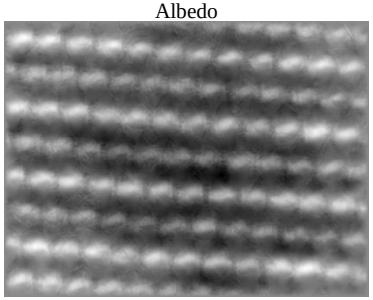

Normalized Depth Map

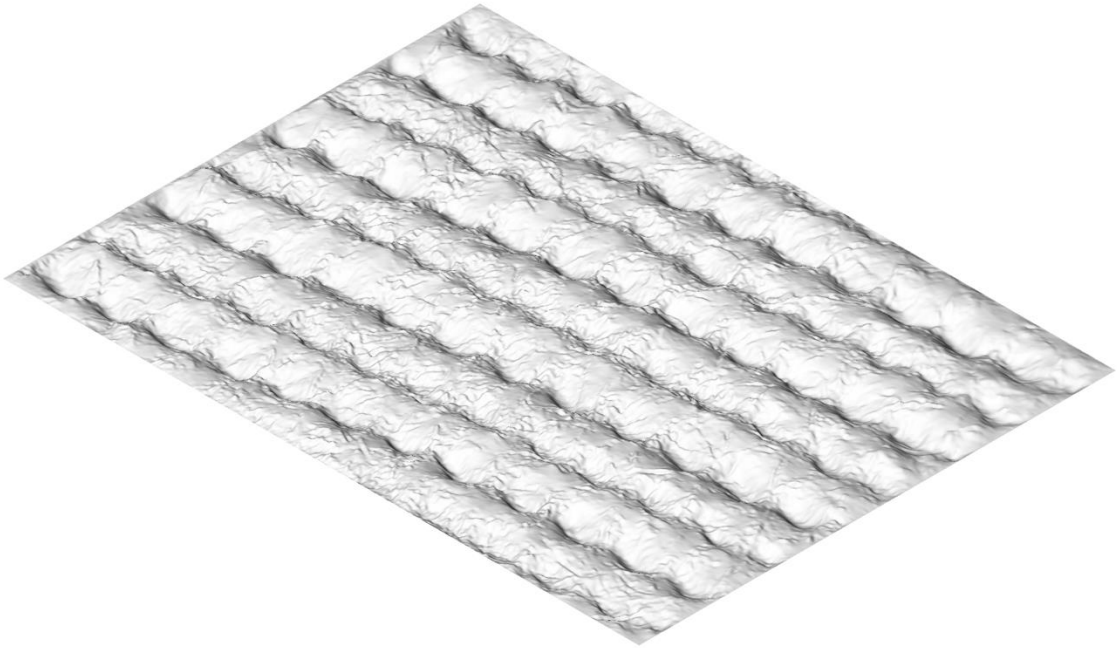

3D Reconstruction Rendering

Polyester (100%) micro-weave

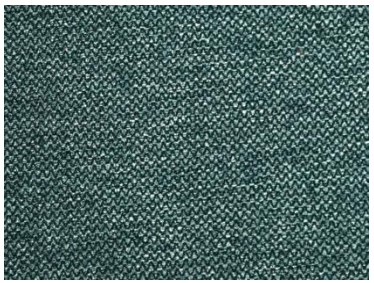

Material Scanned

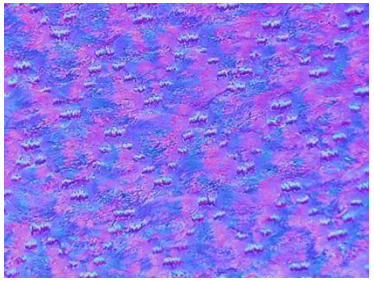

Normal Map

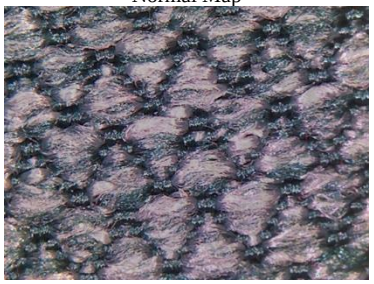

Albedo

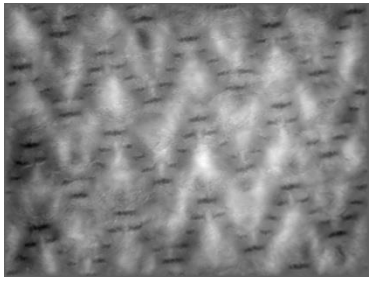

Normalized Depth Map

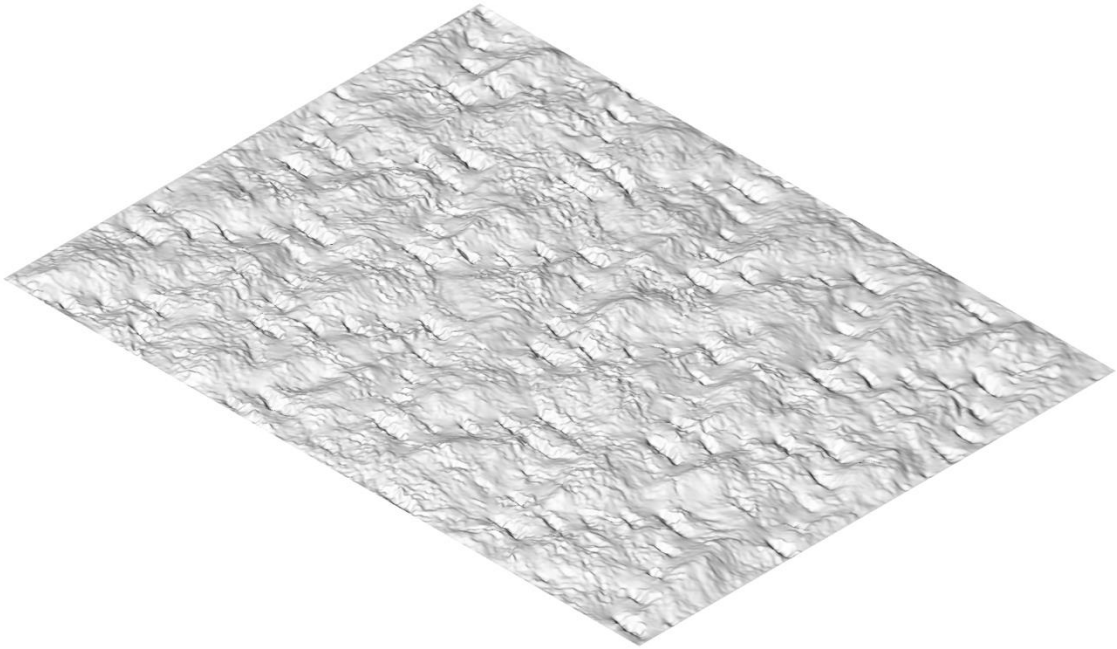

3D Reconstruction Rendering

Cotton (100%) Twill

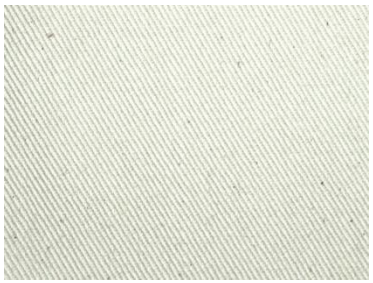

Material Scanned

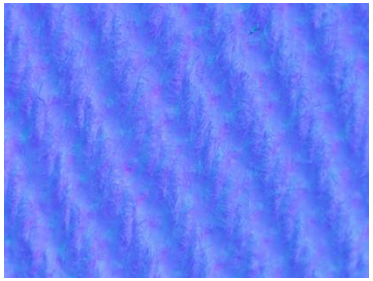

Normal Map

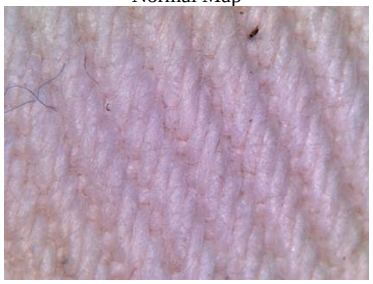

Albedo

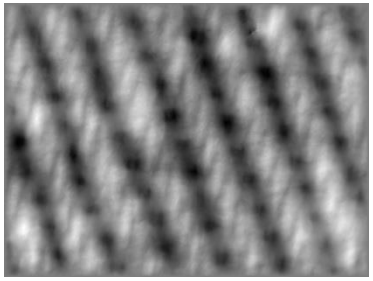

Normalized Depth Map

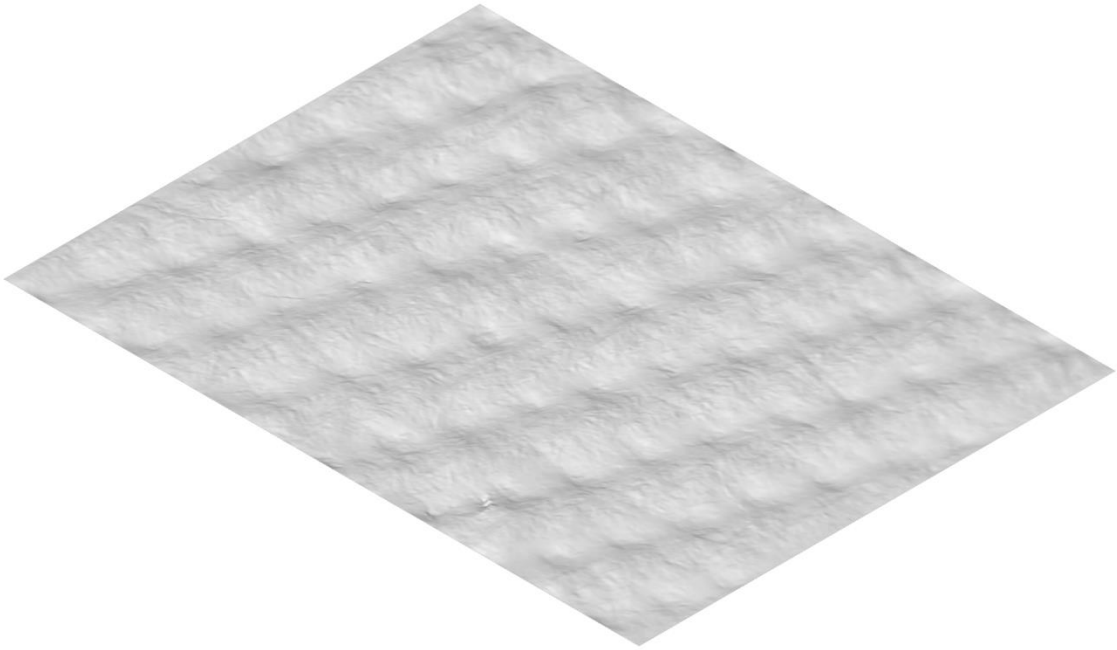

3D Reconstruction Rendering

Polyester (82%), Cotton (18%) Velvet

Material Scanned

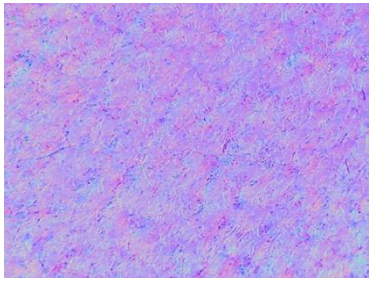

Normal Map

Albedo

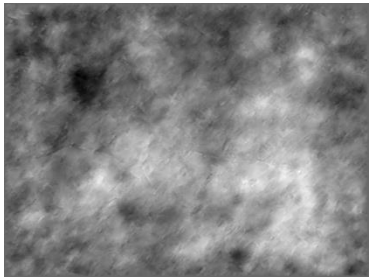

Normalized Depth Map

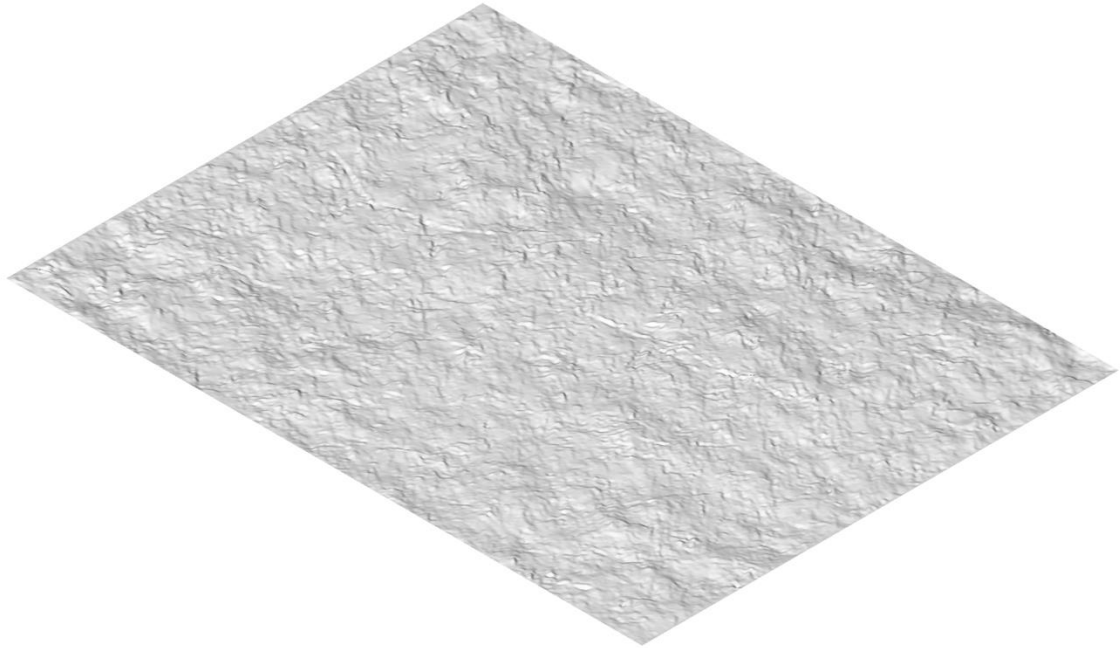

3D Reconstruction Rendering

Polyester (100%) micro-suede

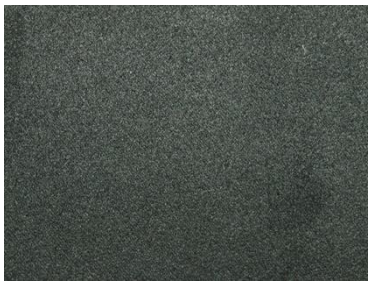

Material Scanned

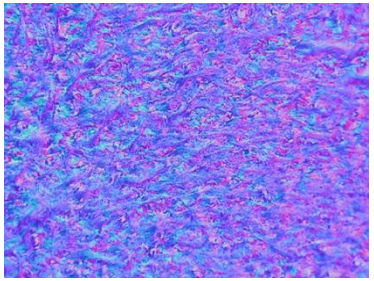

Normal Map

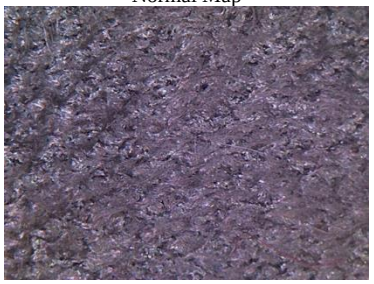

Albedo

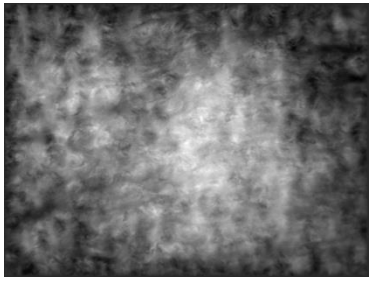

Normalized Depth Map

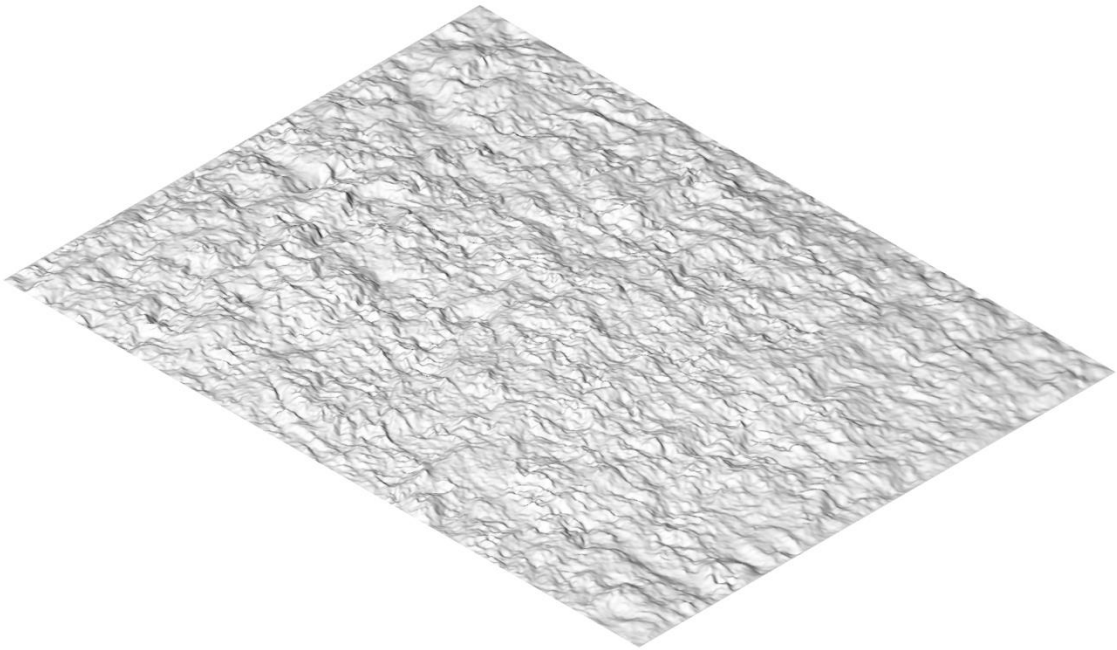

3D Reconstruction Rendering

Polyester (43%), Cotton (39%), Olefin (18%) Jacquard

Material Scanned

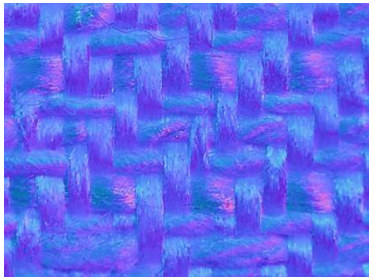

Normal Map

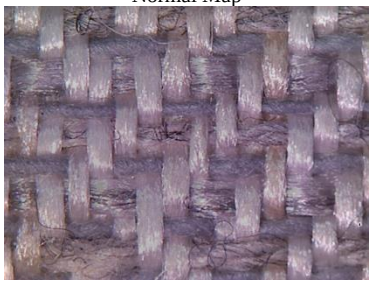

Albedo

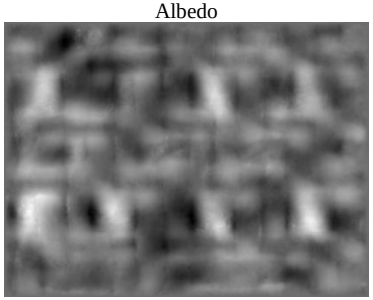

Normalized Depth Map

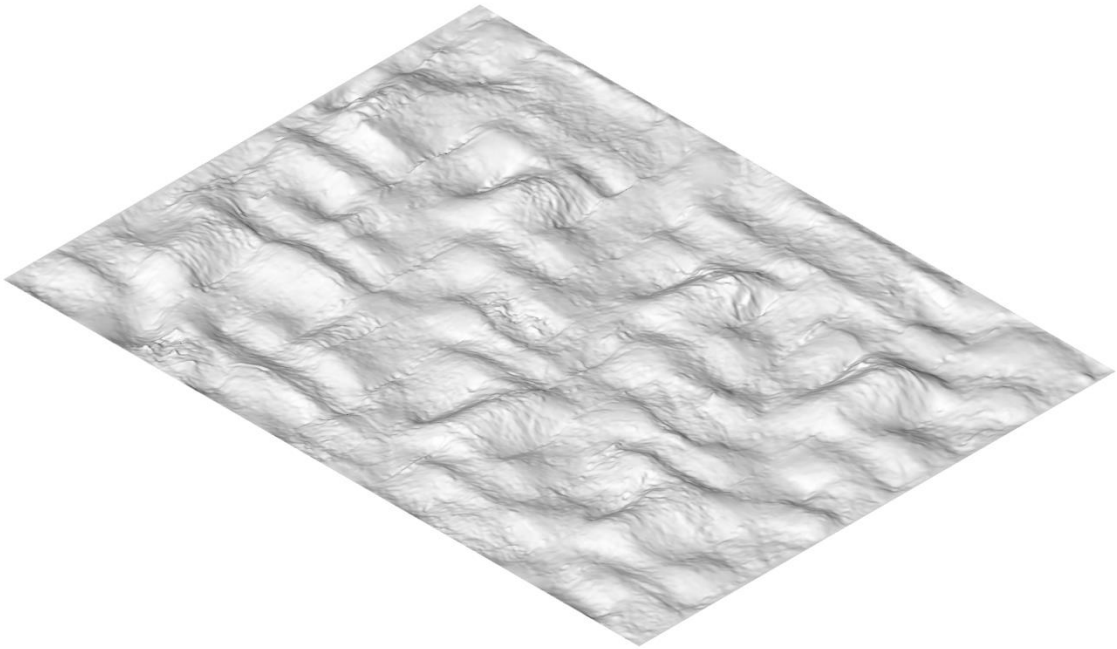

3D Reconstruction Rendering

Polyester (43%), Acrylic (39%), micro-bouclé

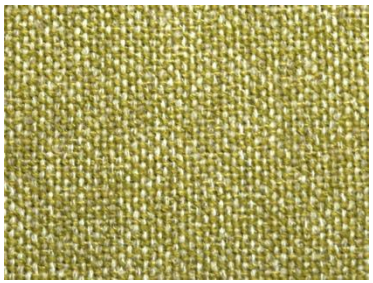

Material Scanned

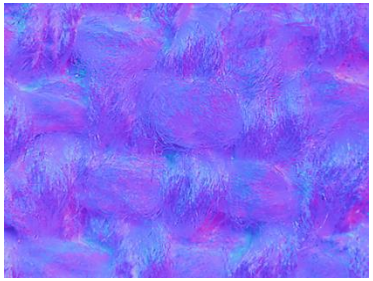

Normal Map

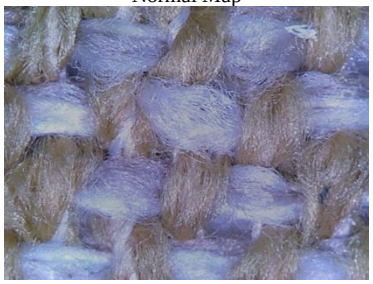

Albedo

Normalized Depth Map

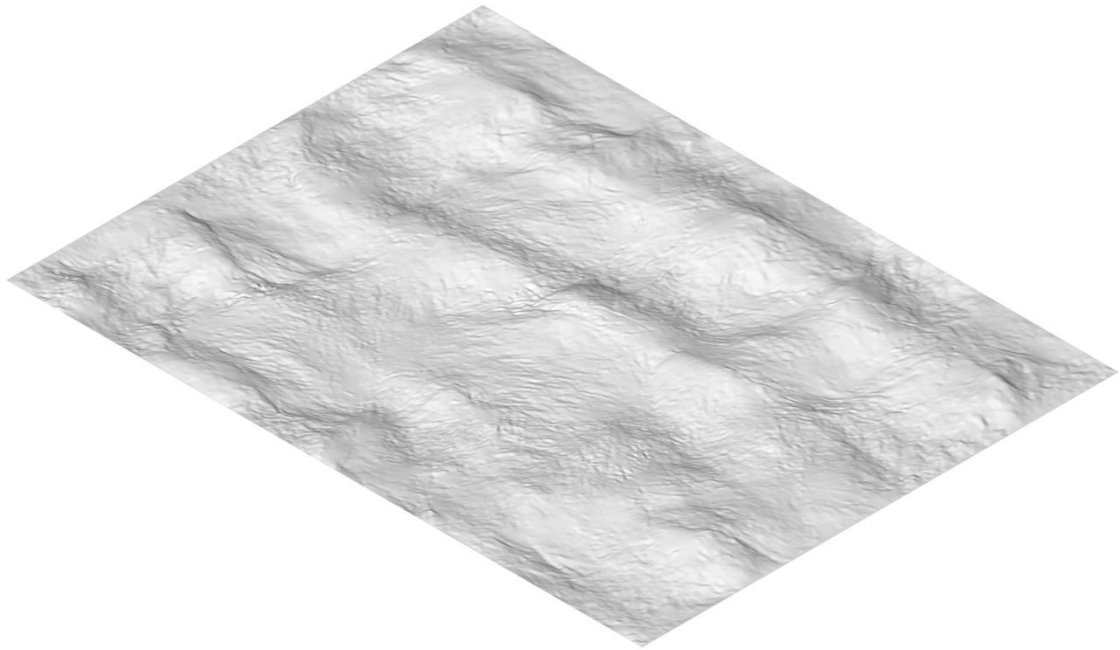

3D Reconstruction Rendering

Polypropylene (98%), Polyester (2%) Bouclé

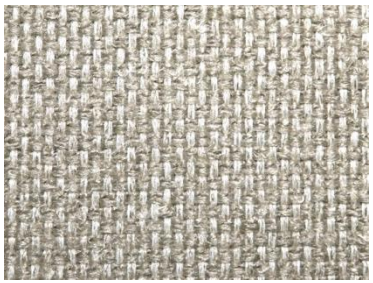

Material Scanned

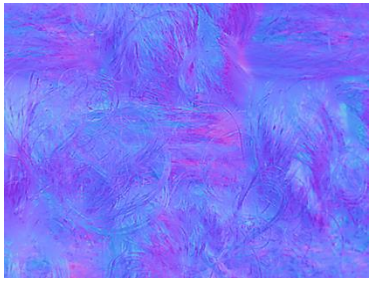

Normal Map

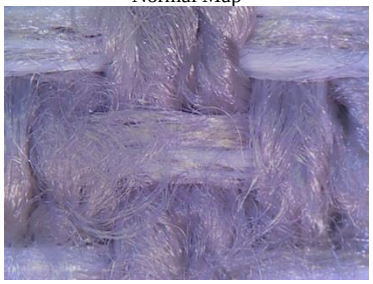

Albedo

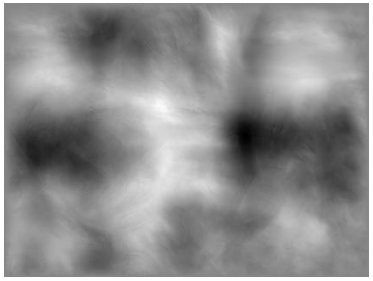

Normalized Depth Map

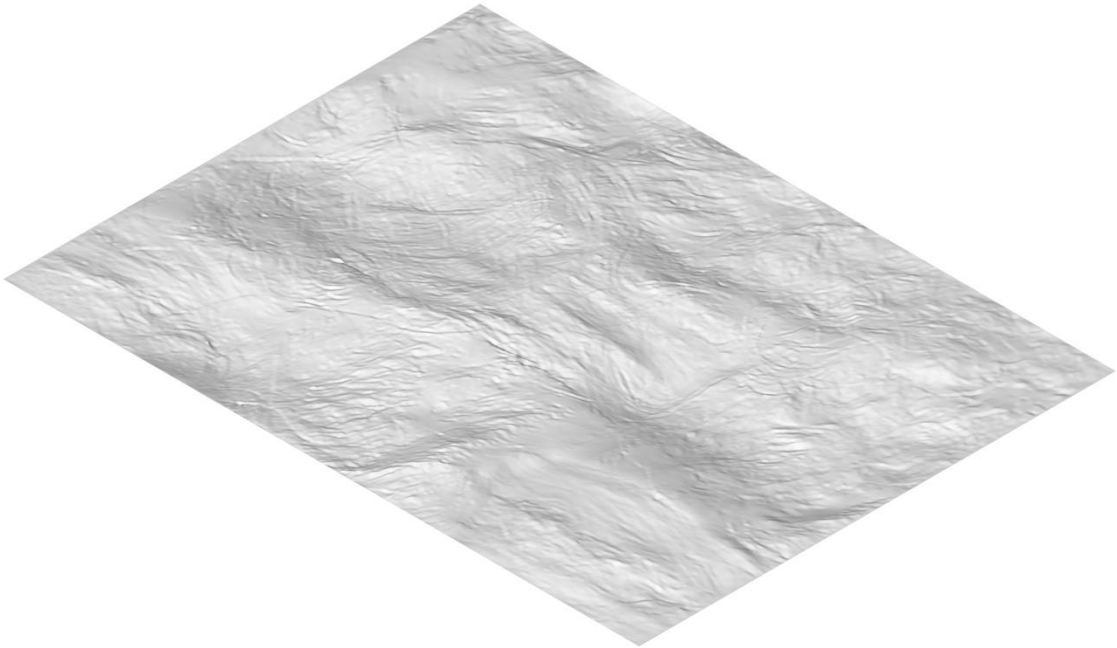

3D Reconstruction Rendering

Olefin (51%), Polyester (49%) Jacquard

Material Scanned

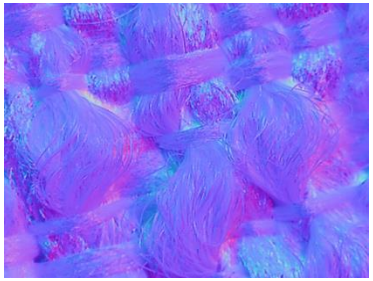

Normal Map

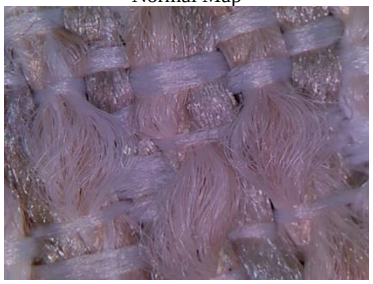

Albedo

Normalized Depth Map

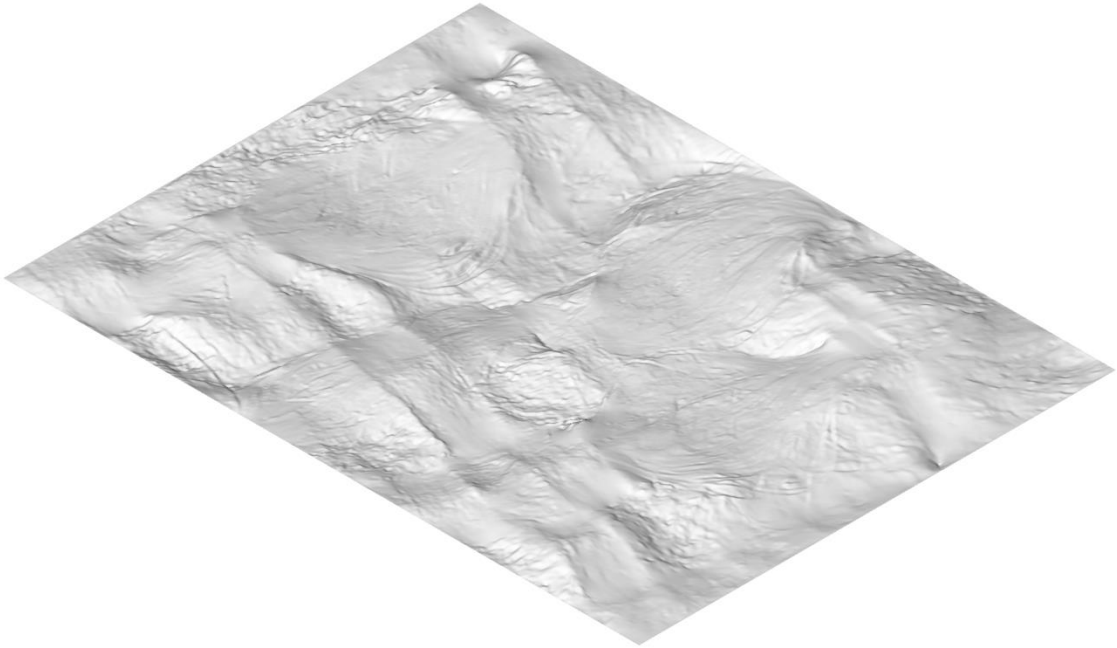

3D Reconstruction Rendering

Polypropylene (75%), Polyester (25%) Bouclé

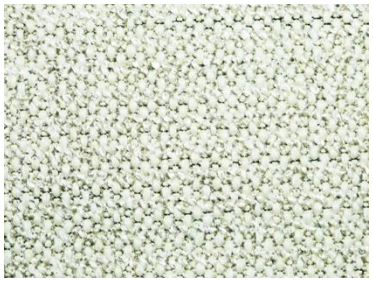

Material Scanned

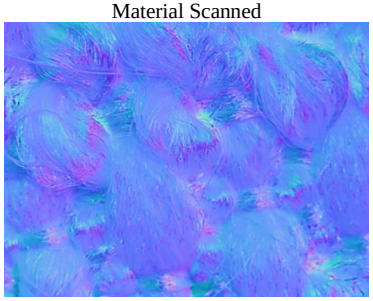

Normal Map

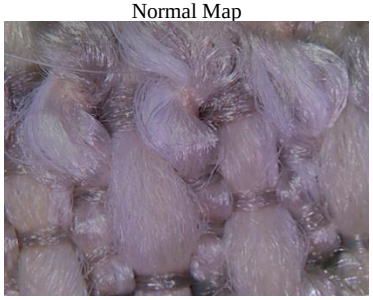

Albedo

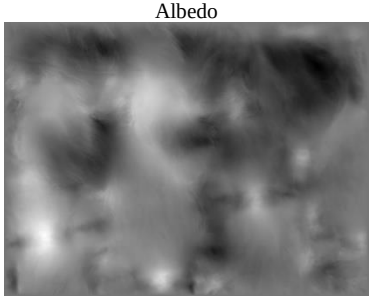

Normalized Depth Map

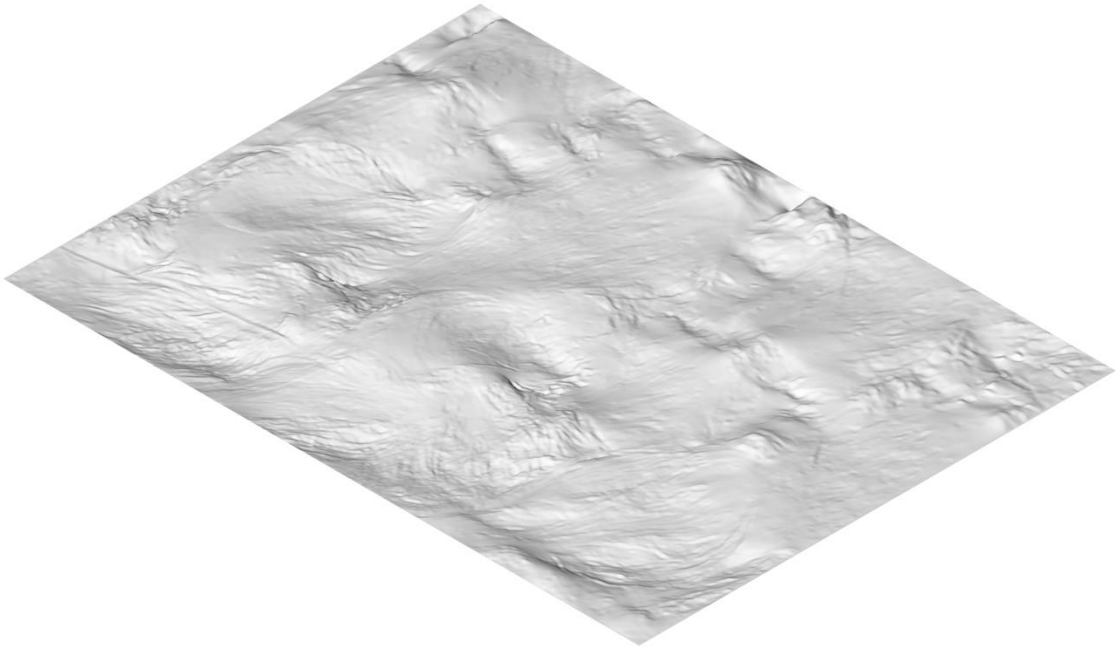

3D Reconstruction Rendering

Cotton (98%), Linen (2%) Weave

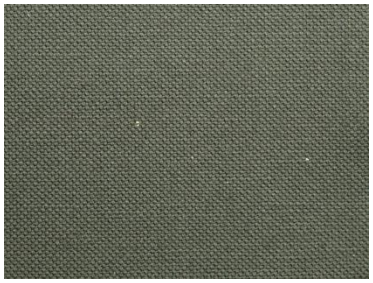

Material Scanned

Normal Map

Albedo

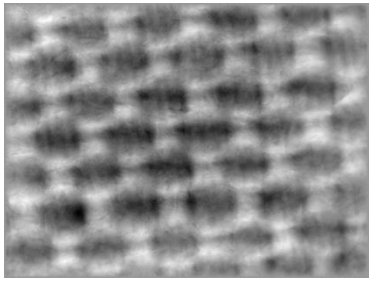

Normalized Depth Map

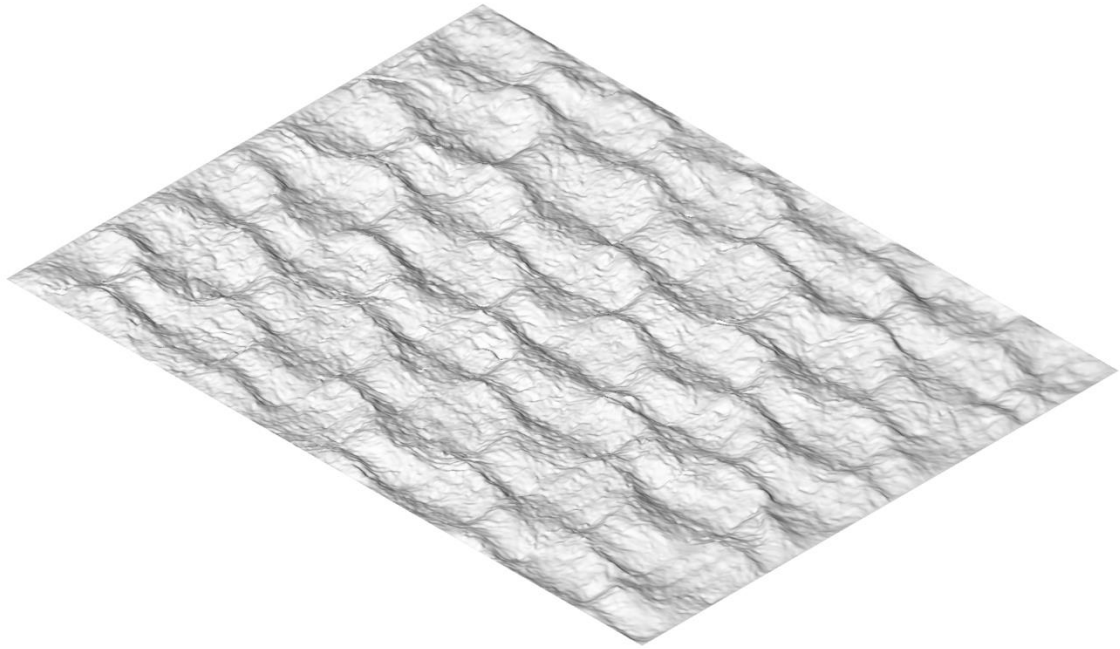

3D Reconstruction Rendering

Polyester (80%), Rayon (20%) Bouclé

Material Scanned

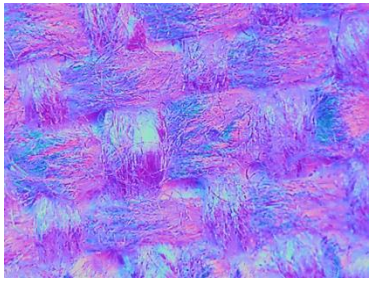

Normal Map

Albedo

Normalized Depth Map

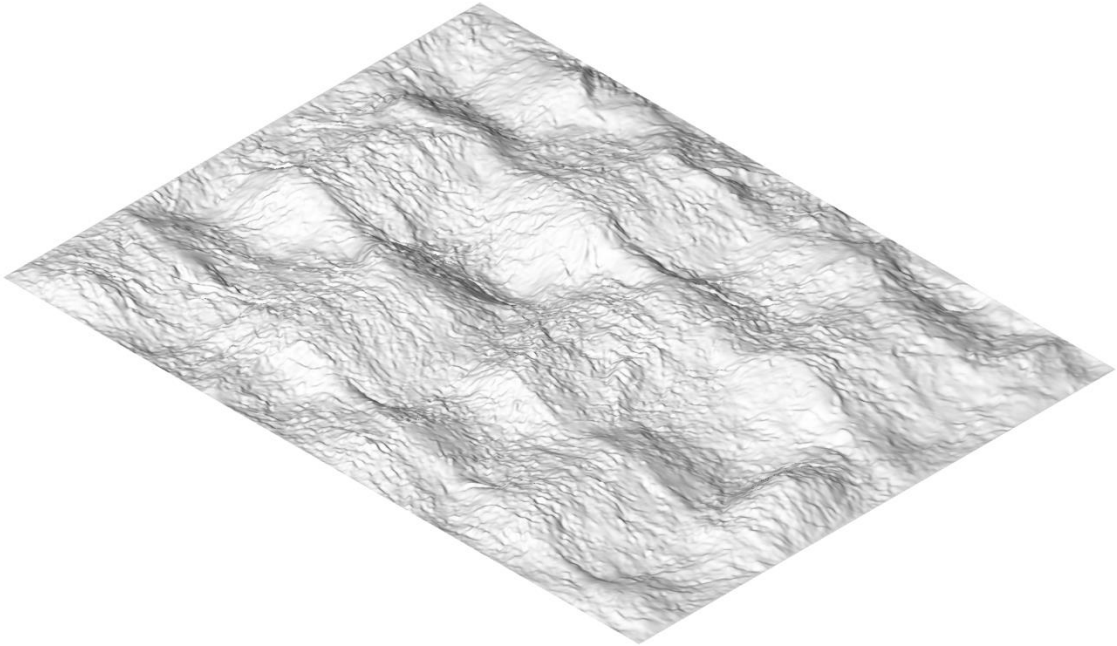

3D Reconstruction Rendering

Polypropylene (64%), Polyester (37%) Bouclé

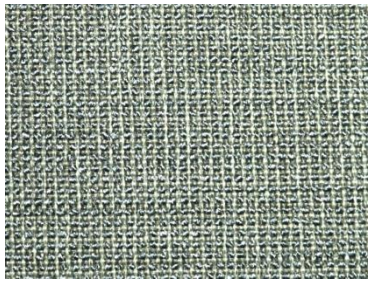

Material Scanned

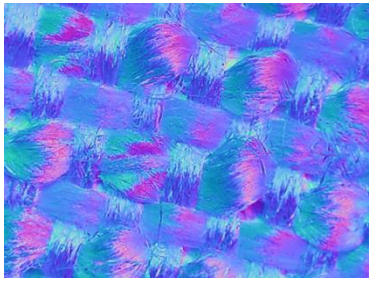

Normal Map

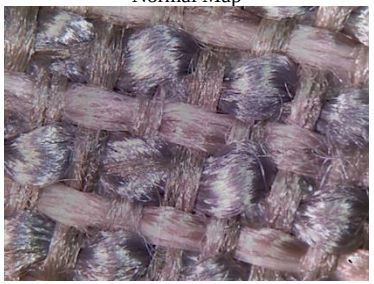

Albedo

Normalized Depth Map

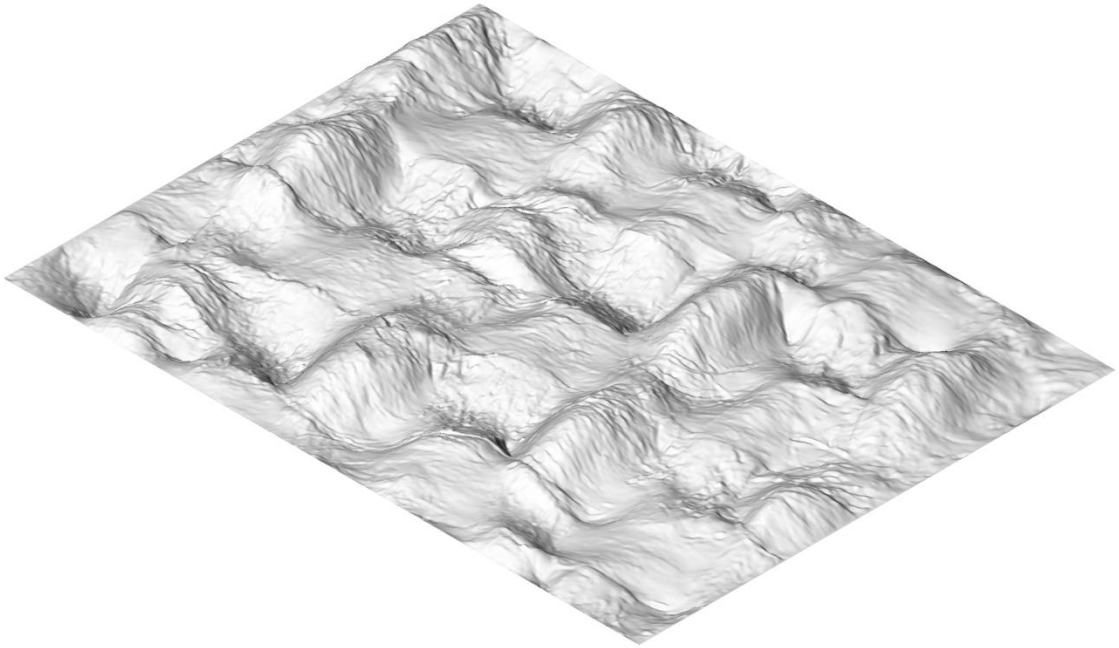

3D Reconstruction Rendering

Polypropylene (98%), Polyester (2%) Bouclé

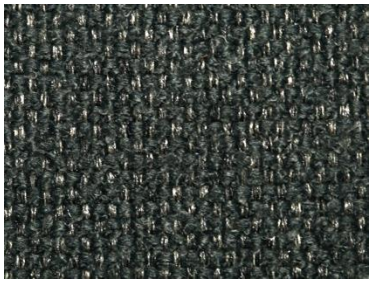

Material Scanned

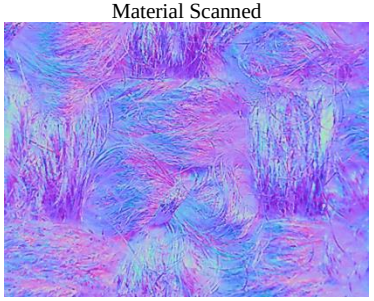

Normal Map

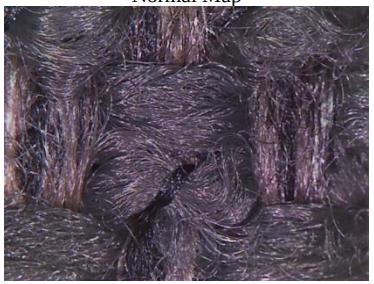

Albedo

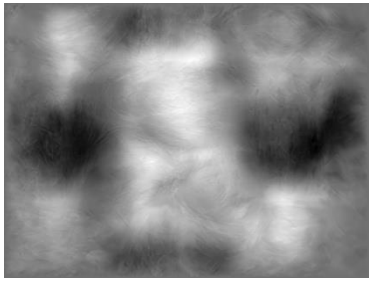

Normalized Depth Map

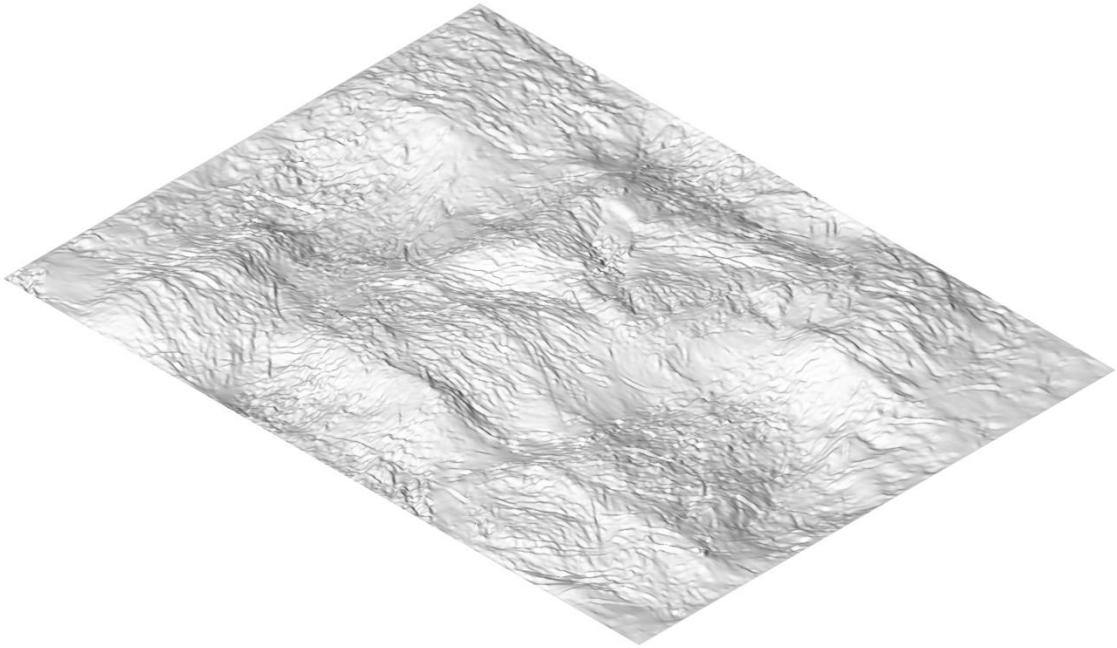

3D Reconstruction Rendering

Polyester (100%) Chenille

Material Scanned

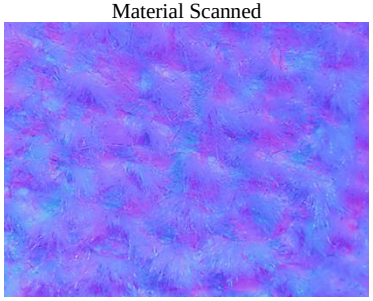

Normal Map

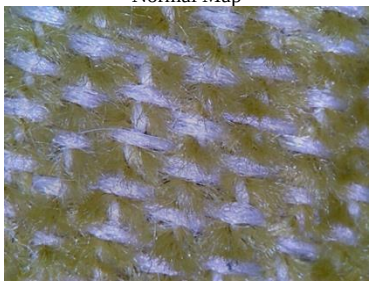

Albedo

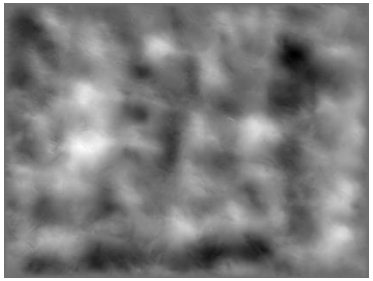

Normalized Depth Map

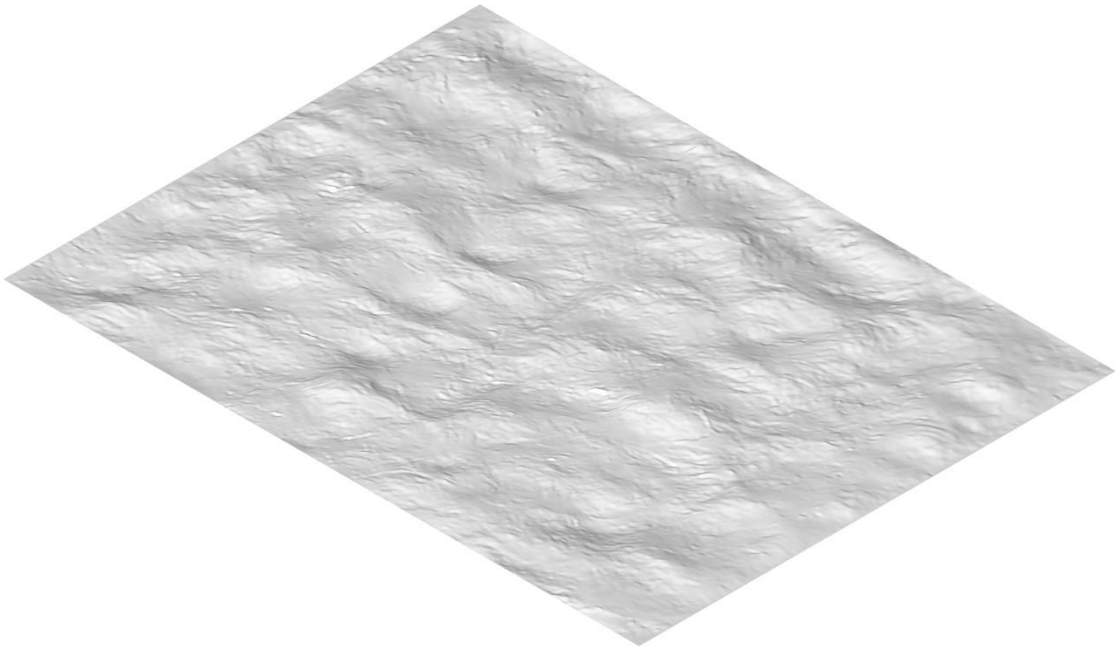

3D Reconstruction Rendering

Polyester (50%), Olefin (50%) Jacquard

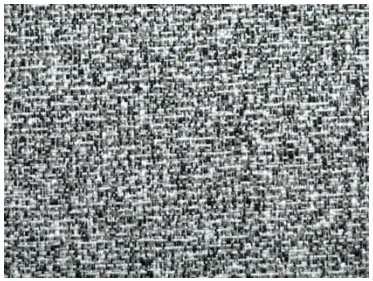

Material Scanned

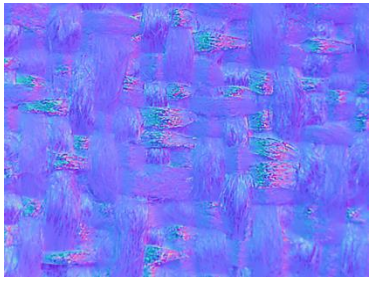

Normal Map

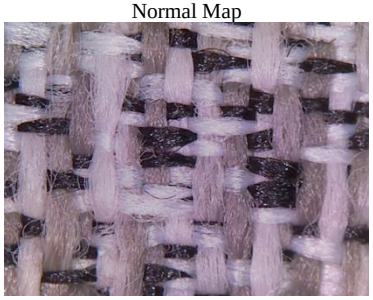

Albedo

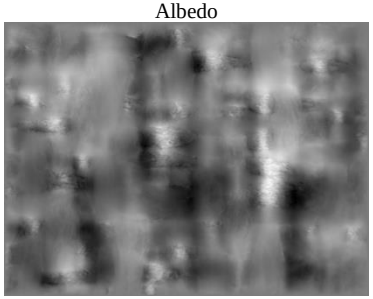

Normalized Depth Map

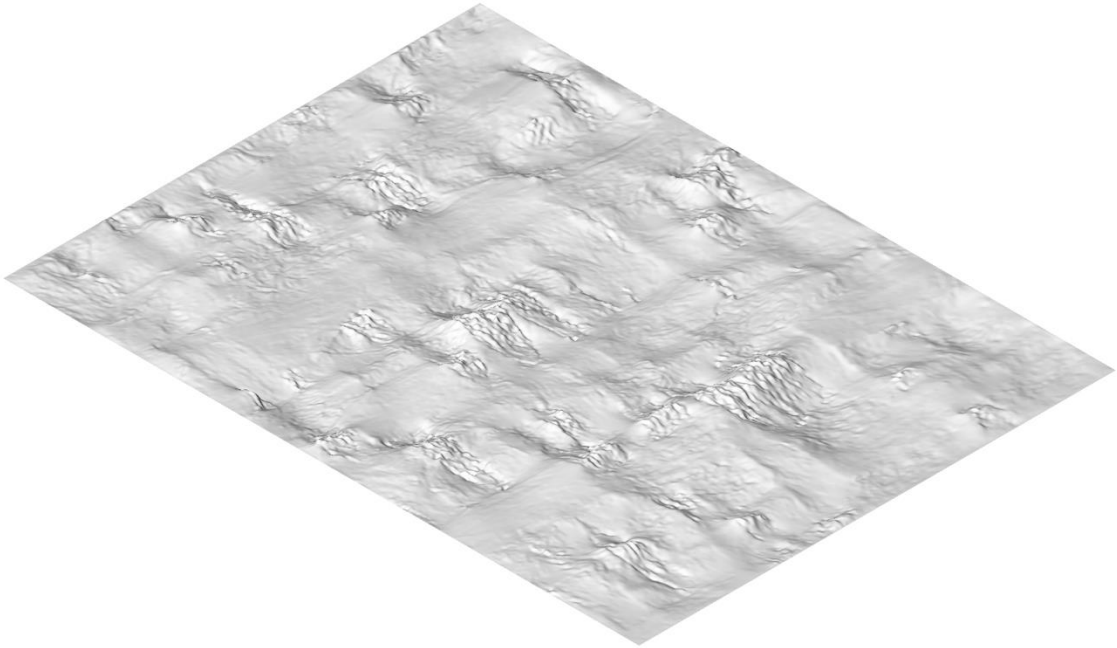

3D Reconstruction Rendering

Polypropylene (100%) Bouclé

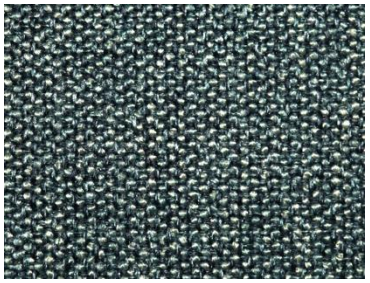

Material Scanned

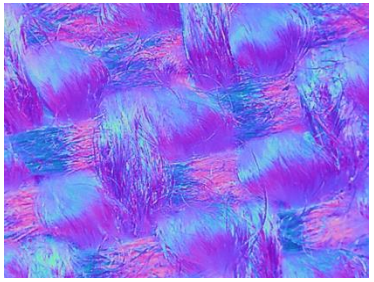

Normal Map

Albedo

Normalized Depth Map

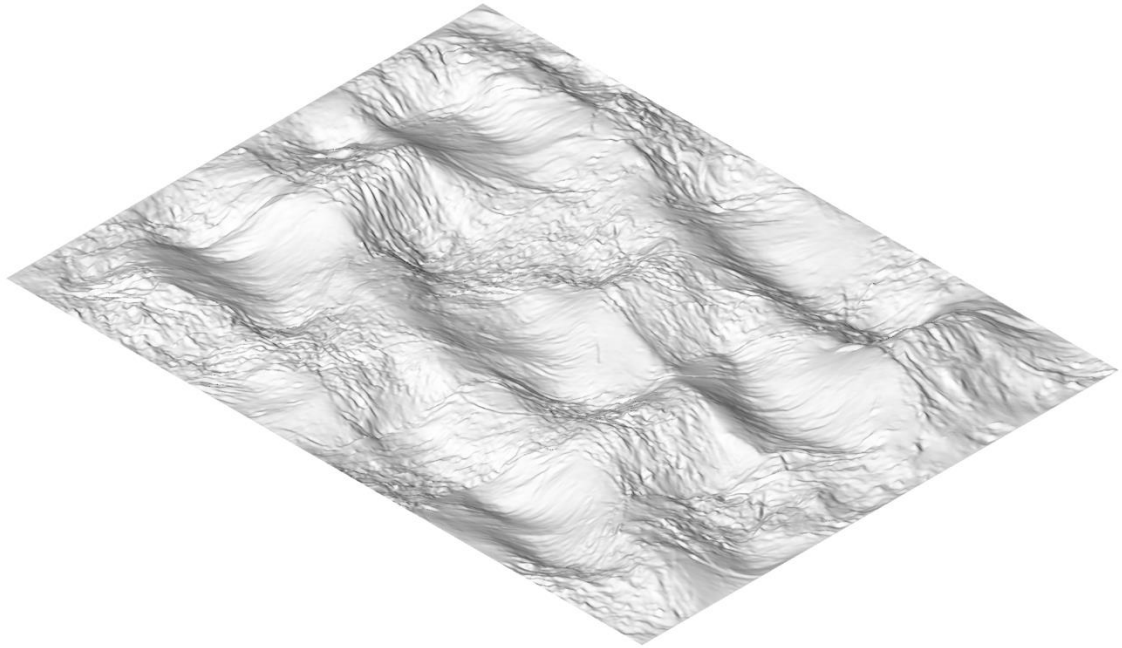

3D Reconstruction Rendering

Top-grain, semi-aniline dyed leather

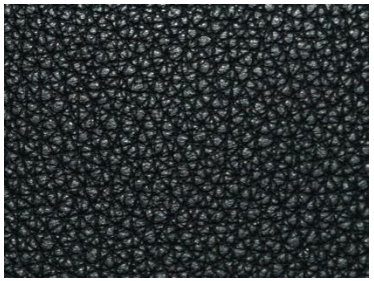

Material Scanned

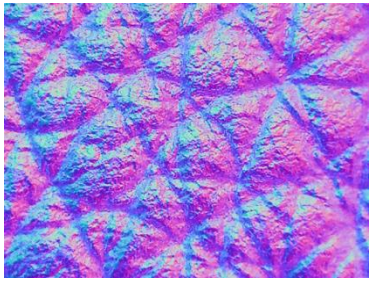

Normal Map

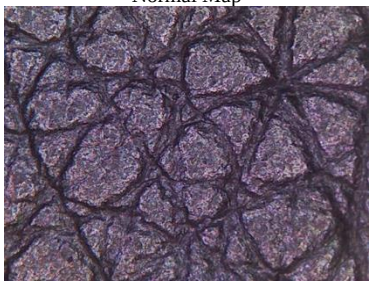

Albedo

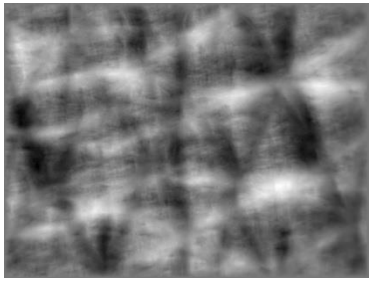

Normalized Depth Map

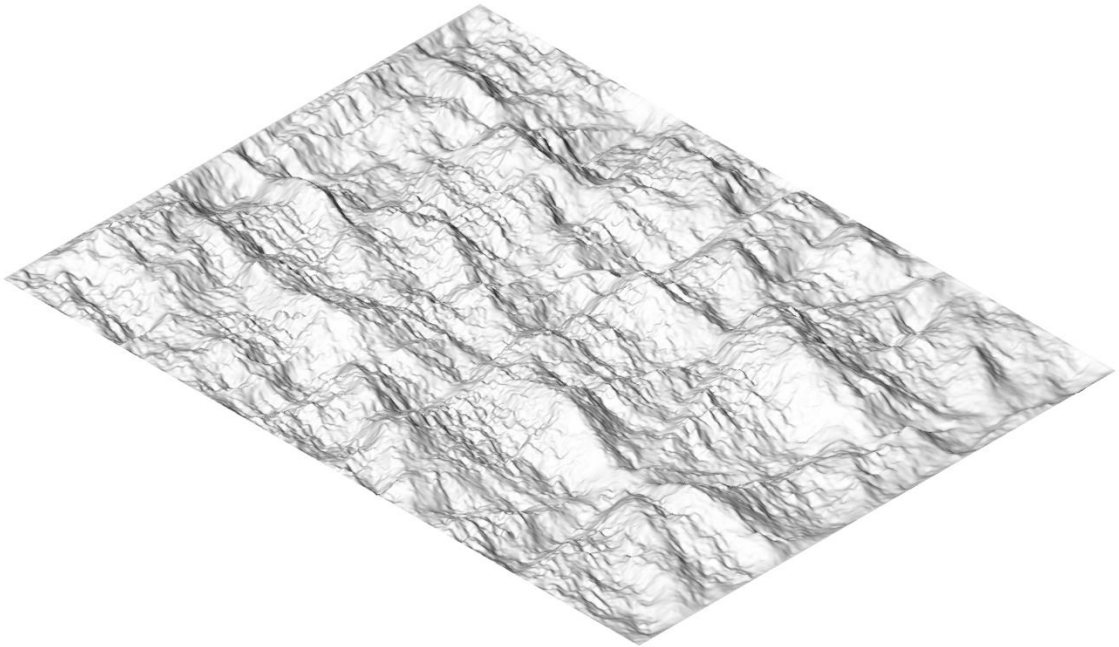

3D Reconstruction Rendering

Top-grain, full-aniline dyed leather

Material Scanned

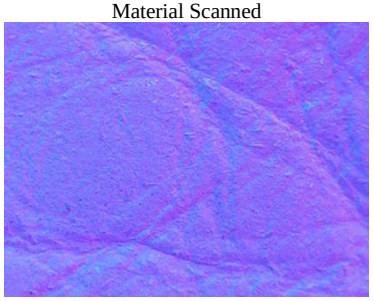

Normal Map

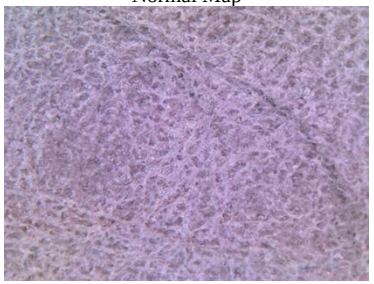

Albedo

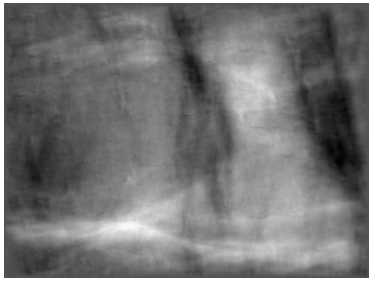

Normalized Depth Map

3D Reconstruction Rendering

Full, Top-grain, semi-aniline dyed leather

Material Scanned

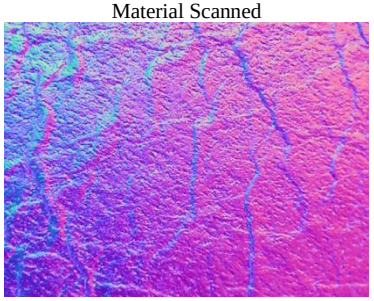

Normal Map

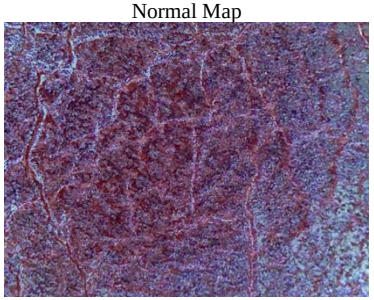

Albedo

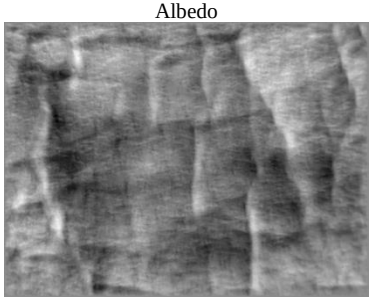

Normalized Depth Map

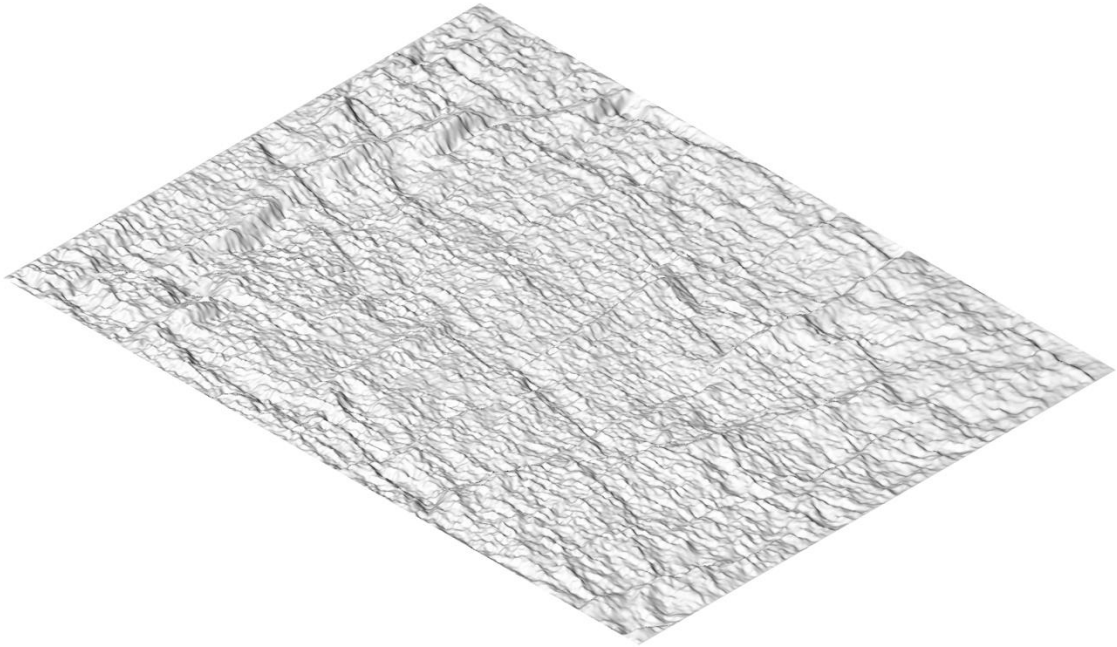

3D Reconstruction Rendering

Agar and Saw Dust

Material Scanned

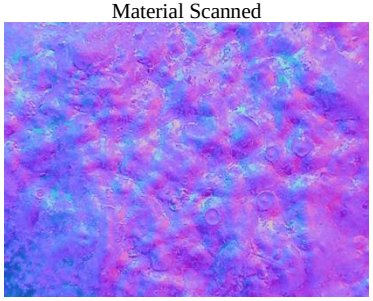

Normal Map

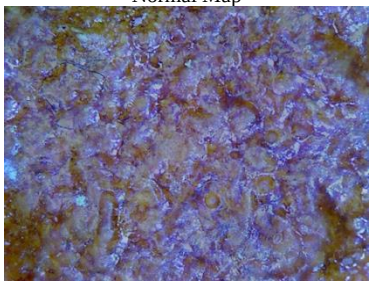

Albedo

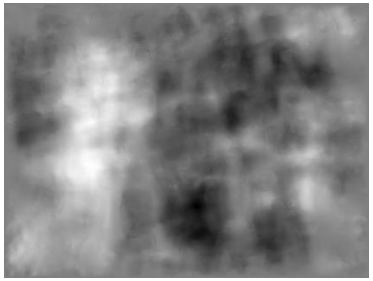

Normalized Depth Map

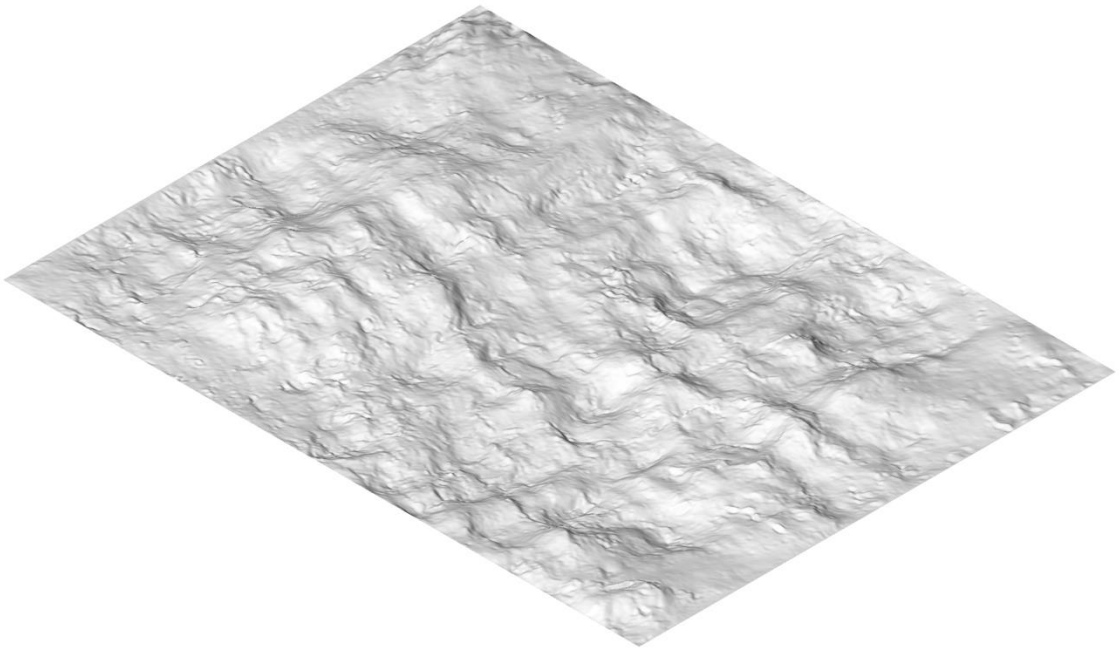

3D Reconstruction Rendering

Agar and Clay

Material Scanned

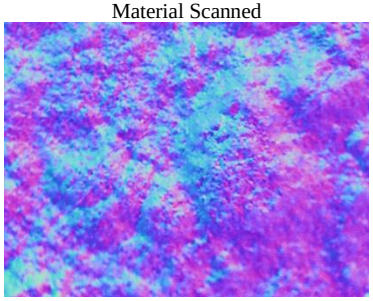

Normal Map

Albedo

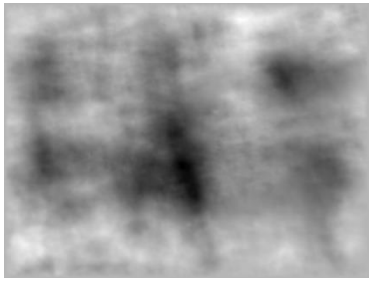

Normalized Depth Map

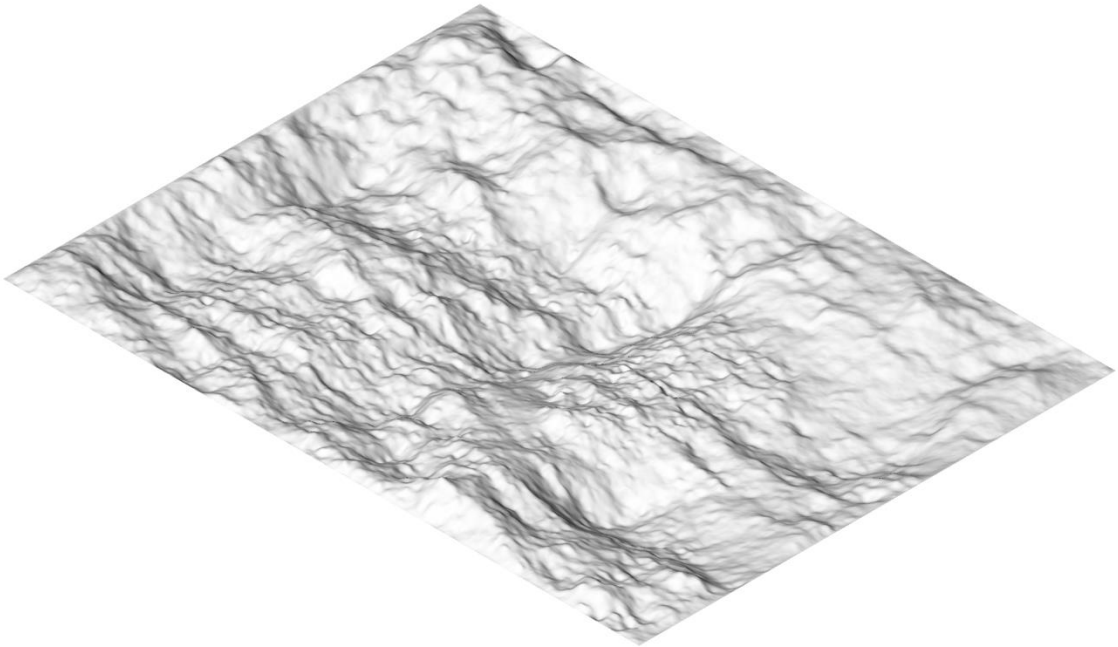

3D Reconstruction Rendering

Tapioca and Coffee

Material Scanned

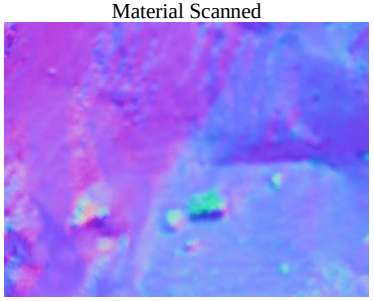

Normal Map

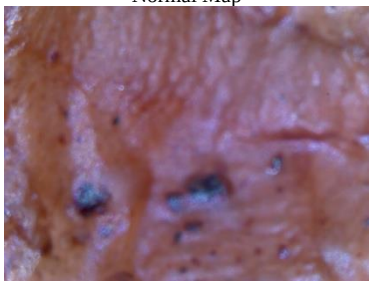

Albedo

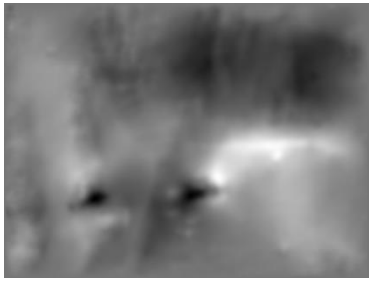

Normalized Depth Map

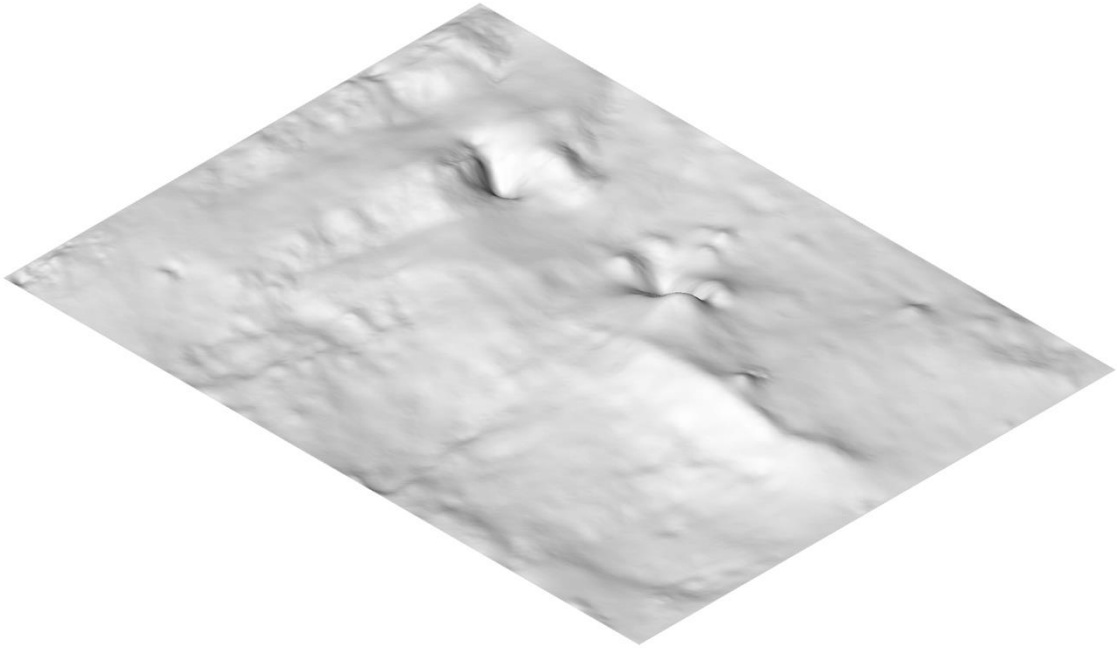

3D Reconstruction Rendering

Agar and Clay

Material Scanned

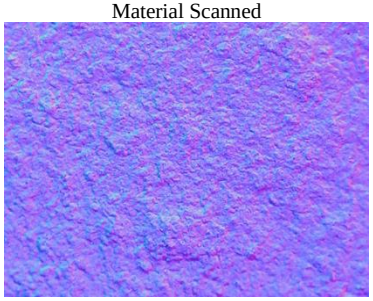

Normal Map

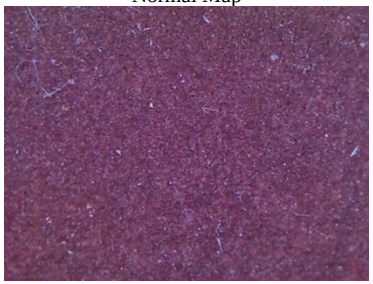

Albedo

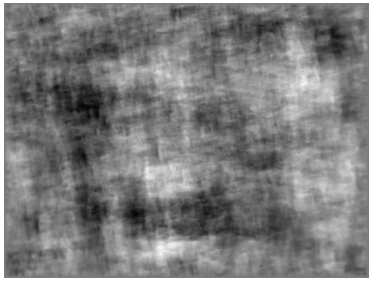

Normalized Depth Map

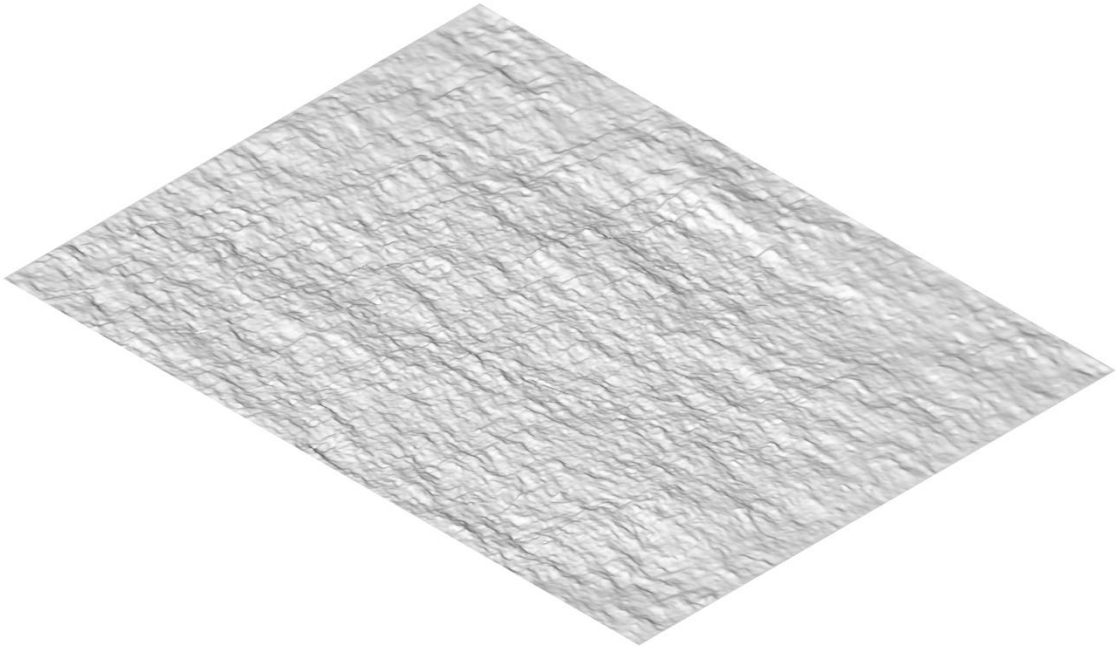

3D Reconstruction Rendering

Tapioca

Material Scanned

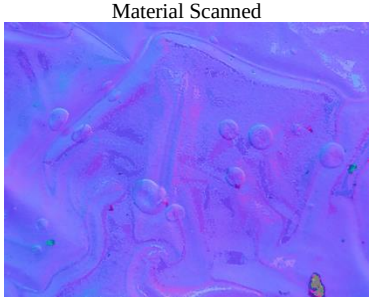

Normal Map

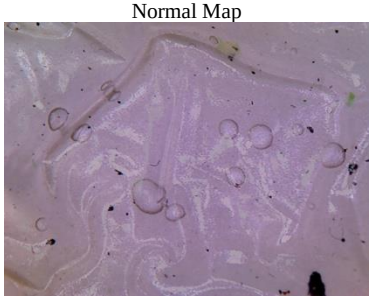

Albedo

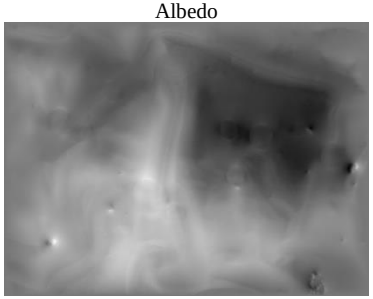

Normalized Depth Map

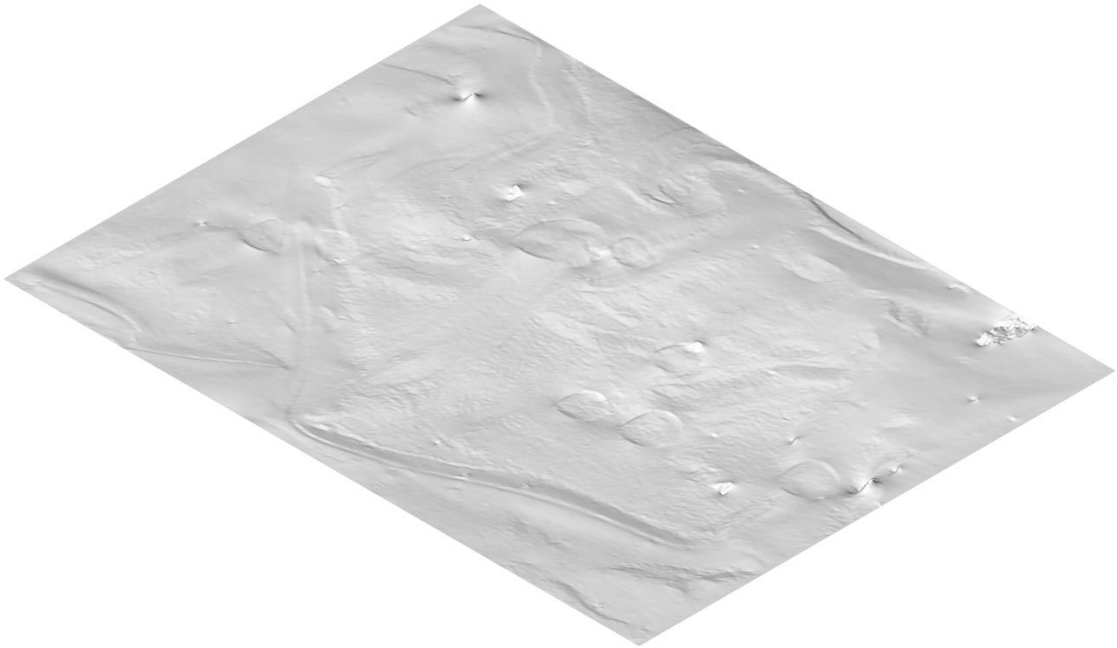

3D Reconstruction Rendering

Powder Print

Material Scanned

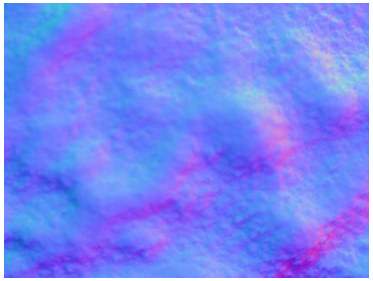

Normal Map

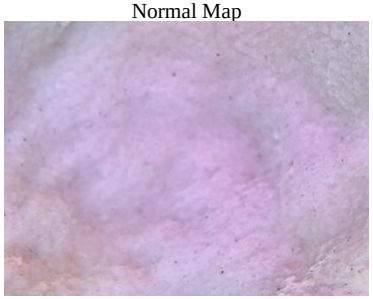

Albedo

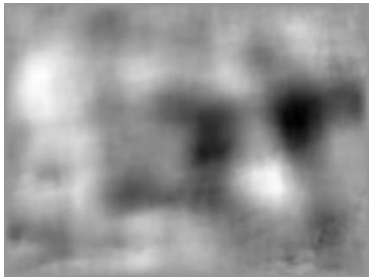

Normalized Depth Map

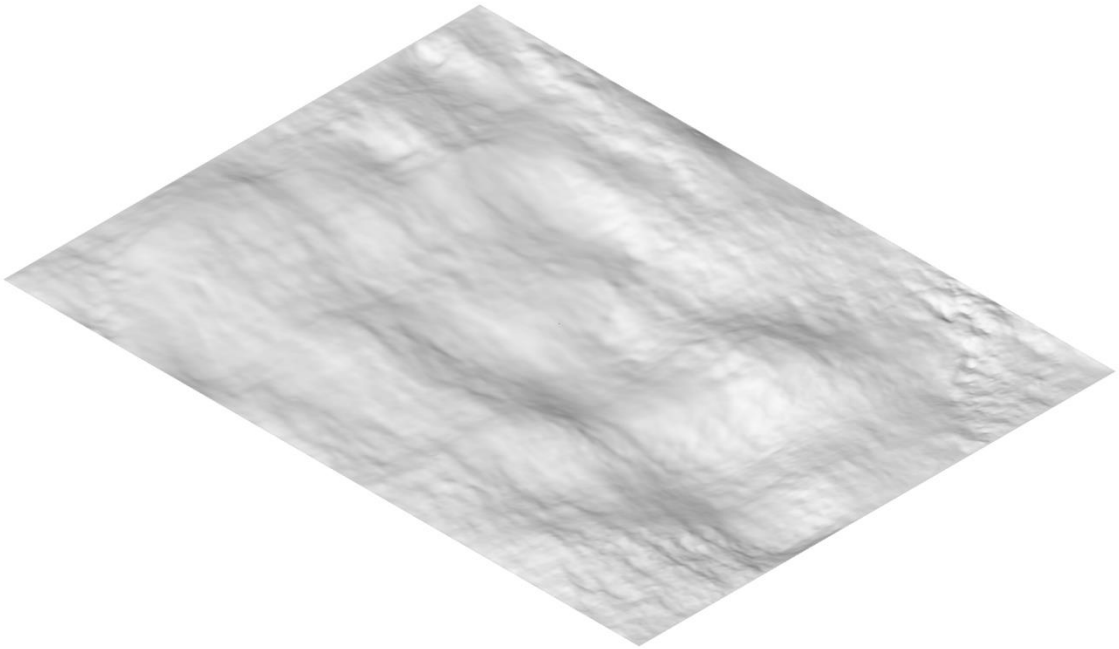

3D Reconstruction Rendering

Resin 3D Print (SLA)

Material Scanned

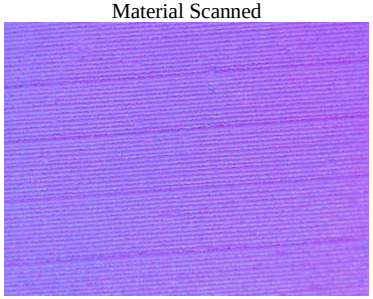

Normal Map

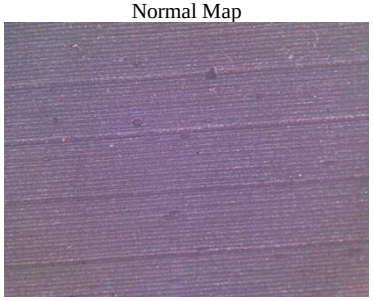

Albedo

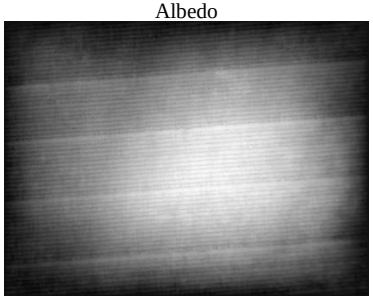

Normalized Depth Map

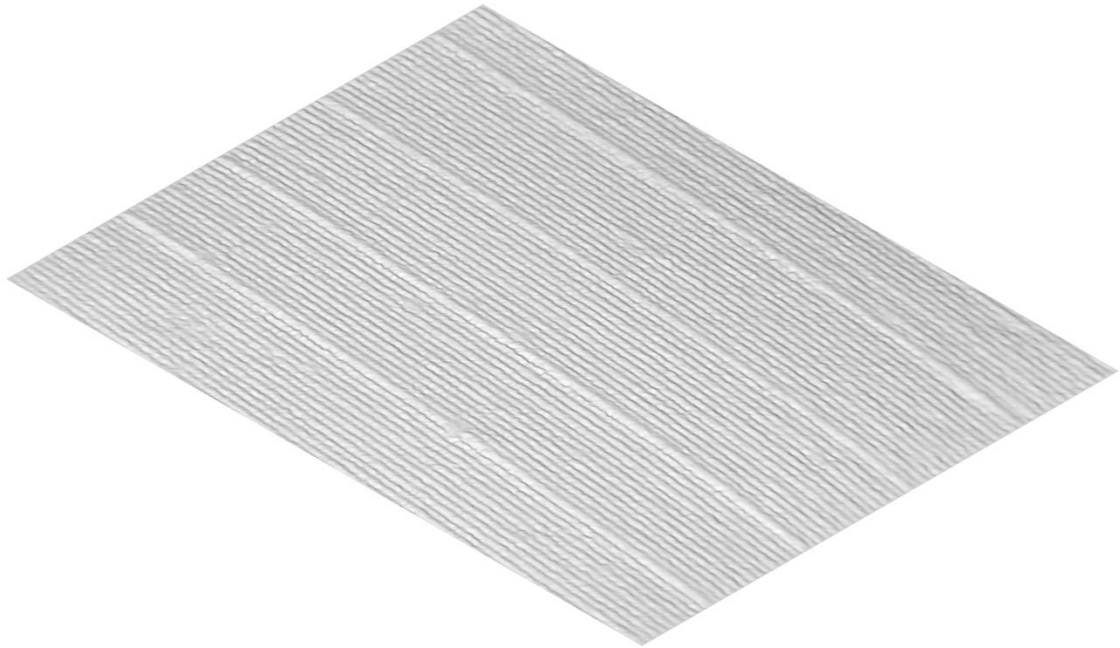

3D Reconstruction Rendering

PLA Print (FDM)

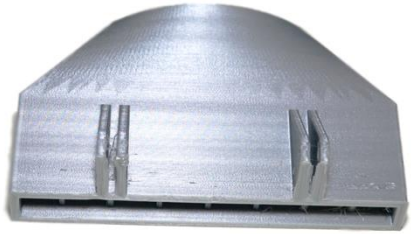

Material Scanned

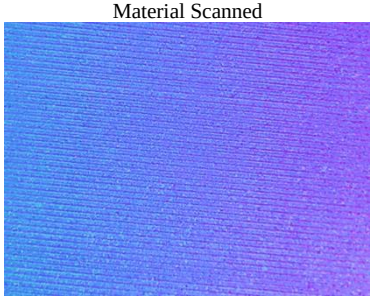

Normal Map

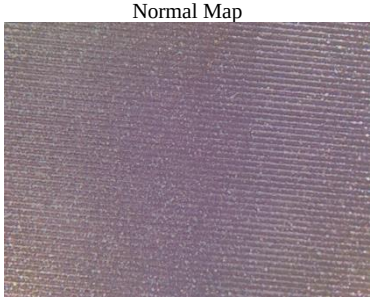

Albedo

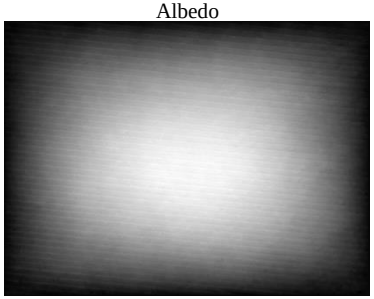

Normalized Depth Map

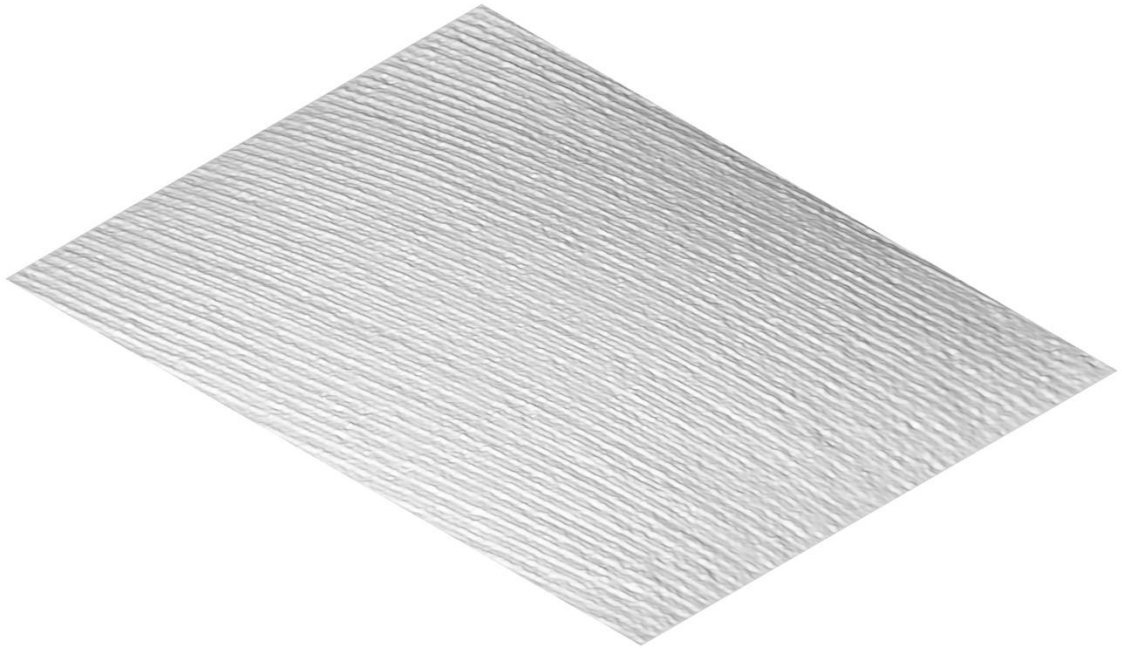

3D Reconstruction Rendering

Appendix B: Material Composition of the 28 Samples

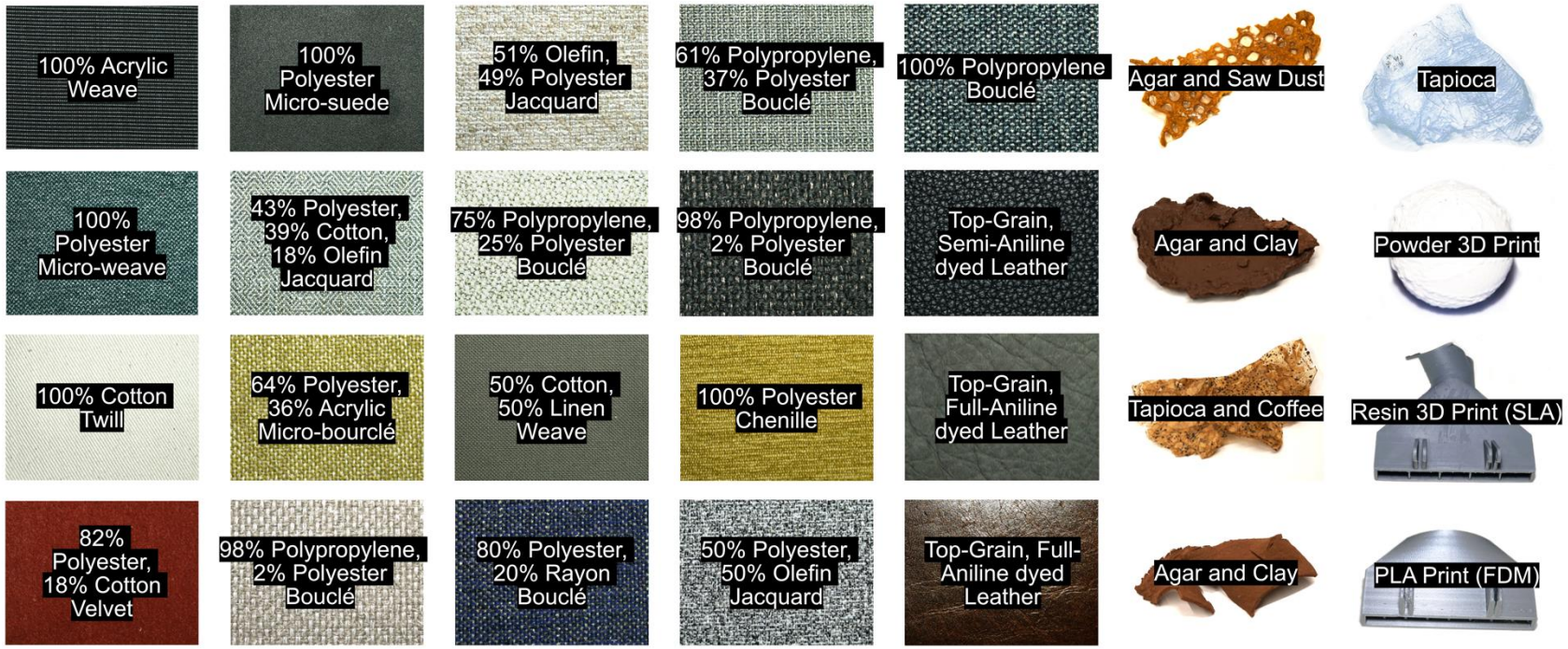

Appendix C: Resin 3D Printed from 8 samples reconstruction (5:1 Scale)

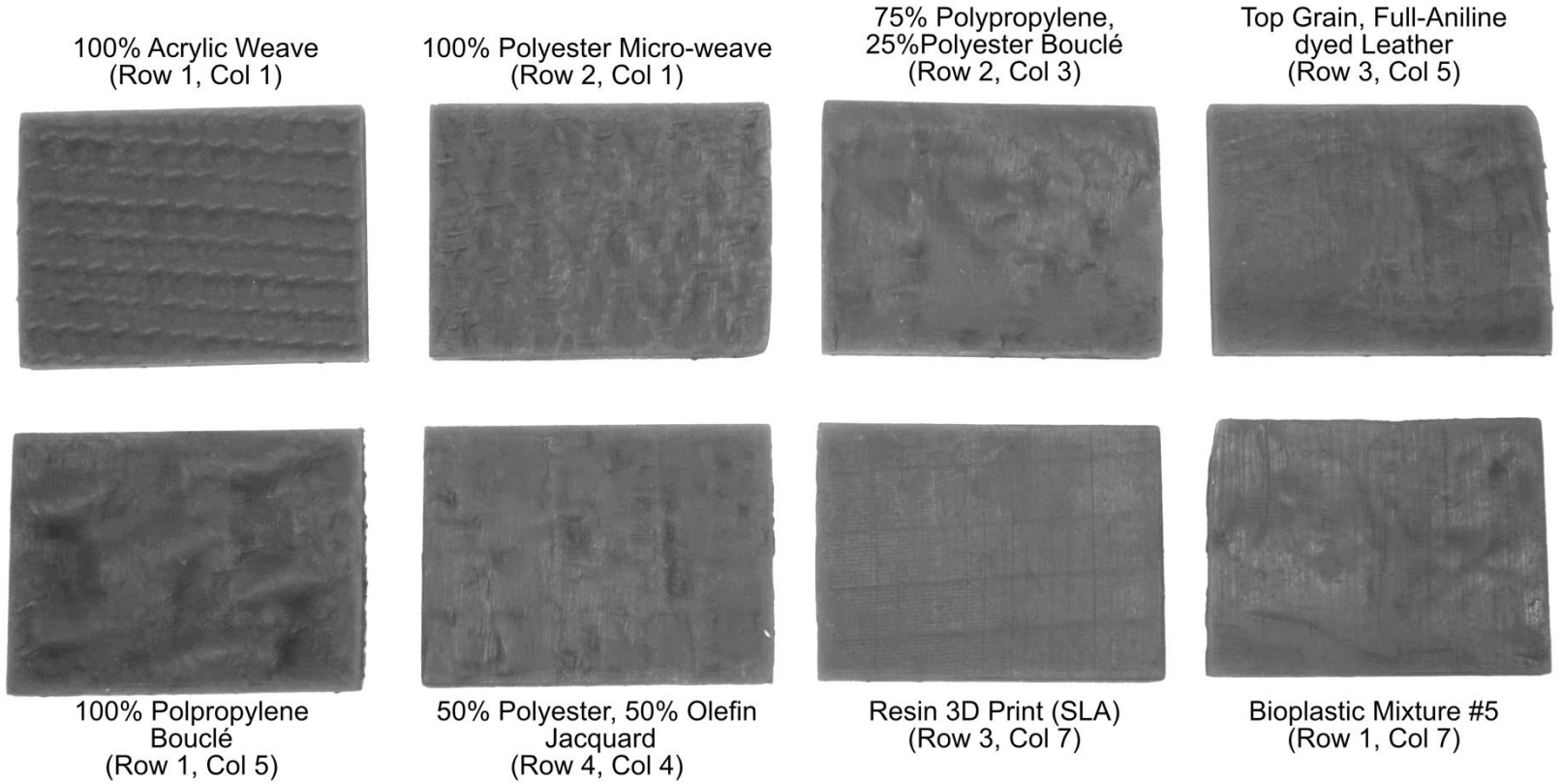

Appendix D: Open-Sourced Github Link

Following is the open-sourced link of the projects including the codes, schematics, hardware lists, and example results.

https://github.com/weiweikee/microscopic_photometric_stereo